AN ABSTRACT OF THE THESIS OF

CHENG-TSONG CHU for the degree of Master of Science in Atmospheric Sciences presented on 23 September 1986

Title: Parameterization of Shallow Convection in the Boundary Layer

Abstract approved: Redacted for Privacy

A shallow convection scheme is derived from several data sets (BOMEX, GATE, AMTEX, BLX83) and developed for the OSU 1-D boundary layer model. Results of the model structure and characteristics of the saturation point (SP) profile are compared against the constant cloud diffusivity scheme of Tiedtke (1983) and the ECMWF boundary layer parameterization scheme.

The results indicate that the primary mechanism that transports moisture away from the lower boundary layer is the boundary layer turbulent flux and that the boundary turbulent mixing alone is capable of maintaining an apparent moisture source near the inversion. While the sensible heat flux over ocean becomes quite small after a few hours of model simulation, the virtual heat flux remains positive and the boundary layer remains in the unstable regime.

Parameterization of Shallow Convection in the Boundary Layer

by

Cheng-Tsong Chu

A THESIS

submitted to

Oregon State University

in partial fulfillment of
the requirements for the
degree of

Master of Science

Completed 23 September 1986

Commencement June 1987

APPROVED:

Redacted for Privacy

Professor of Atmospheric Sciences in charge of major

Redacted for Privacy

Chairman of the Department of Atmospheric Sciences

Redacted for Privacy

Dean of Gradu

Date thesis is presented 23 September 1986

TABLE OF CONTENTS

LIST OF FIGURES

LIST OF FIGURES (Continued)

LIST OF FIGURES (Continued)

LIST OF TABLES

PARAMETERIZATION OF SHALLOW CONVECTION IN THE BOUNDARY LAYER

1. INTRODUCTION

Shallow convection is thought to be one of the crucial sub-grid scale mechanisms for transporting moisture and heat from the planetary boundary layer to the free atmosphere. It is also thought to be an important mechanism that provides a balance against large scale sinking motion and maintains a steady state well mixed subcloud layer under undisturbed trade wind situations. By it's vertical transfer of water vapor, it supports the growth of the deep, precipitating cumulus towers. Without this mechanism moisture will accumulate in the lower boundary layer and cut down the latent heat and sensible heat fluxes from the surface. Yanai et al. (1973) introduced a budget approach to implicitly calculate the first order sub-grid scale turbulent flux from large scale observation data. They defined Q1 (apparent heat source) to be the heating due to radiation, the release of latent heat by net condensation, and the divergence of the vertical eddy transport of sensible heat, and Q2 (apparent moisture sink) to be the net condensation and the divergence of the vertical eddy transport of moisture. They found the Q2 profile in the tropical ocean to possess peaks in the upper troposphere as well as in the lower troposphere. The moisture sink in the upper troposphere is interpreted as due to convective precipitation. The moisture sink in the lower troposphere and relative minimum in Q2 between the two peaks are

interpreted as due to transport of moisture upward from the lower troposphere and detrainment of liquid water and water vapor in mid-troposphere by the non-precipitating shallow clouds. They concluded that the relative minimum between the two peaks which counteracts the drying by environmental sinking motion is due to the water vapor and liquid water detrainment from the clouds, especially the shallow clouds in the lower troposphere. Nitta and Esbensen (1974) used a similar approach to estimate the large-scale heat and moisture budgets over the tropical Atlantic Ocean during Phase 3 (22-30 June 1969) of the Barbados Oceanographic and Meteorological Experiment (BOMEX). For undisturbed period (22-26 June 1969) with weak cumulus convection, the sub-grid scale Q1 and Q2 profiles both show a minimum near the bottom of the trade wind inversion layer. This phenomenon is interpreted as the effect of moistening and cooling due to moisture detrained and re-evaporated at the top of the shallow cumulus. There are some other works that obtained similar results by using Air Mass Transformation Experiment (AMTEX) data (e.g. Esbensen, 1975; Nitta, 1976; Murty, 1976; Nitta and So, 1980). As an example, we show Q1 and Q2 profiles derived from AMTEX 75 data in Fig 1.1 which is taken from Nitta and So (1980).

The importance of the shallow convection is not only demonstrated by the budget studies but also in numerical modeling studies. Tiedtke (1983) showed that it is necessary to parameterize such processes in the general circulation model. He found that with both the Arakawa-Schubert (1974) and the Kuo (1965) deep convection schemes, moisture accumulated in the lower boundary layer

and there lacks another mechanism that can transport the excess moisture up to the upper air environment. By employing a simple constant cloud diffusivity profile as a shallow convection scheme in the European Centre for Medium-Range Weather Forecasts (ECMWF) operational model, Tiedtke was able to not only get rid of the excess moisture near the surface and significantly improve the model's forecast but also reproduce the BOMEX and ATEX (Atlantic Trade Wind Experiment, 1969) sounding data in one-dimensional model simulations.

Direct calculations of the turbulent heat and moisture flux (e.g. LeMone and Pennell, 1976; Nicholls, 1980) using data from the GARP (Global Atmospheric Research Program) Atlantic Tropical Experiment (GATE, 1980), however, have found little evidence of the effect of the shallow cumulus. The study of California stratus by Albrecht (1985) using aircraft data, on the other hand, does seem to show an enhancement of the moisture flux. It is possible that the cloud amount may play a role in the magnitude of the fluxes as the GATE studies are for days with little shallow convection.

Betts and Miller (1984) proposed a new convective adjustment scheme for sub-grid scale mixing processes by using mixing line concept based on saturation point (SP) thermodynamics (Betts, 1982a, 1982b). When a parcel of air originated at a pressure level P with temperature T and dew point T_d is lifted dry-adiabatically in the vertical, the parcel temperature will decrease as the ambient pressure decreases. The pressure and temperature at which the parcel becomes saturated is the saturation point for the

parcel. The SP profile of a sounding is a useful tool to diagnose the atmosphere structure. The mixing line is chosen as a line of the SPs on the thermodynamic diagram that represents the possible state of the mixture of air with one saturation point and air with another saturation point. An example is taken from Betts (1982) (Fig. 1.2). Observational studies have shown that SPs of the atmosphere below an inversion usually fall along the mixing line between the surface and the atmosphere above the inversion. As diabetic processes move the SPs away from the mixing line, this parameterization scheme adjusts the temperature and moisture field to move the SPs back toward the mixing line. This scheme has been tested recently in the ECMWF operational model and produces results similar to that of Tiedtke (1983). In our study we shall use the mixing line concept as a tool to examine the resulting characteristics of the model structure.

One of the goals of this work is to derive a shallow convection scheme using BOMEX, AMTEX, and BLX83 (Boundary Layer Experiment 1983 in Oklahoma) data. To be consistent with the PBL model treatment, we seek to parameterize the effect of shallow clouds using diffusivity formulation in which the cloud diffusivity profile depends on the cloud amount. The cloud amount forecast equation is derived from the BLX83 data and is only relative humidity dependent. Troen and Mahrt (1983) developed a PBL column model to parameterize the turbulent mixing within the boundary layer for a global spectral model of the Air Force Geophysics Laboratory (AFGL) (Brenner et al., 1982). Extensive tests of the

model have been performed (Troen and Mahrt, 1983; Pan and Mahrt, 1986) and the results indicate that the model is capable of producing realistic simulations of the boundary layer under various atmospheric and lower surface conditions. The shallow convection scheme is developed for this model. Results of the sensitive tests are compared against the constant cloud diffusivity scheme of Tiedtke (1983).

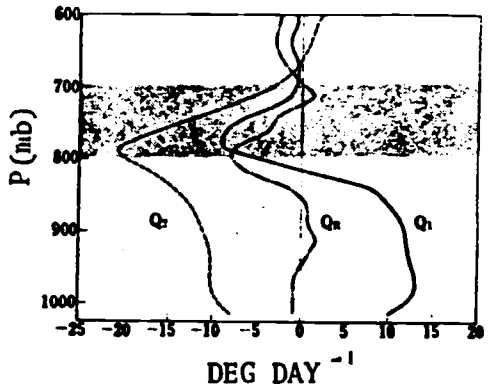

Figure 1.1. Averaged Q1 and Q2 profiles from AMTEX75 (after Nitta and So, 1980).

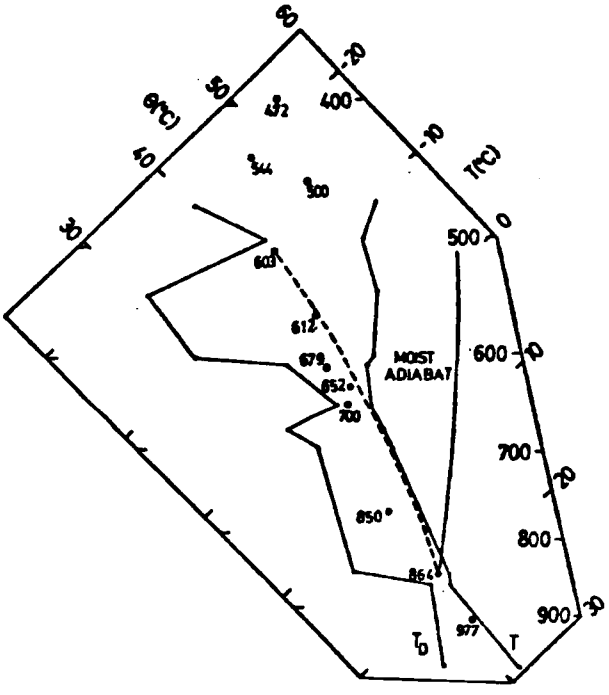

Figure 1.2. 1800 Z sounding on 19 July 1977 at Pittsburgh showing conventional plot of T(p) and Td(p) as solid lines, and SP as open circles, labeled with data pressure level p. The dashed line is the mixing line between the SP's of 603 mb air and 864 mb air.

2. THE DATA

Data from BOMEX, AMTEX74 and GATE were chosen for this study. While the data covered different synoptic situations, we chose to use data during undisturbed periods with a trade wind inversion capping the unstable boundary layer when only shallow convective clouds are present. Following are some of the characteristics of each data set (see Table 2.1 for summary).

2.1. BOMEX

The Barbados Oceanographic and Meteorological Experiment (BOMEX) was conducted during May and June 1969 over the area east of the Barbados. The season was chosen to provide a wide range of convective activities in the absence of well-developed storms. The primary objective of this experiment was to determine the rate of transfer of water vapor, heat, and momentum from the tropical ocean to the atmosphere. This experiment is divided into three phases. Only Phase 3 from June 22 to 26 is used in this study because of a particular shortage of data early on the 22nd and late on the 26th. This period was marked by relatively undisturbed trade-wind weather with light southerly wind near the sea surface turning into stronger northerly wind higher up. Strong easterly wind appeared in the lower boundary layer and decreased slowly below the inversion. Cloud cover was estimated from ATS-3 image-enhancement satellite picture and is about 40% to 50% during the period. Sea

surface temperature was 28°C, the period-averaged sensible heat flux was 15 W m^{-2} and the latent heat flux was 167 W m^{-2}.

2.2. AMTEX74

The Air-Mass Transformation Experiment in 1974 (AMTEX74) was conducted during 14 to 28 February 1974 over the Kuroshio region around the Nansei Island of Japan. During this season the cold air mass is strongly modified when it passes over the oceanic regions to the east of the Asian continent. Due to the large amount of heat and moisture supplied from the sea surface, the cumulus activity is strongly enhanced as the air travels farther over the ocean. The primary objective of AMTEX is to clarify the role of the cumulus clouds and the boundary layer eddies in the air mass transformation process and their relationship to the development of disturbances. This experiment is divided into three periods. Only the first period (from 14 to 16 February) was used, during which a local high pressure center is located to the northeast of the AMTEX area and southerly wind prevailed in the lower layer below the inversion. During this period the average sea surface temperature was 16°C, cloud cover was 45%, the surface latent heat flux is 252 W m^{-2} and sensible heat flux was 42 W m^{-2}. Below the inversion southerly wind speed increased with height and turned into strong westerly wind above the inversion. Sinking motion was stronger than for the other cases used in this study.

2.3. GATE

The Atlantic Tropical Experiment (GATE) was conducted during 1974. The experiment was divided into three phases but only data from Phase three is used due to shortage of data for undisturbed situations during the first two phases. During this period the boundary layer was capped by a weak trade wind inversion and boundary layer itself was nearly neutral and only slightly unstable. Average cloud cover was only 10% with little cumulus activity. The boundary layer structure appeared well-mixed for most days so that the modeled counter-gradient effect becomes important for the heat and moisture flux profiles. According to observation the northerly wind component was stronger than the easterly or westerly wind component. Sea surface temperature was about 26°C, average latent heat flux was 90 W m^{-2} and sensible heat flux was 10 W m^{-2}.

Table 2.1. Summary of the surface sensible heat flux, latent heat flux, average cloud cover and sea surface temperature (SST) of the BOMEX, AMTEX, GATE undisturbed period data.

Data	Sensible Heat Flux (W m^{-2})	Latent Heat Flux (W m^{-2})	Cloud Cover (%)	SST (°C)
BOMEX	15	167	45	28
AMTEX	42	252	45	16
GATE	10	90	10	26

CHAPTER 3. THE MODEL

3.1. The OSU PBL Model

In the Oregon State University Planetary Boundary Layer model (OSU PBL) the surface fluxes are computed according to the Louis (1979) formula and the layer below 50 m is consider to be the constant-flux layer. Above this layer, temperature (θ), moisture (q), and momentum (u,v) fluxes due to the boundary layer turbulent mixing with environment are parameterized as diffusive processes:

$$\frac{\partial X}{\partial t} = \frac{\partial}{\partial z} K \left(\frac{\partial X}{\partial z} - \gamma\right) \tag{3.1}$$

where X = [u,v,θ,q], K is the parameterized coefficient of diffusivity and γ is the parameterized counter-gradient effect (see Troen and Mahrt, 1983 for detail).

For stable cases, the momentum diffusivity is defined as

$$K_m = u_* \, k \, z \, (1 - z/h)^2 \, \Phi_m^{-1} \, (z/L), \text{ for } z \leq h, \tag{3.2}$$

where

$$\Phi_m = 1 + 4.7 \cdot z/L.$$

For unstable cases, momentum diffusivity is defined as

$$K_m = \begin{cases} u_* \, k \, z \, (1 - z/h)^2 \, \Phi_m^{-1}(z/L), \text{ for } z \leq 0.1h \\ w_s \, k \, z \, (1 - z/h)^2, \text{ for } 0.1h < z \leq h, \end{cases} \tag{3.3}$$

where

$$\Phi_m = (1 - 7.0 \cdot z/L)^{-1/3},$$

$$ws = u_* \cdot \Phi m^{-1} \, (.1 \, h/L).$$

The variable u_* is the surface friction velocity, w_s is the velocity scale, k is the Von Karman constant, ϕ_m is the nondimensional shear, and L is the Obukhov length. For both stable and unstable cases, the heat and moisture diffusivity coefficients are parameterized as

$$K_h = K_m \cdot P_r \quad , \tag{3.4}$$

where P_r is the Prandtl number and is computed in the model.

The variable h is the height of the boundary layer and is determined in this model as the height where the bulk Richardson number calculated over the layer below h is equal to the chosen critical Richardson number (Ri_{cr}). The bulk Richardson number is defined as

$$Ri_B = \frac{g\left(\theta_v(h) - \theta_s\right)h}{T_o \left|\vec{V}(h)\right|^2} \tag{3.5}$$

where $\theta_v(h)$ and θ_s are the virtual potential temperatures at the top of the boundary layer and near the surface, respectively. In this model Ri_{cr} is chosen to be 1.

The counter-gradient effect in the present formulation for heat flux is parameterized as

$$\gamma = 10 \frac{\overline{(w'\theta')}_o}{w_s \, h} \tag{3.6}$$

and a similar formulation for moisture flux is also included.

3.1.1. Model Limitation and Assumption

Since this is a 1-D column model, there is no horizontal advection process affecting the model structure during the sensitivity tests. We prescribed the initial vertical profile of horizontal (u,v) and vertical (w) motion, temperature (T) and mixing ratio (q). Additional assumptions are made as follows:

1. Large scale vertical motion field is a constant profile through out the sensitivity test period. The turbulent and convective process can only change the wind, temperature and mixing ratio fields within the boundary layer.
2. Super-saturation is removed by assuming that the excess moisture is carried away by the trade wind and advected downstream.
3. The sea surface temperature is assumed as a constant throughout the sensitivity test period.
4. Model's top is 4 Km which constrains the boundary layer top below this level. Between 50 m and 1.05 Km, the model resolution is 200 m. Above 1.05 Km, the model resolution is 100m.

3.2. The OSU Cloud Scheme

3.2.1. Cloud Cover

A formula for predicting the unstable boundary layer shallow cumulus amount is derived from the BLX83 aircraft and the AMTEX sounding data. The best parameter was found to be the relative humidity at the Lifting Condensation Level (LCL) within the boundary layer. A least square fit of a quadratic polynomial is used to predict the cloud amount CC:

$$CC = A0 + A1 \cdot RH + A2 \cdot RH^2, \quad \text{for } RH \geq 57\% \qquad (3.7)$$

and the coefficients calculated from the data are: A0 = -0.7417, A1 = -1.25665, and A2 = 2.264E-2. In Figure 3.1 we present the observed relationship between cloud cover and relative humidity at the cloud base. The solid line in Figure 3.1 represents the function in Eq. (3.7).

Slingo (1980) also developed a cloud parameterization scheme derived using GATE data for use in the British Meteorological Office's tropical model. Slingo's formulae for low cloud cover (Fig. 3.1) with and without inversion are:

(a) For $(d\theta/dp)min \leq -0.07(K/mb)$, we assume the existence of inversion and use the formula

$$CC = -16.67(d\theta/dp)min + \delta(RH-80)^2/400 - 1.167 , \qquad (3.8)$$

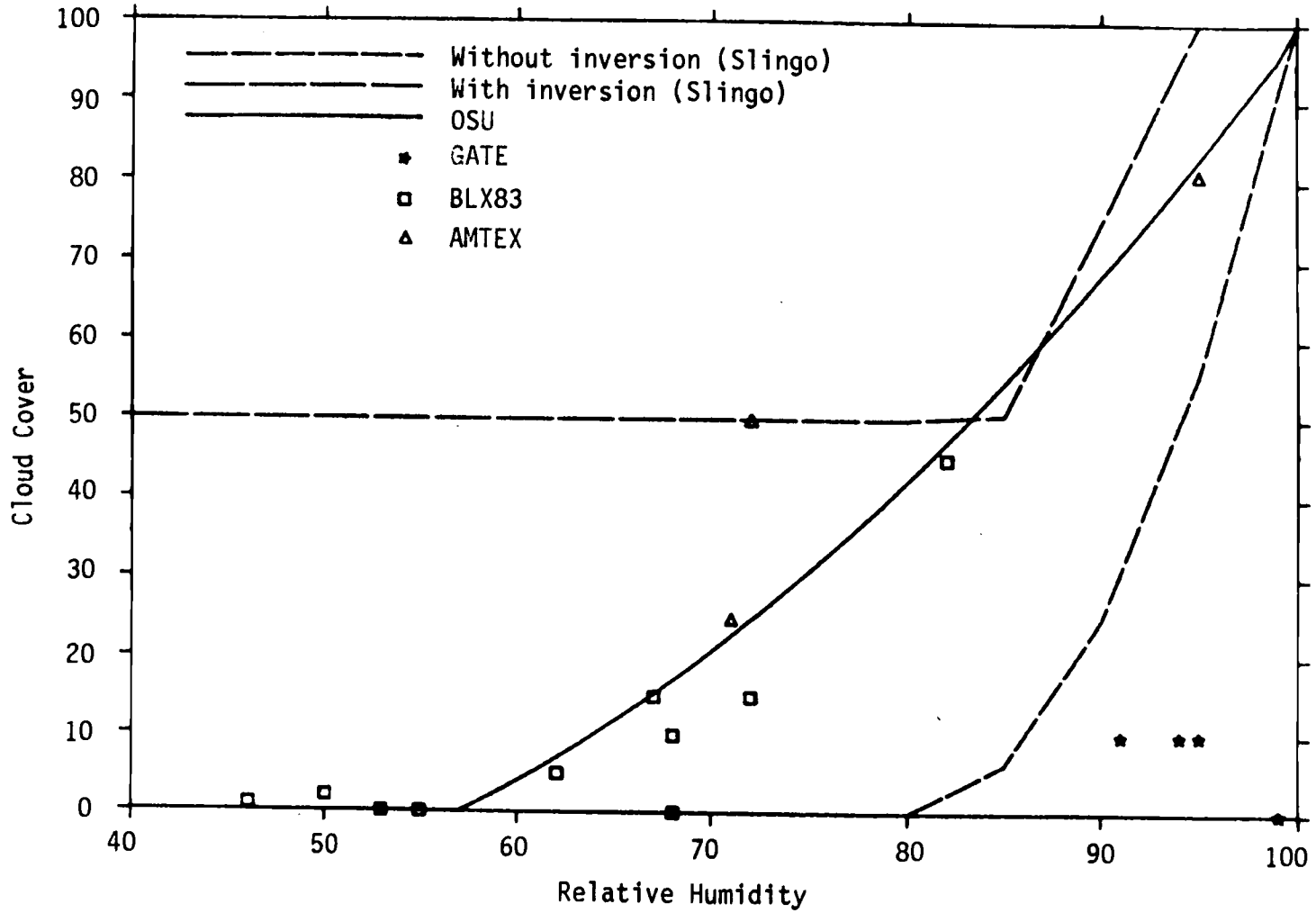

Figure 3.1. Comparison of the cloud cover prediction equations (Eqs. (3.7) and (3.8), (3.9)). For the Slingo scheme with inversion, we use $-d\theta/dp = 0.1$ (K/mb).

where

$$\delta = \begin{cases} 1 & RH \geq 80\% \\ 0 & RH < 80\% \end{cases}$$

to estimate the cloud amount.

(b) For $(d\theta/dp)min > -0.07(K/mb)$, we calculate the cloud amount as

$$CC = \begin{cases} (RH-80)^2/400, & \text{for } RH \leq 80\% \\ 0, & \text{for } RH \leq 80\%. \end{cases} \qquad (3.9)$$

For the case with inversion we use $d\theta/dp = -0.1(K/mb)$. For comparison, we take the BOMEX undisturbed period when $d\theta/dp$ is $-0.11(K/mb)$ and cloud cover is about 50%. The relative humidity just below the inversion is at 91% and at LCL is at 84%. In this case the Slingo formula predicts a cloud cover of 70% while our formula predicts 55% cloud cover. It can be seen that the Slingo formula will over estimate the cloud amount in the presence of an inversion when the relative humidity falls below 80%.

3.2.2. Cloud Diffusivity

Because the observed moisture fluxes from either budget studies (AMTEX and BOMEX) or aircraft measurements (California stratocumulus experiment reported in Albrecht, 1985) represent the combined fluxes from both the boundary layer turbulence and the shallow convection, we need to consider both mechanisms to model the observed fluxes. Within the framework of the PBL parameterization scheme, it is decided that a diffusion type parameterization scheme will be used to model the moisture flux due to shallow

convection. We therefore seek to model the moisture flux $\overline{w'q'}$ as

$$\overline{w'q'} = -(K_h + K_c)(\frac{\partial \bar{q}}{\partial z} - \gamma) \qquad (3.10)$$

where K_h is the coefficient of diffusivity due to boundary layer turbulence and K_c is the coefficient of diffusivity due to the shallow cumulus within the boundary layer. Furthermore, the boundary layer turbulent flux is calculated using the Troen and Mahrt (1983) method (Eq. 3.1-6). The combined diffusivity (K_h + K_c) (Fig. 3.2) is first calculated for each data set from profiles of $\overline{w'q'}$ and $\bar{q}$. We observe a peak in the lower boundary layer diffusivity profile. Troen and Mahrt (1983) demonstrated that the profile of K with a maximum at z/h = 1/3 fits the profile derived from large-eddy simulation experiments (Wyngaard and Brost, 1983). By assuming that the diffusivity coefficient for shallow convection (K_c) be small near ground, we estimate the diffusivity coefficient for the boundary layer (K_h) using the profile of calculated K (=K_h + K_c) below .5 z/h. When a maximum K value is observed near the level z/h = 1/3, it is inserted into Eqs. (3.3) and (3.4) and we can obtain a vertical profile of the K_h. We can further derive a diffusivity profile for the cloud (K_c) after subtracting K_h from K (see Fig 3.3). We found that this profile can be approximately fitted by a Gaussian Distribution function (see Fig. 3.4 a,b) if we know the peak value of this function and the standard deviation. Based on the observation that the ratio of the height of the Lifting Condensation Level (LCL) and

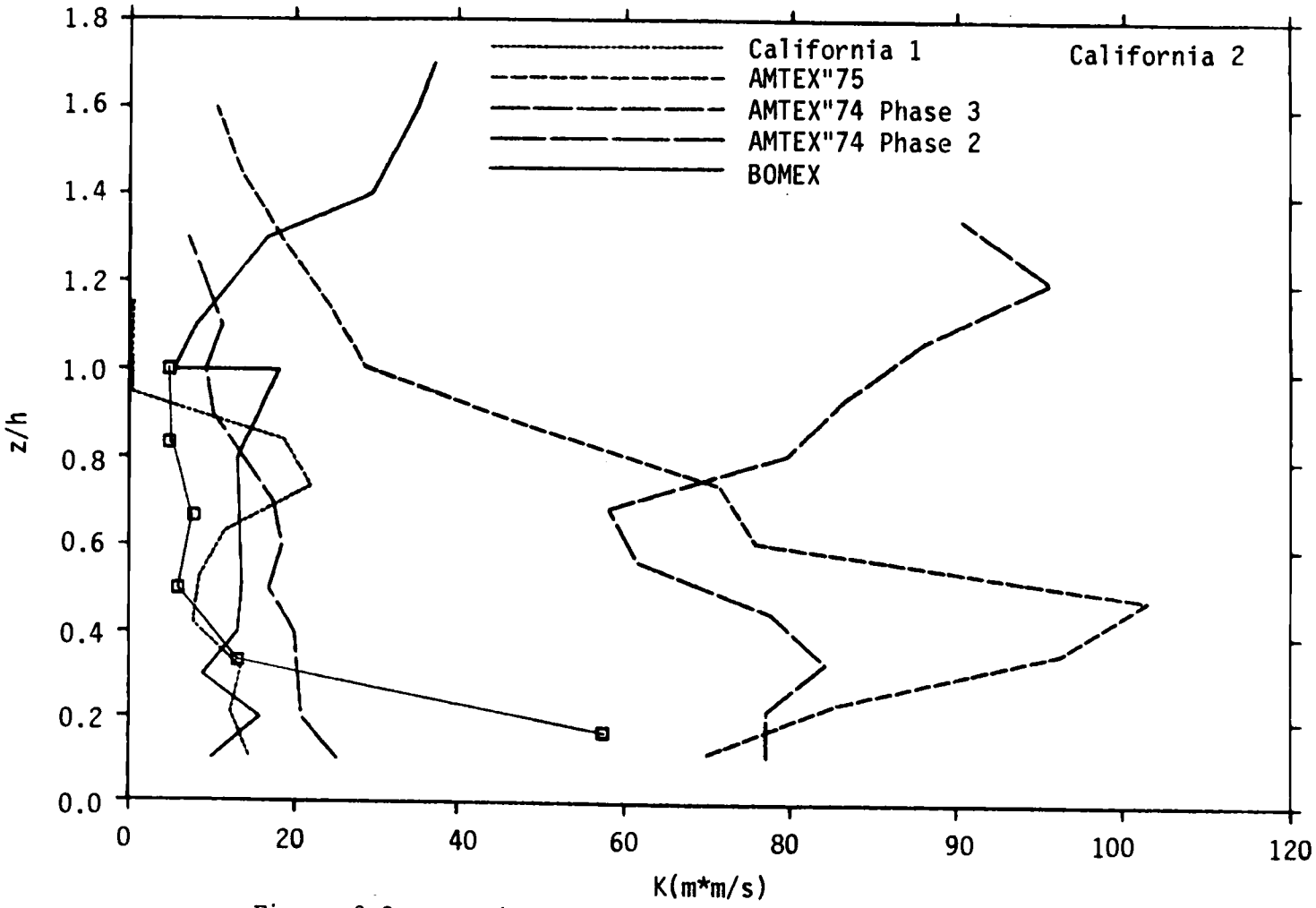

Figure 3.2. Vertical distribution of (K_c + K_h) calculated from the BOMEX, AMTEX and California coast stratocumulus experiment data.

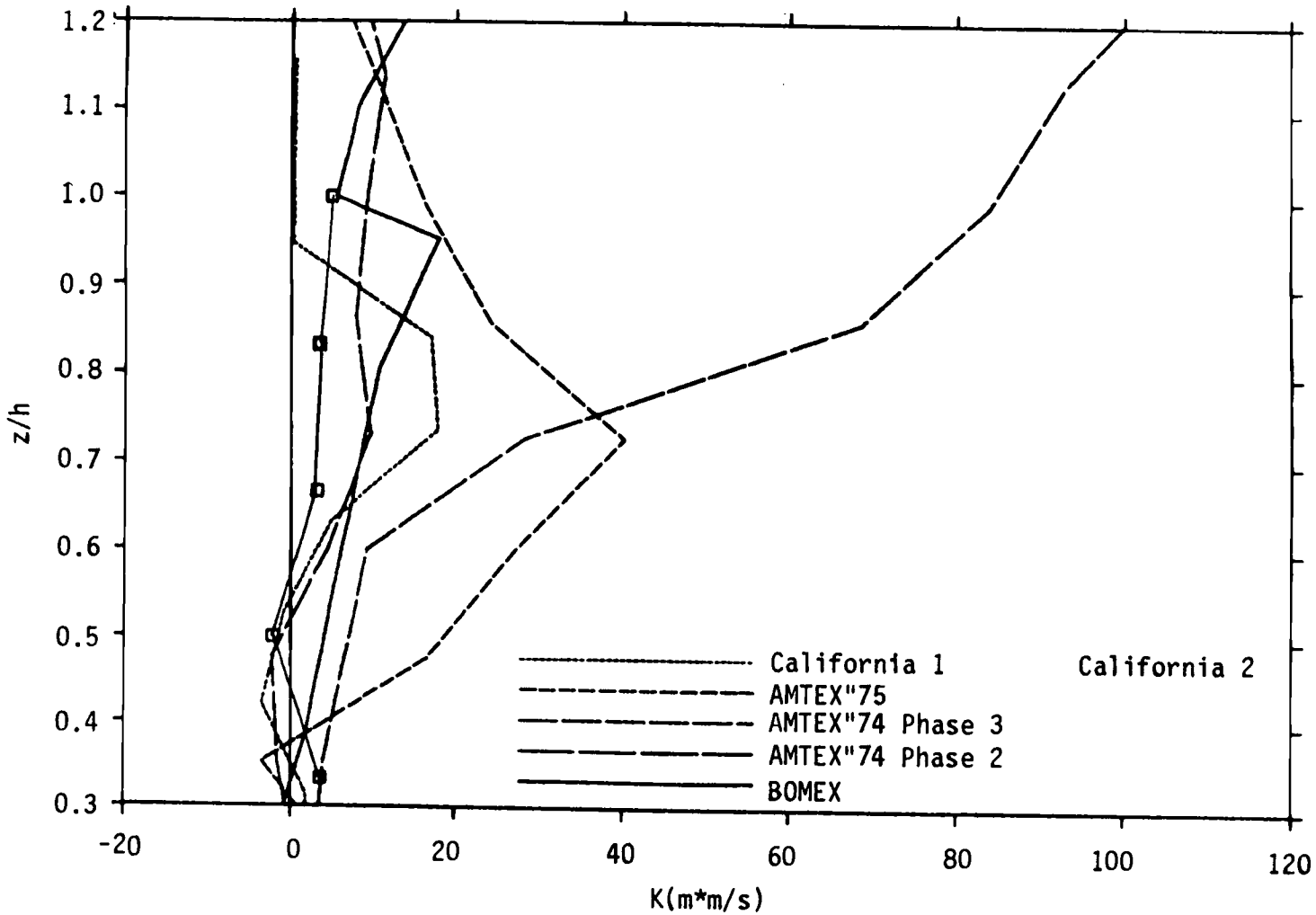

Figure 3.3. Vertical distribution of K_c deduced from the BOMEX, AMTEX and California coast stratocumulus experiment data.

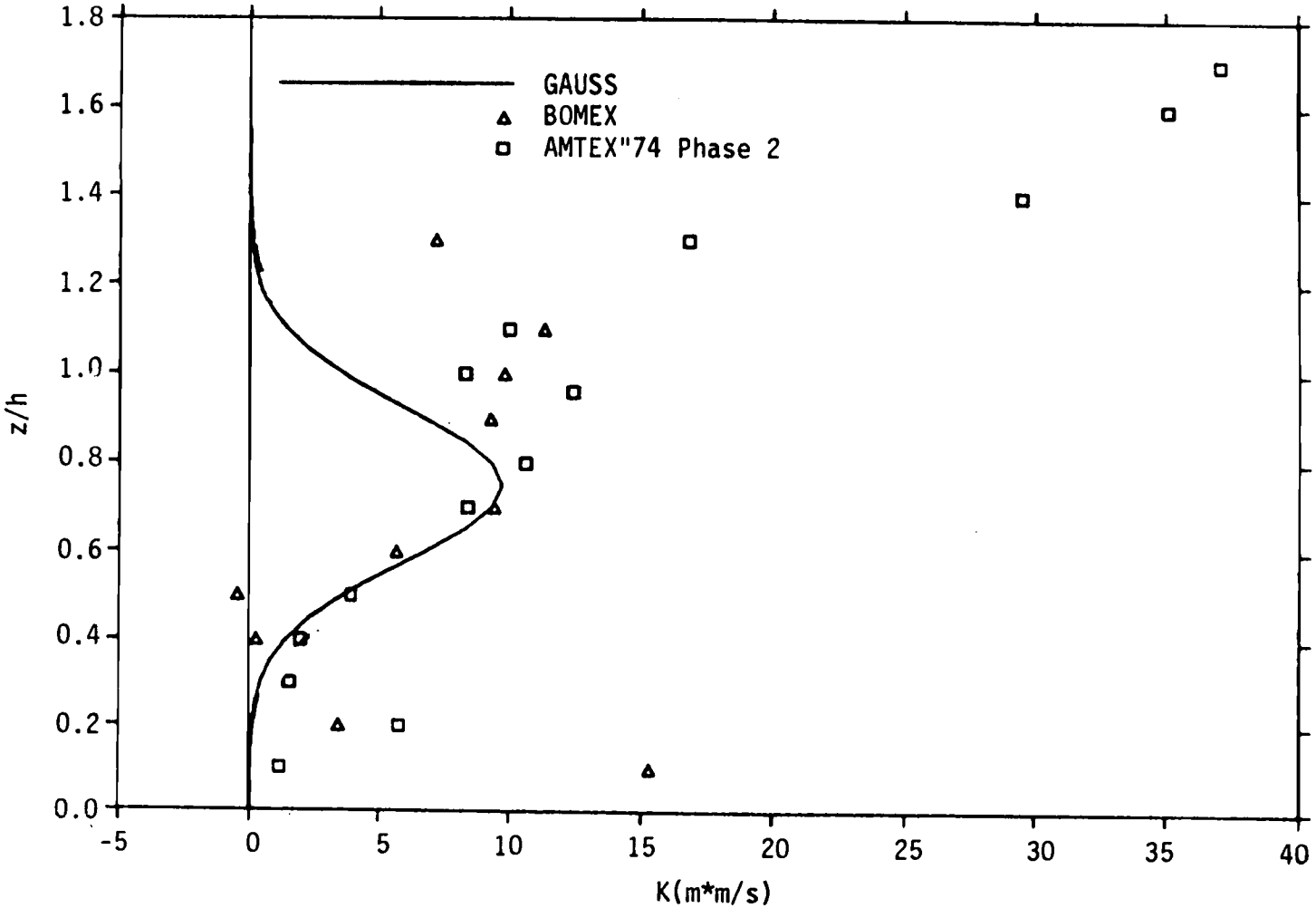

Figure 3.4. Examples of the best fit K profile calculated from observation data (a) For the BOMEX, AMTEX74. (b) For the AMTEX75.

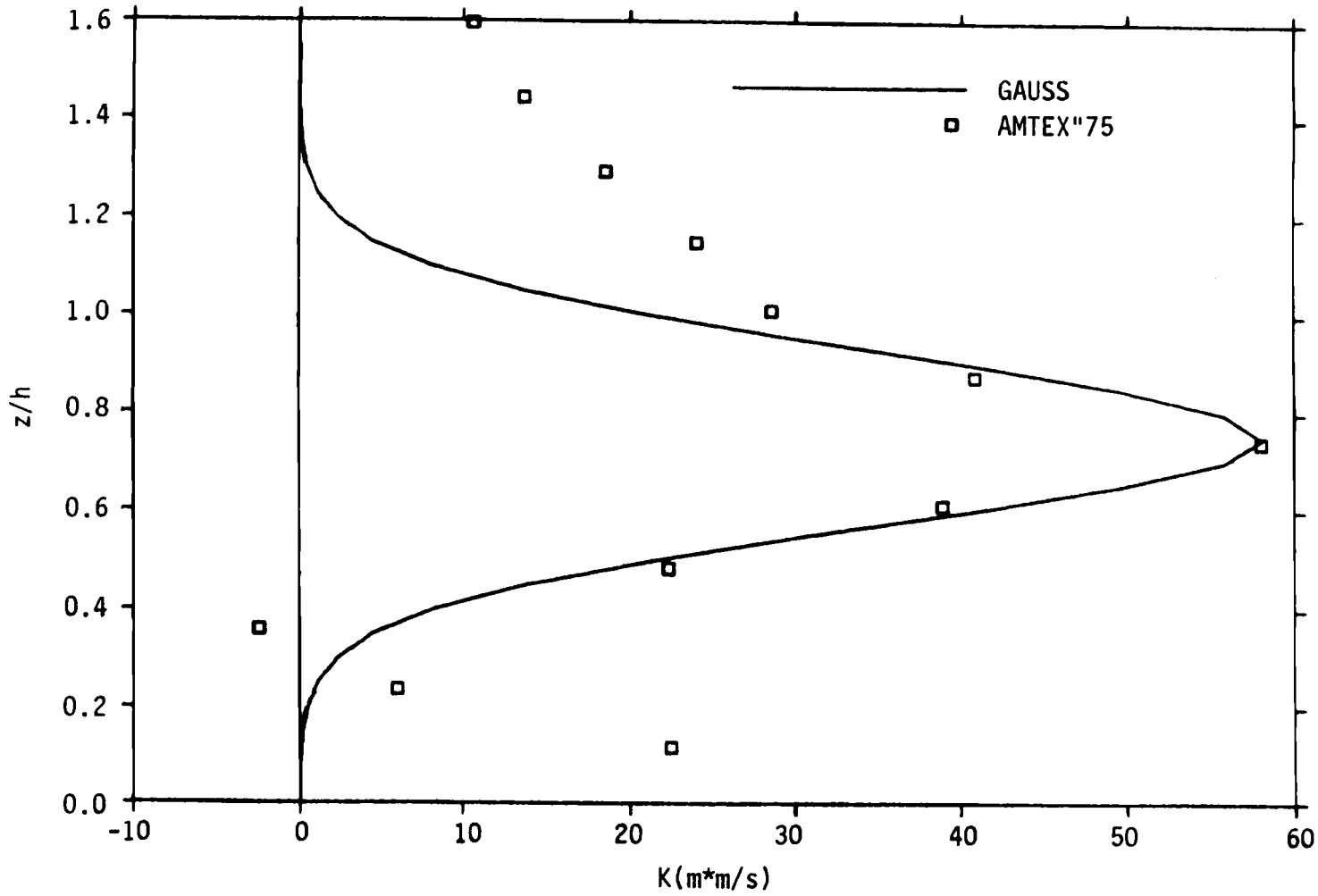

Figure 3.4. (Continued)

the boundary layer height (h) is about 0.3 and that K_c approximately vanishes above z/h = 1.2, we thus parameterize the profile of cloud diffusivity as

$$K_c = K_{max} \exp[-(ZH - Center)^2/\delta^2], \quad 0.3 \leq ZH \leq 1.2 \qquad (3.11)$$

where

$$\delta^2 = (1.0 - Center)^2 ,$$

$$Center = Z_{max}/h,$$

K_{max} is the peak value, ZH is z/h, Z_{max} is the height where the maximum value took place, and Center is about 0.75 for the data we used here.

There are several parameters (stability, Richardson Number, humidity, etc.) that have been tested to predict the magnitude of the variable K_{max}, but only the cloud cover is significantly related to K_{max}. The relationship between them can be fitted by a least-square linear equation (Fig. 3.5) as below:

$$K_{max} = A1 \cdot CC + A2, \text{ for } CC \geq 34\% , \qquad (3.12)$$

where A1 = 1.872, and A2 = -63.59. We further assume a linear relation for cloud cover less than 34% as follows:

$$K'_{max} = A3 \cdot CC . \qquad (3.13)$$

where A3 = 0.3555. Sensitivity experiments reveal that simulation results are insensitive to whether the K'_{max} term is included or not. It is probably because the term is usually quite small.

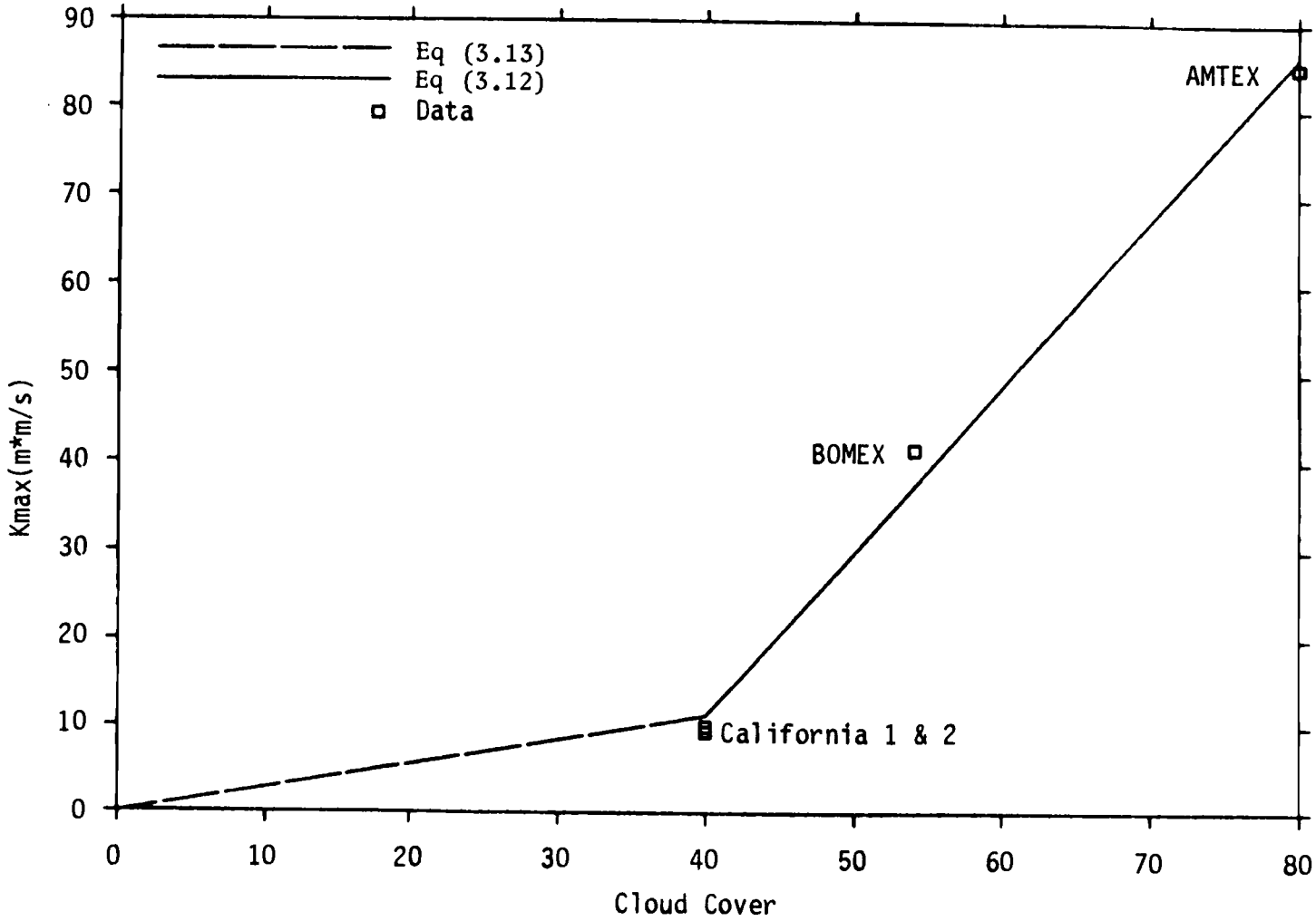

Figure 3.5. K_{max} vs. Cloud Cover plot of observation data and the least square fit lines.

In order to apply the shallow convection parameterization in real data situations it is necessary that the Eqs. (3.11) can represent a variety situations when K_{max} may exist at different levels within the boundary layer. Since we are only interested in the physical process within the boundary layer, we assume that cloud diffusivity vanished when ZH is greater than 1.2 or smaller than 0.3. The ratio between the LCL height and the boundary layer height is close to the 0.3 in all cases we examined and the cloud top is usually about the same height as the boundary layer. Thus, we can rewrite δ^2 as a function of the LCL height by assuming that the distance between Z_{max} and LCL versus the distance between the boundary top and LCL is a constant ratio. We then arrives at the equation:

$$\text{Center} = z_{max}/h = 9/14 + 5/14 \cdot Z_{lcl} \quad , \qquad (3.14)$$

where Z_{lcl} is height of the LCL.

There are no similar treatments to the heat and momentum fluxes partly because it is not clear at the present how the cloud redistributes heat and momentum. Observational evidences seem to indicate that the effect of shallow cumulus on heat and momentum budget is weak. We are therefore neglecting them for the time being. Preliminary results show that if heat and momentum are similarly treated as moisture, boundary layer will grow and the inversion will be wiped out within a very short time period. Further studies are necessary to examine the effect of the shallow cumulus in the heat and momentum budget.

3.3. The ECMWF PBL and Shallow Convection Parameterization Scheme

The European Centre for Medium Range Weather Forecast Planetary Boundary Layer (ECMWF PBL) parameterization scheme (Louis, 1979) does not have explicit treatment for unstable, stable or neutral boundary layer. It uses a Richardson number to determine each grid level's instability :

$$Ri = \frac{g \cdot dz \cdot d\theta}{\theta (dv)^2} \quad . \tag{3.15}$$

One then applies the following formula to compute the diffusion coefficient K_m and K_h

$$K_m = l^2 \left| dv/dz \right| F(Ri) \tag{3.16}$$

where

$$F(Ri) = \begin{cases} 1 - \dfrac{b \cdot Ri}{1 + c \left| Ri \right|^{1/2}} & , \text{ unstable } (Ri < 0) \\ \dfrac{1}{(1 + b' \cdot Ri)^2} & , \text{ stable and neutral } (Ri \geq 0), \end{cases}$$

$$l = \frac{k \cdot z}{1 + \dfrac{k \cdot z}{\lambda}}$$

and

$$c = C^* \frac{l^2 \cdot b \cdot \left[(z+dz)/z^{1/3} - 1 \right]^{3/2}}{z^{1/2} \cdot dz^{3/2}} \quad .$$

The parameter F(Ri) is a stability function, k is the Von Karman constant (0.4 in this study), l is the mixing length, λ is the asymptotic mixing length and is adjustable (currently being chosen as 100m), b = 9.4, b' = 4.7 and C* is 7.4 for momentum and 5.3 for heat and moisture.

The shallow convection scheme used in Teidtke (1983) is quite simple. A constant diffusivity coefficient (25 m^2 s^{-1}) is assumed throughout the entire cloud deck for momentum, heat and moisture. The cloud base is assumed to be the condensation level for surface air and the cloud top is the level of non-buoyancy, but not higher than 750mb. In the OSU PBL model the cloud top is determined where the relative humidity falls below 57% (Eq. 3.7).

4. RESULTS

4.1. Real Data Simulations With The OSU Scheme

In this section we will present the results of several 1-D model simulations of the undisturbed trade wind situations and compare the simulated atmospheric profiles with and without the proposed shallow cumulus parameterization scheme to study the impact of the new scheme. The maintenance of the trade wind inversion is generally thought to be due to a balance between the large-scale sinking motion of the subtropical high-pressure system and the turbulent mixing within the boundary layer. To simulate this balance, it was necessary to include the observed vertical motion in the simple 1-D model. Without large-scale advection, however, the model predicted temperature field near the surface will in time approach the temperature at the sea-surface. The virtual heat flux from the ocean and the boundary layer turbulence will both be reduced. These results will eventually lead to the collapse of the boundary layer. With this inherent limitation of the 1-D model, we will only present short-range (1-2 days) model simulations.

For a given initial profile of wind, temperature and moisture, we keep the model top level wind field and the entire vertical motion field fixed with time and allow boundary layer mixing to modify the rest of the parameters. Because the observed atmospheric profiles are usually stably stratified, the simulated

boundary layer will grow vertically as turbulent mixing starts. We will refer to the initial state as the time 0 state and the predicted state by the number of hours from the initial time. In addition to the temperature and dew-point profiles, we will also display the saturation point (SP) profile. When the SP profile is close to a straight line, as is often observed, the atmosphere is well-mixed. In the 1-D model, turbulent and shallow cumulus mixing are the only mechanisms that can modify the SP profile. We have found the SP profile to be a good tool to examine the effect of the parameterization schemes.

4.1.1. BOMEX

Figs. 4.1a,b and 4.2a,b show the model predicted atmospheric profiles using BOMEX June 22 to June 26 average sounding as initial state after 1 hour and 12 hours runs with and without the shallow convection. By comparing these figures we find that, after 12 hours, both cases maintain a well defined inversion at the top of the boundary layer. This is due to the sinking motion warming the top of the inversion and the cooling of the upper part of the boundary layer (discussion about the cooling will be given in section 4.2). Below the inversion, slight folding of the SP profile (Figs. 4.1a and 4.2a) indicates that the turbulent mixing in the boundary layer has modified the atmosphere within the boundary layer in less than one hour. The nearly linear character of the SP profile also suggest that the boundary layer is well-

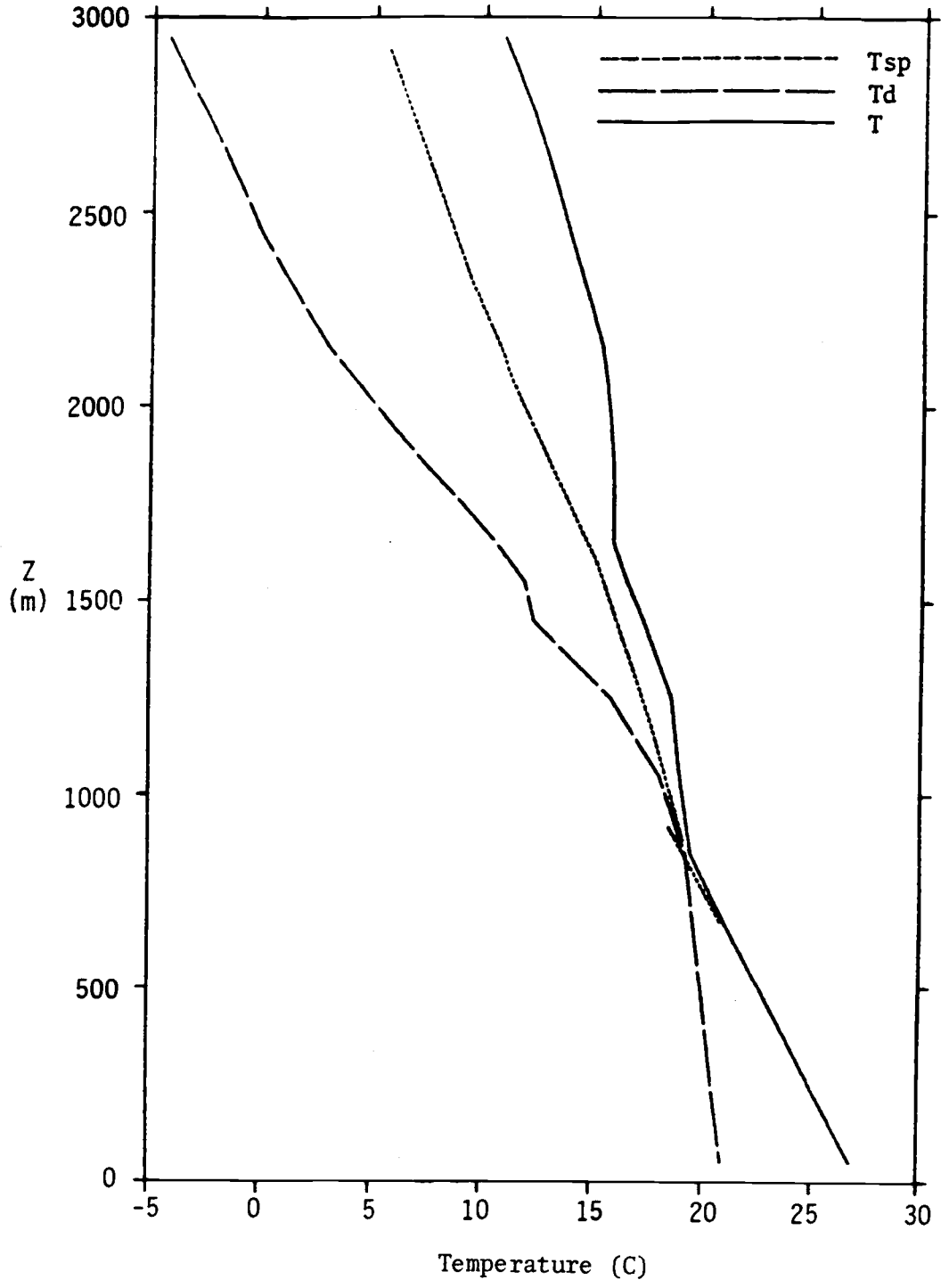

Figure 4.1. Temperature, dew point and saturation point profiles for the BOMEX case with the OSU shallow convection scheme (a) at hour 1, and (b) at hour 12.

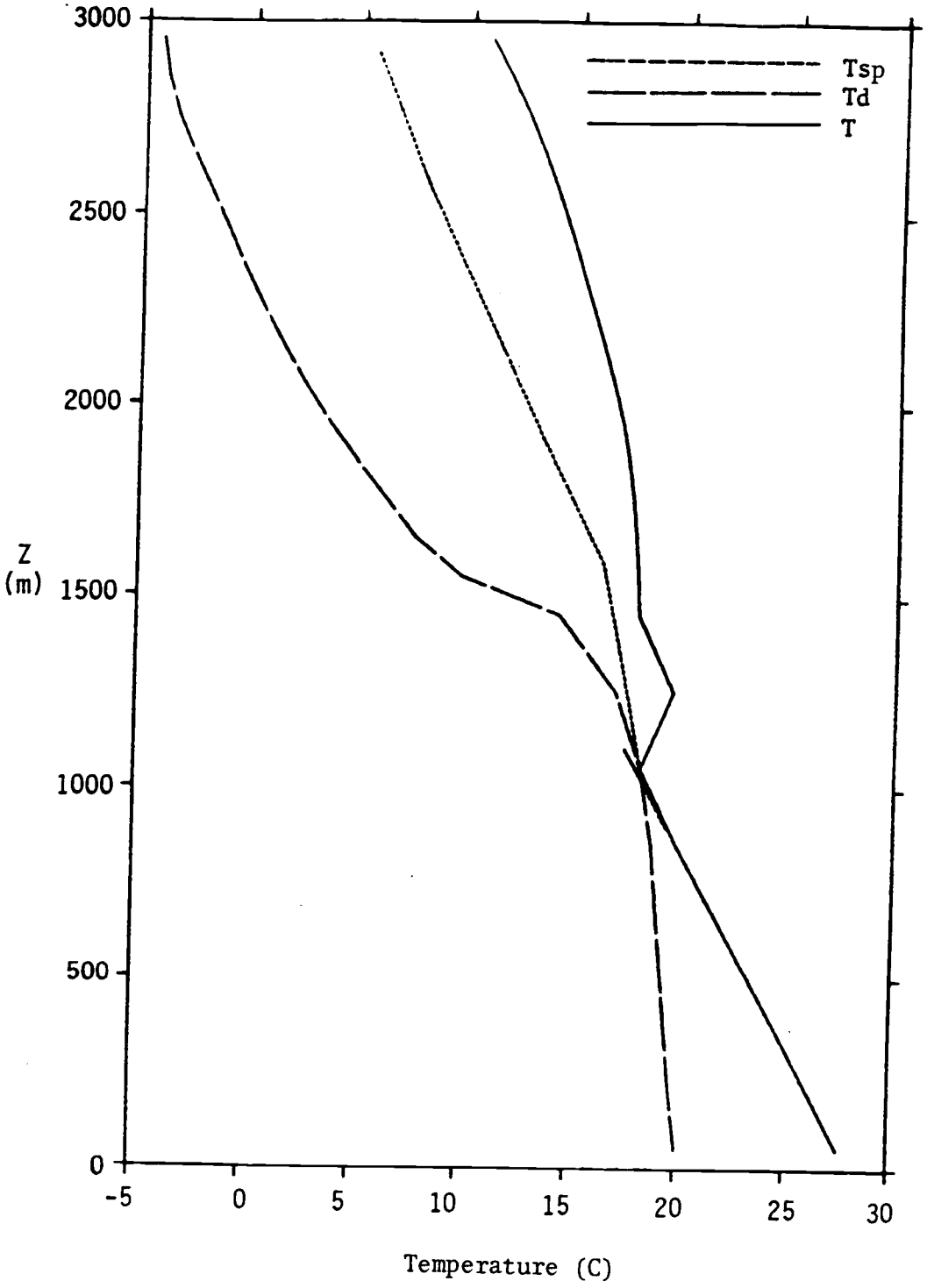

Figure 4.1. (Continued)

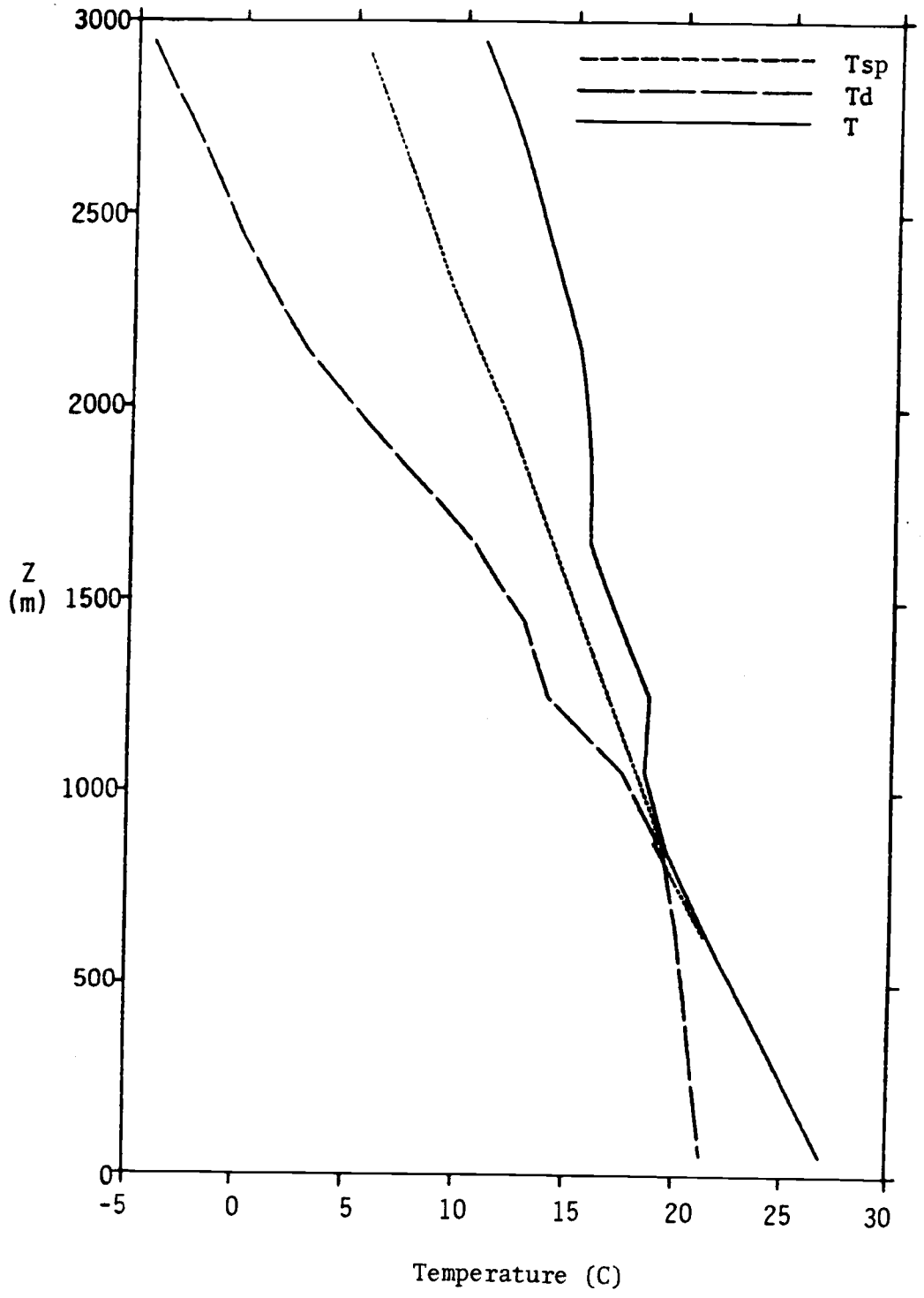

Figure 4.2. Temperature, dew point and saturation point profiles for the BOMEX case without the OSU shallow convection scheme (a) at hour 1, and (b) at hour 12.

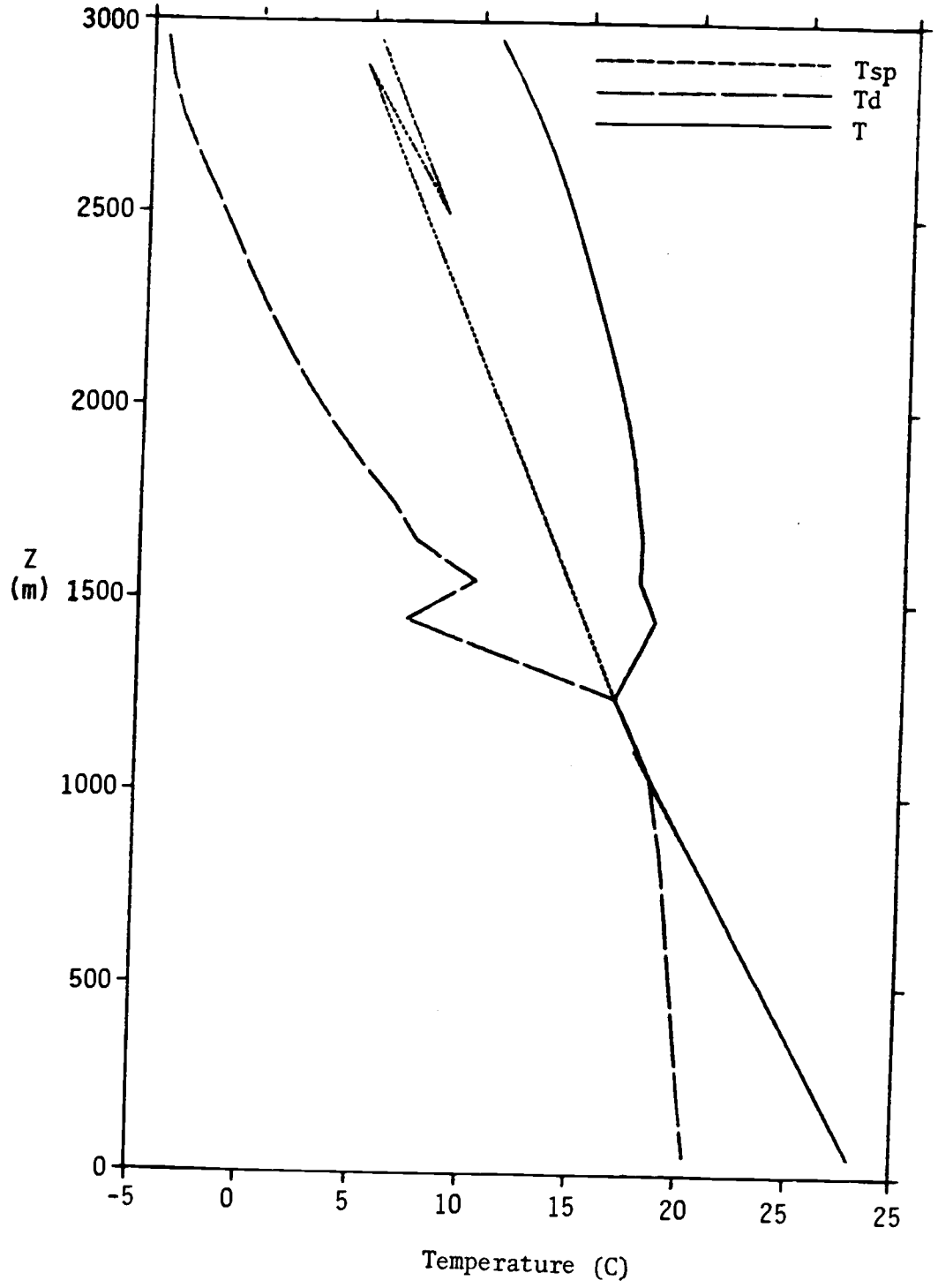

Figure 4.2. (Continued)

mixed. The temperature profiles in both Figs. 4.1a and 4.2a are very close to the dry-adiabatic, constant potential temperature lapse-rate. The dew-point profiles fall closely on a constant mixing-ratio line. The boundary layer coefficient of diffusivity formulation slightly over-estimates the mixing near the top of the boundary layer and results in a mixing ratio profile that increases slightly with height above 500m. Above the boundary layer, the large scale sinking motion is adiabatic and does not alter the SP character so that the environmental SP profiles are maintained. The effect of the shallow cumulus parameterization is quite small at this time. When shallow cumulus is parameterized, the enhanced diffusion will transport more moisture into the upper boundary layer and, in fact, will transport some moisture above the inversion. This is designed to simulate the penetrating tops of some of the cumulus that can exist above the inversion.

At hour 12, the effect of the shallow cumulus parameterization in more evident. Above 1.5 Km, the model structures are identical as they should be. Boundary layer is significantly deeper for the case without shallow cumulus (1.3 Km) than with cumulus (1.0 Km). This is because the cloud moisture diffusivity above the boundary layer top (h) mixes the dry stable air into the boundary layer and creates a deeper transition layer below the inversion top. Between the inversion base and 1.5 Km, the model with shallow cumulus (Fig. 4.1b) is moistened while the model without shallow cumulus (Fig. 4.2b) actually dries out because of imperfect vertical advection (an upstream scheme is applied and the constant sinking motion

has a maximum below 1.5 Km). The boundary layer in the 1.0 - 1.3 Km interval is saturated for the run without shallow cumulus (Fig. 4.2b). This result demonstrates that the parameterized boundary layer mixing alone is capable of transporting significant amounts of moisture into the upper boundary layer. This also can be seen from the model diagnostic Q2 profiles shown in Figs. 4.3a,b where the moisture flux convergence near the top of the boundary layer is greater in the case without shallow convection than with shallow convection beyond one hour. This is because the later one mixes the dryer air down from above the top of the boundary layer as well as transports moisture out of the boundary layer, this can prevent moisture from accumulating in the upper boundary layer. For this run the predicted cloud cover for both cases is reasonable (the averaged amount is about 50% compare to 45% for the observation).

4.1.2. GATE

Model results (Fig. 4.4) show that, after 12 hours of boundary layer turbulent mixing, the LCL moves down closer to the inversion base but is still above the top of the boundary layer. Our cloud cover prediction formula can not be applied in this case. The simulation results will be identical for both with and without the shallow convection scheme so that only one is shown. In the actual observation the GATE undisturbed period is nearly neutral, it has been suggested that the cloud formation was due to the local fluctuations of LCL. Furthermore, the GATE date in the lower

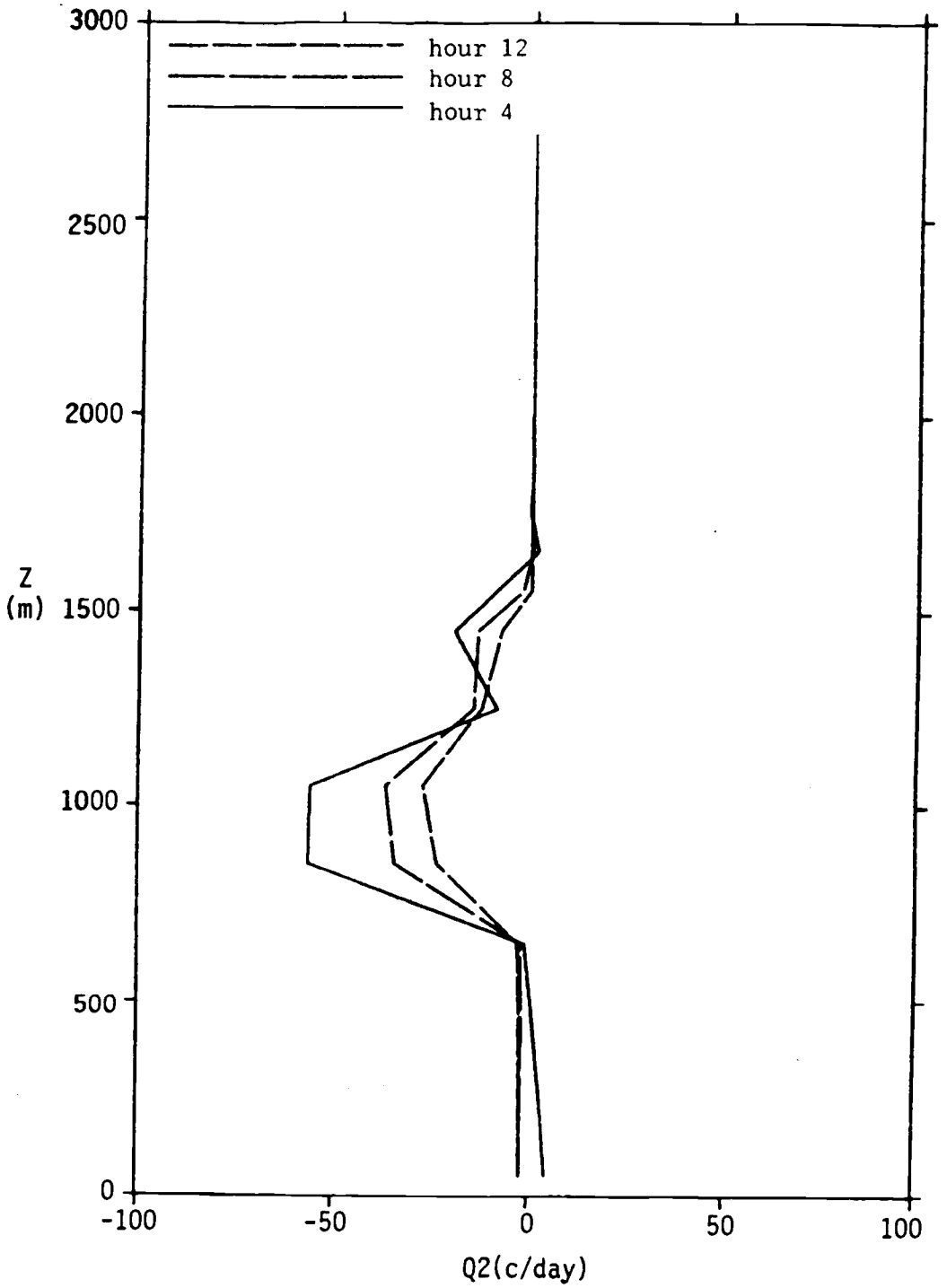

Figure 4.3. Model diagnostic Q2 profiles for the BOMEX case at hours 4, 8, 12 (a) with the OSU shallow convection scheme, and (b) without the OSU shallow convection scheme.

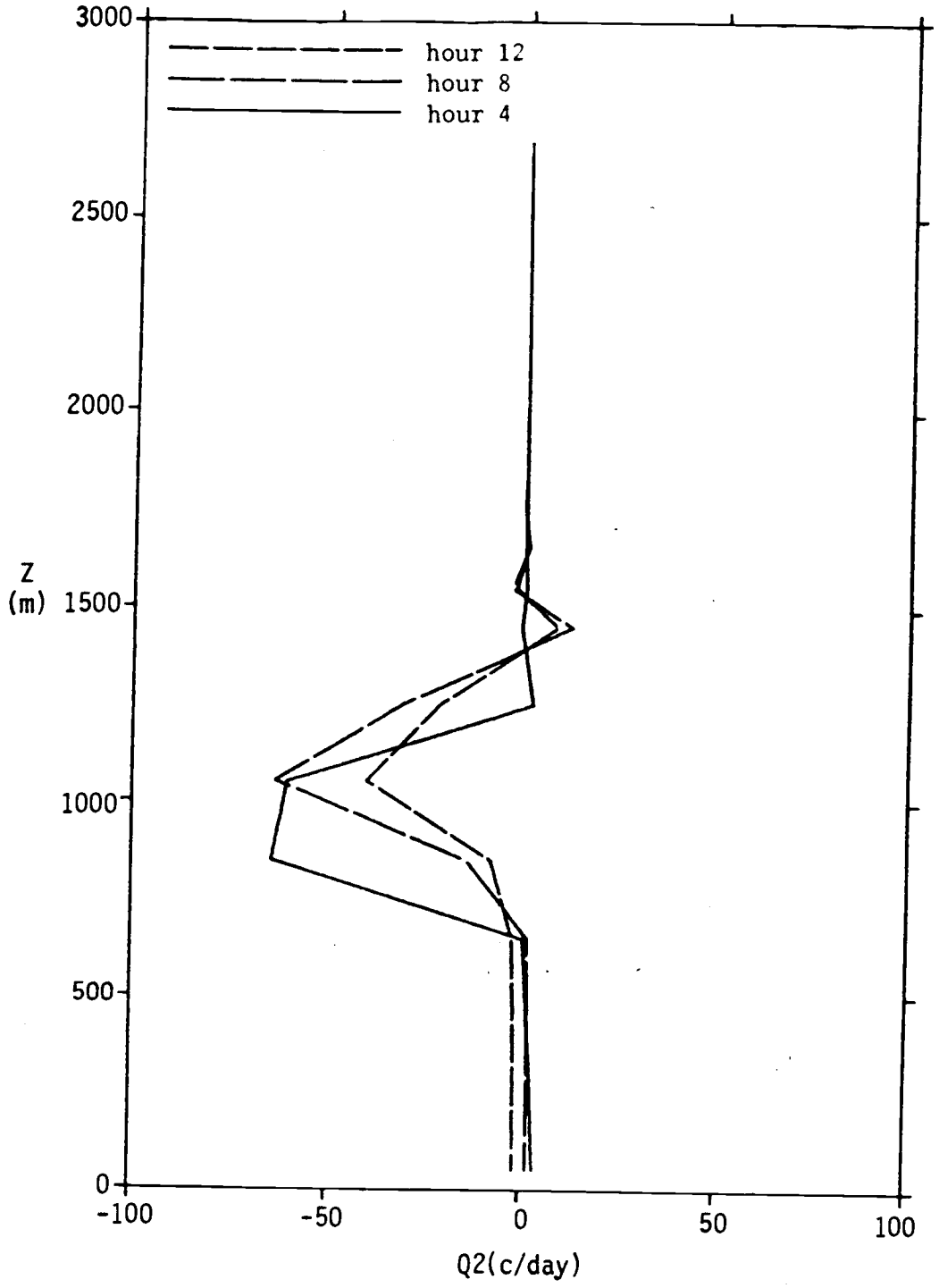

Figure 4.3. (Continued)

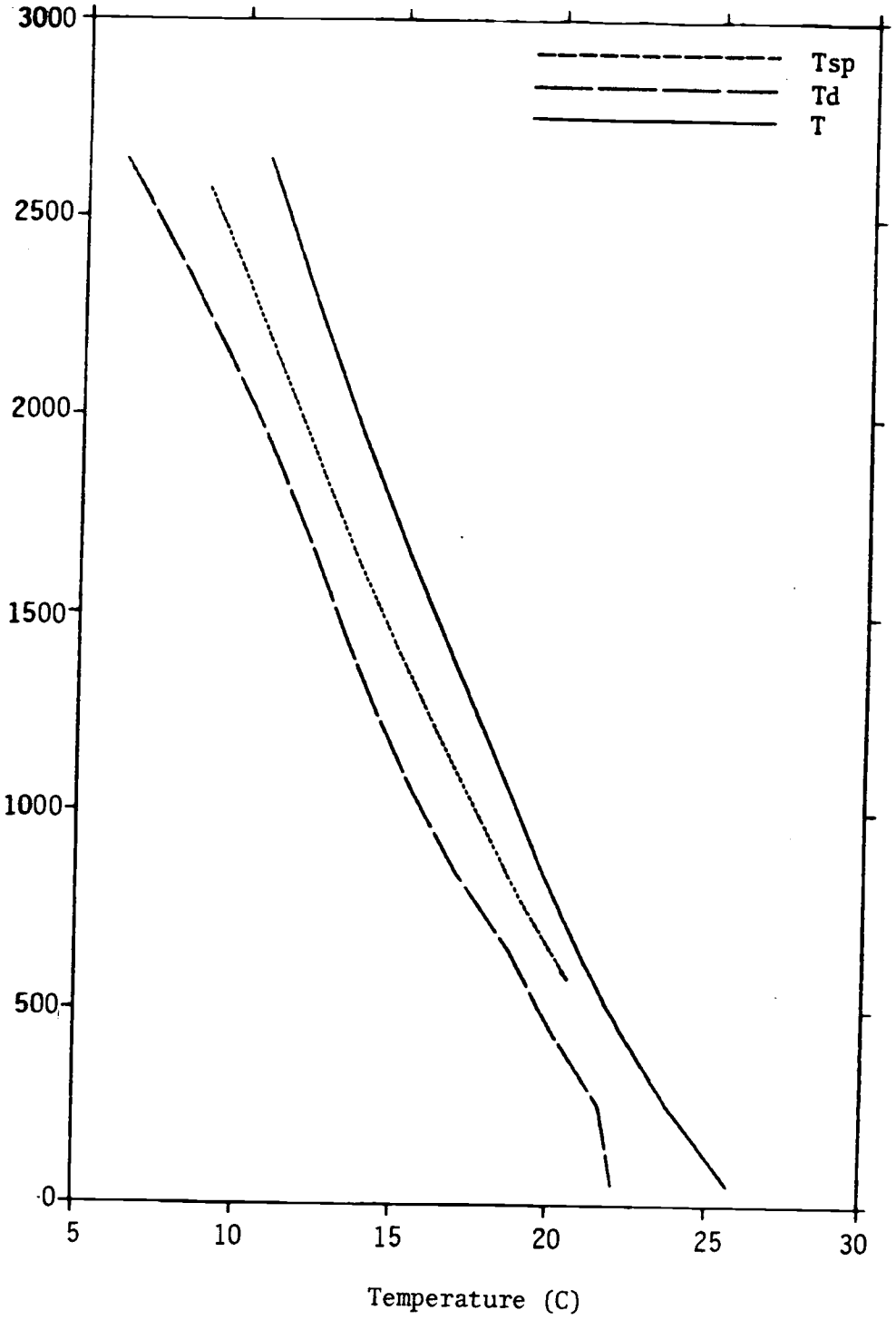

Figure 4.4. Temperature, dew point and saturation point profiles for the GATE case (a) at hour 1, and (b) at hour 12.

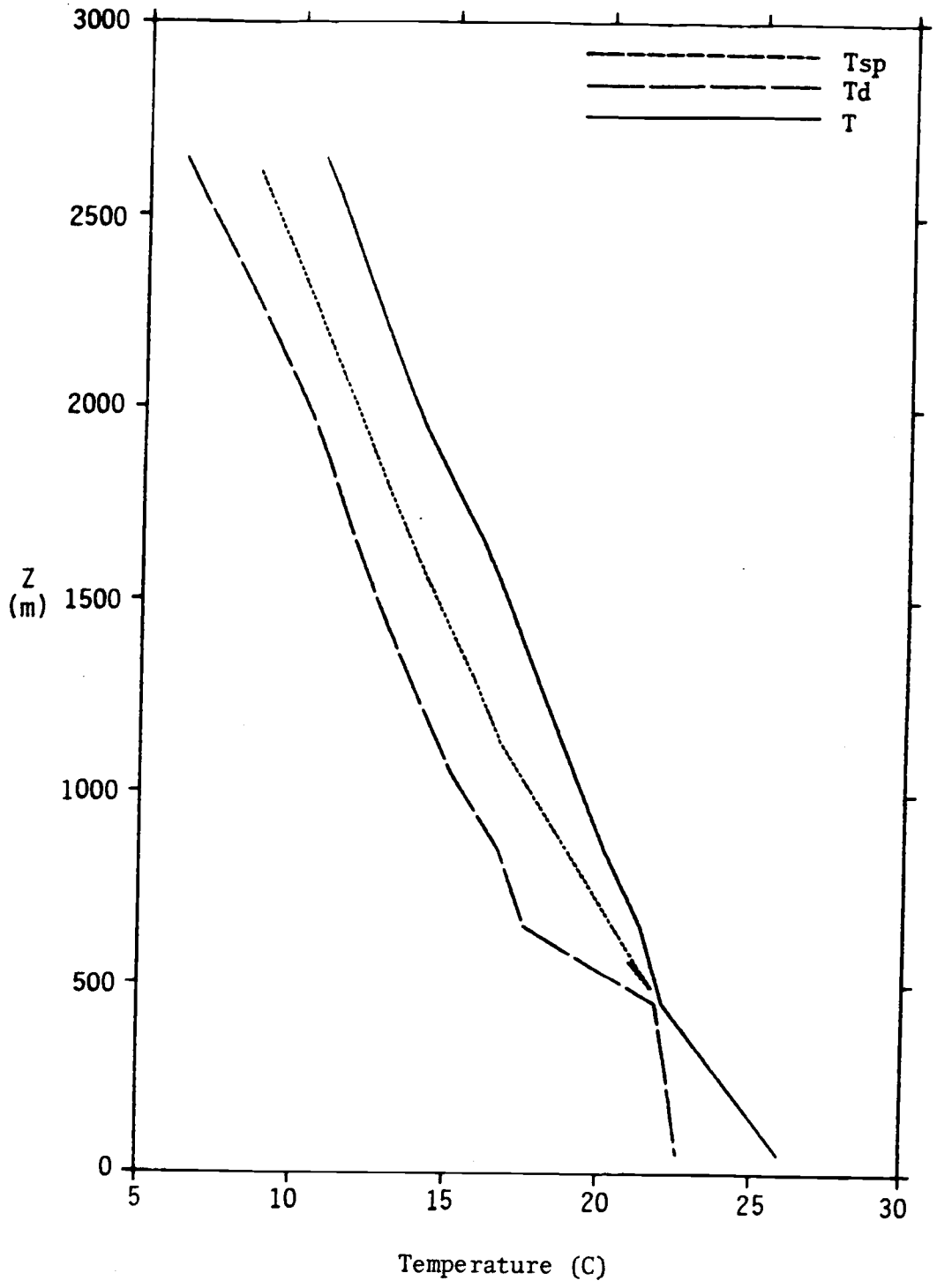

Figure 4.4. (Continued)

troposphere are known to have large error margin (Esbensen, 1986, personal communication). Calculation of the diffusivity profiles from data (Fig. 4.5) shows that moisture flux contribution from the cloud to the total moisture flux is small, as we suggested before that the cloud amount may be an important factor. Even without the shallow convection we still obtain good agreement with the observation (a steady state boundary layer structure is maintained for 12 hours after 8 hours). Due to the weak turbulent mixing there is not much moisture pumped up to the upper boundary layer. The Q2 profile (Fig. 4.6) shows that the maximum moisture flux convergence is just above the surface (i.e. moisture starts to accumulated in the lower boundary layer which gives a large positive correction of the surface virtual temperature). As a result the surface virtual heat flux becomes slightly larger than zero even though the surface sensible heat flux is negative. Observational study by Nicholls and LeMone (1980) also shows the dominant role of water vapor in maintaining positive buoyancy in the GATE area which kept this nearly neutral situation slightly unstable.

Unlike the others cases we studied, the boundary layer does not become saturated after 12 hours even though the boundary layer is quite well-mixed (Fig. 4.4b).

4.1.3. AMTEX

Even during the undisturbed period, the boundary layer is deep and well-mixed in the observation and in the model structure

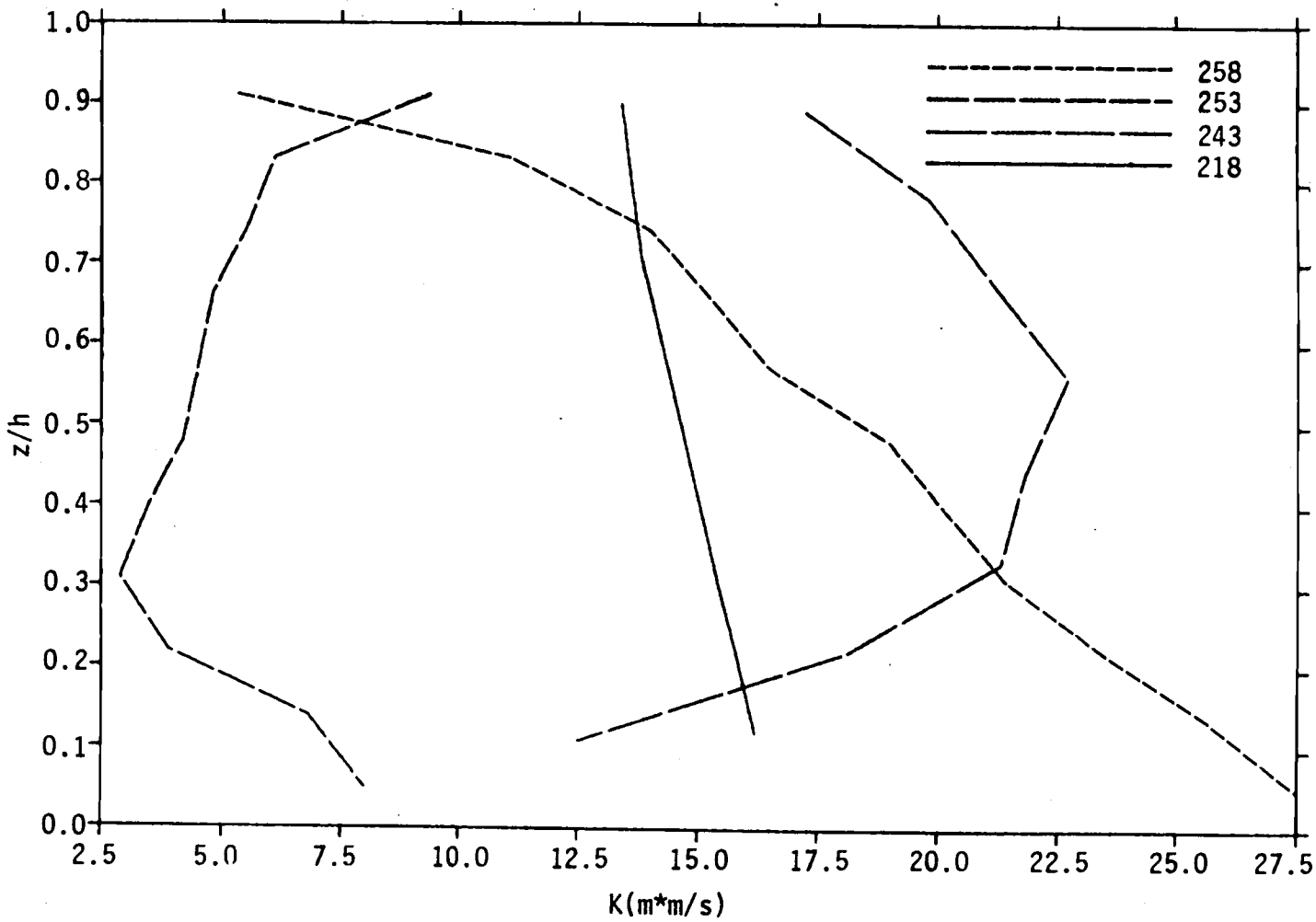

Figure 4.5. Diffusivity profile ($K_c + K_h$) for the GATE cases.

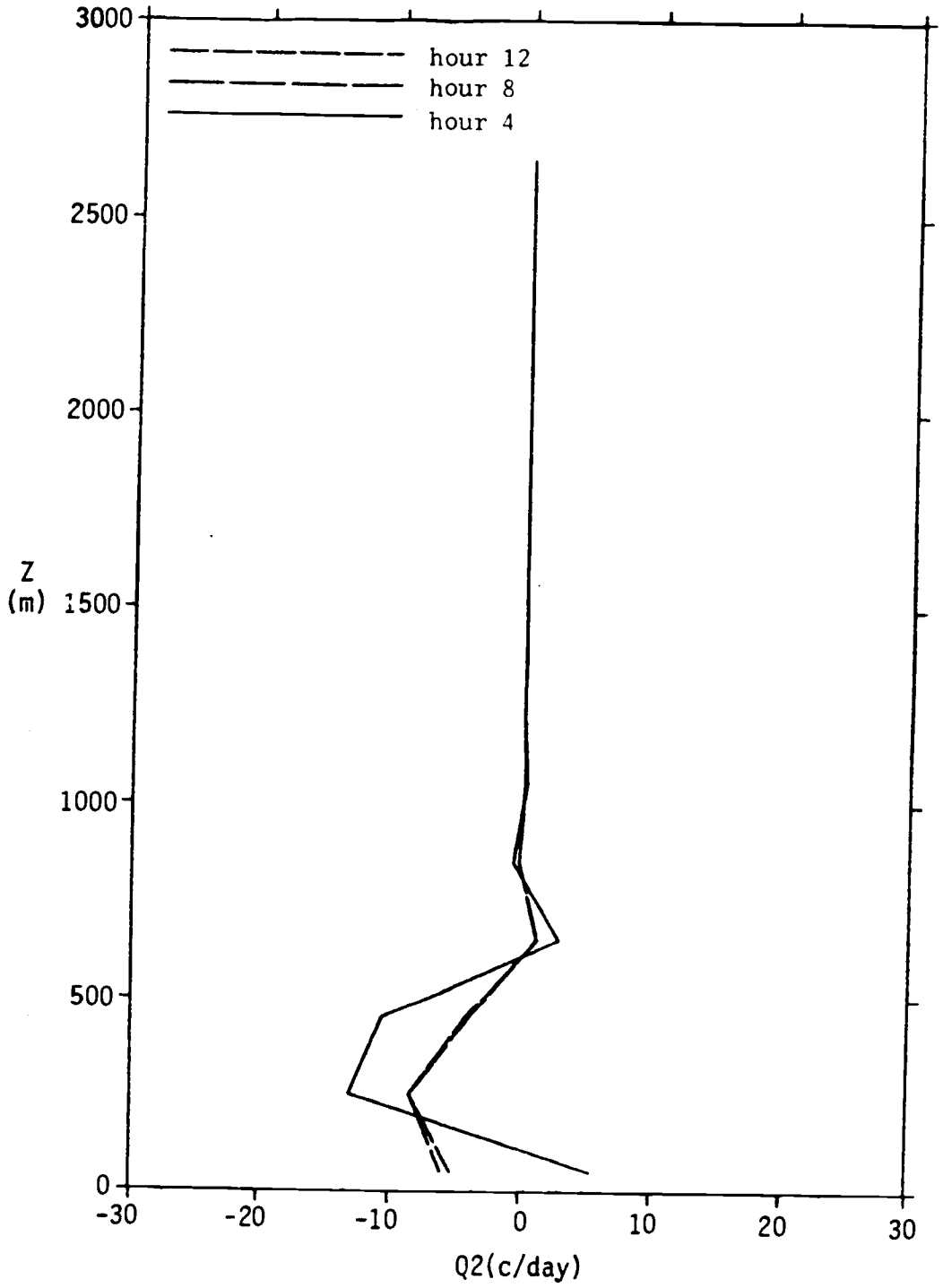

Figure 4.6. Model diagnostic Q2 profiles for the GATE case at hours 4, 8, 12 with the OSU shallow convection scheme.

(Figs. 4.7, 4.8) indicating vigorous turbulent activity. The only difference between the simulation with and without the shallow convection is in the model structure above the boundary layer. There is little difference between them within the boundary layer. The inversion layer is not wiped out by such strong turbulent mixing and an approximated steady state boundary layer can be maintained for more than 10 hours after hour 12.

The Q2 profile (Fig. 4.9a,b) for the case with the shallow convection has a second peak above the boundary layer which is not realistic. However, comparing these two figures we can see the effect of cloud diffusivity mixing the moisture up and dry air down such that the value of the Q2 peak at hour 12 shows a smaller moisture flux convergence (Fig. 4.9a) similar to the BOMEX simulation.

4.2. Comparison With Observation

Judging by the moisture flux profiles deduced from the observed Q2 profiles, shallow convection indeed has certain influence on the environment. In the 1-D model, we also notice differences in the SP profiles when shallow cumulus is parameterized indicating changes in the environment. The model results further demonstrated that the often observed minimum in the Q2 profiles (Fig. 4.10) near the base of the inversion is due to the convergence of boundary layer turbulent flux as well as due to shallow convection. In cases when the cloud amount is small, boundary layer turbulent mixing can explain all or most of the

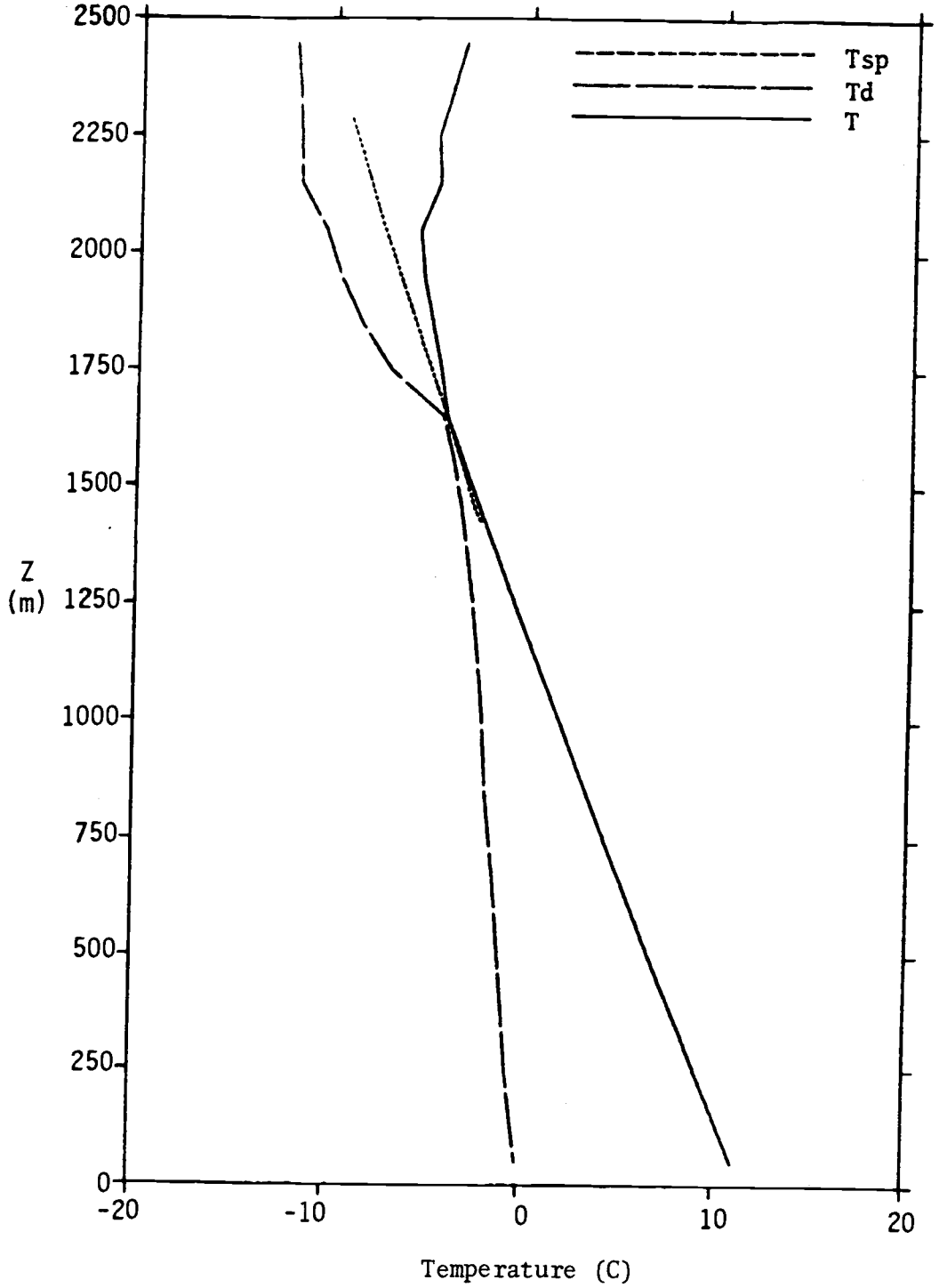

Figure 4.7. Temperature, dew point and saturation point profiles for the AMTEX case with the OSU shallow convection scheme (a) at hour 1, and (b) at hour 12.

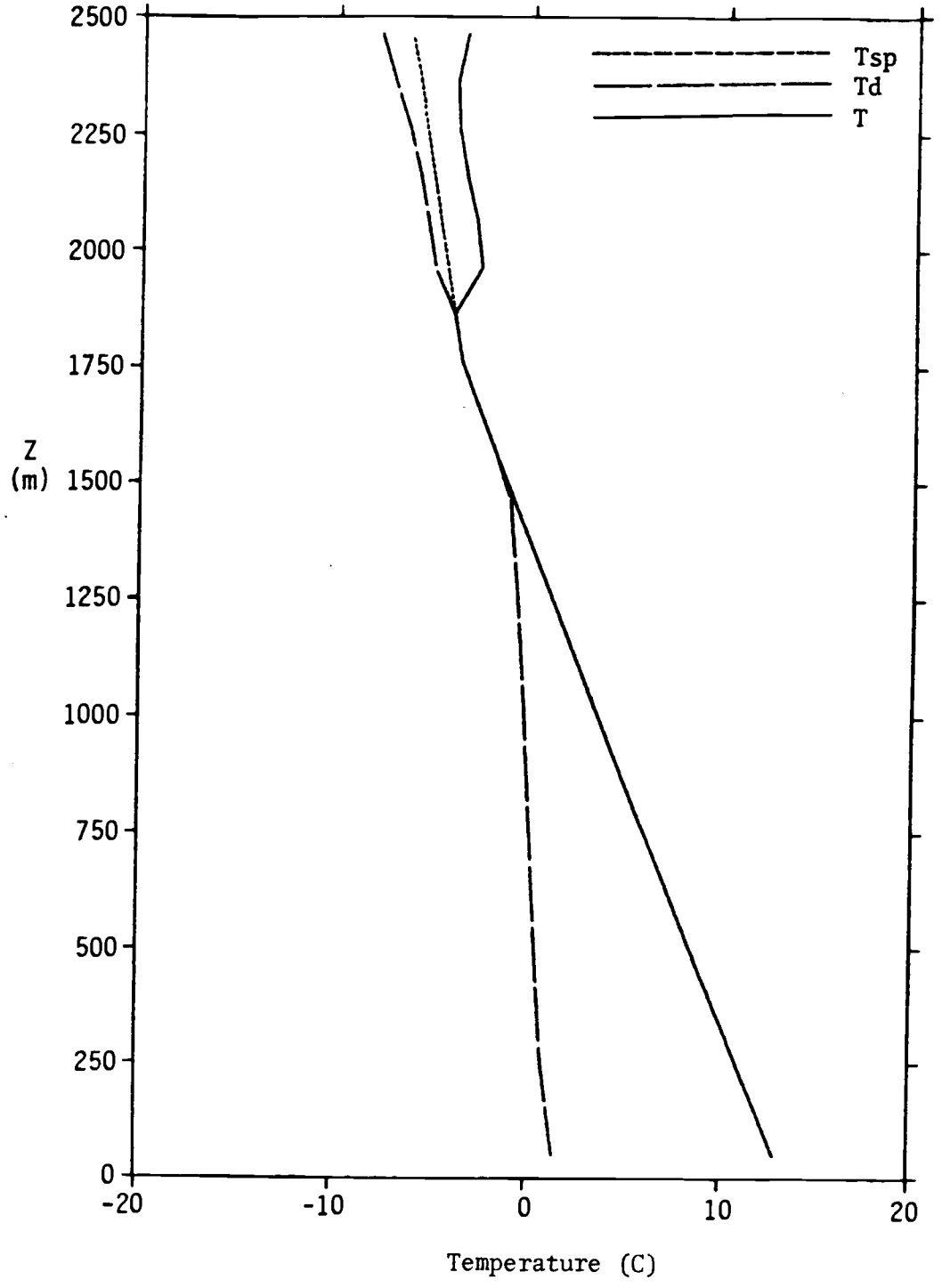

Figure 4.7. (Continued)

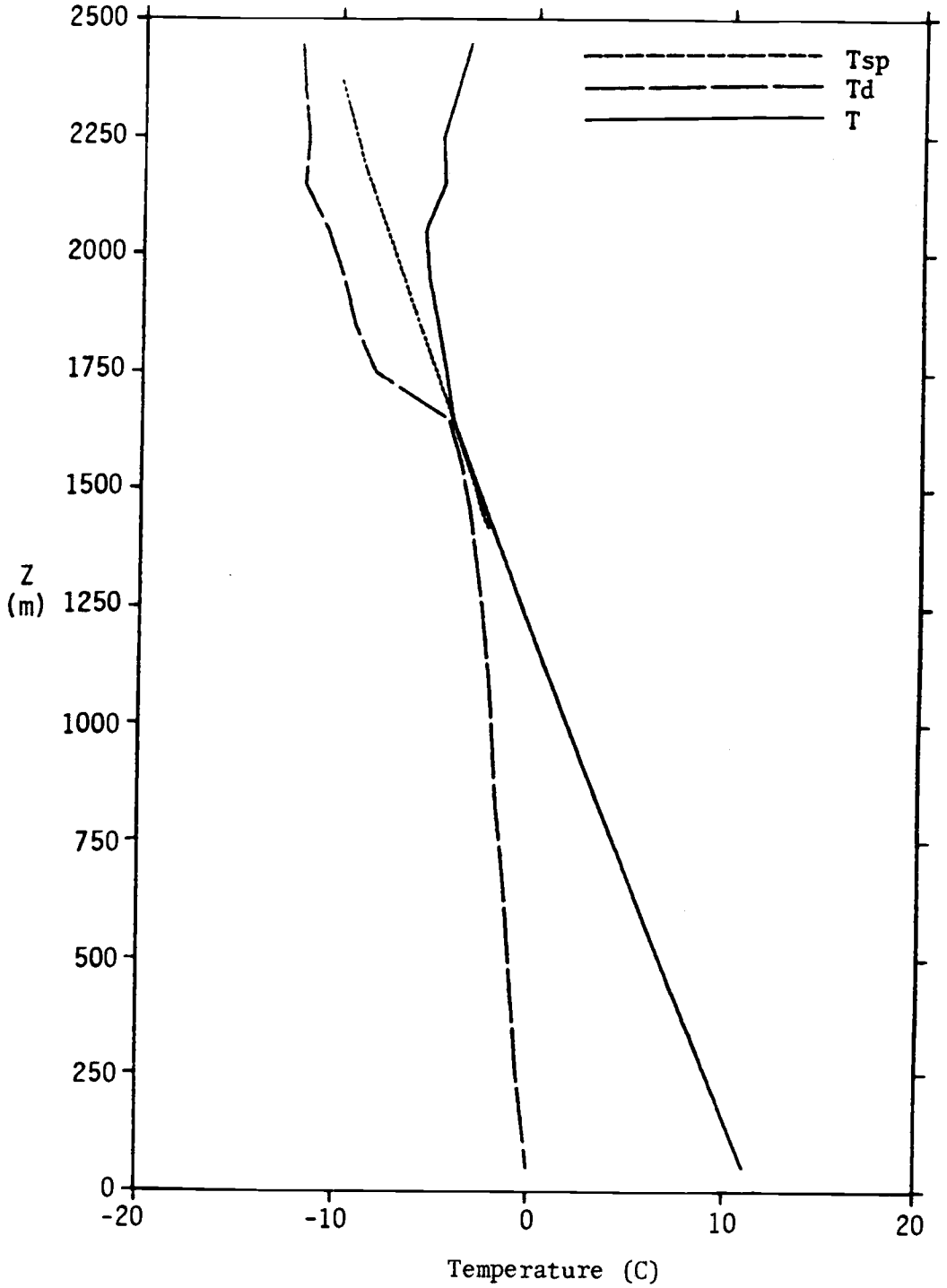

Figure 4.8. Temperature, dew point and saturation point profiles for the AMTEX case without the OSU shallow convection scheme (a) at hour 1, and (b) at hour 12.

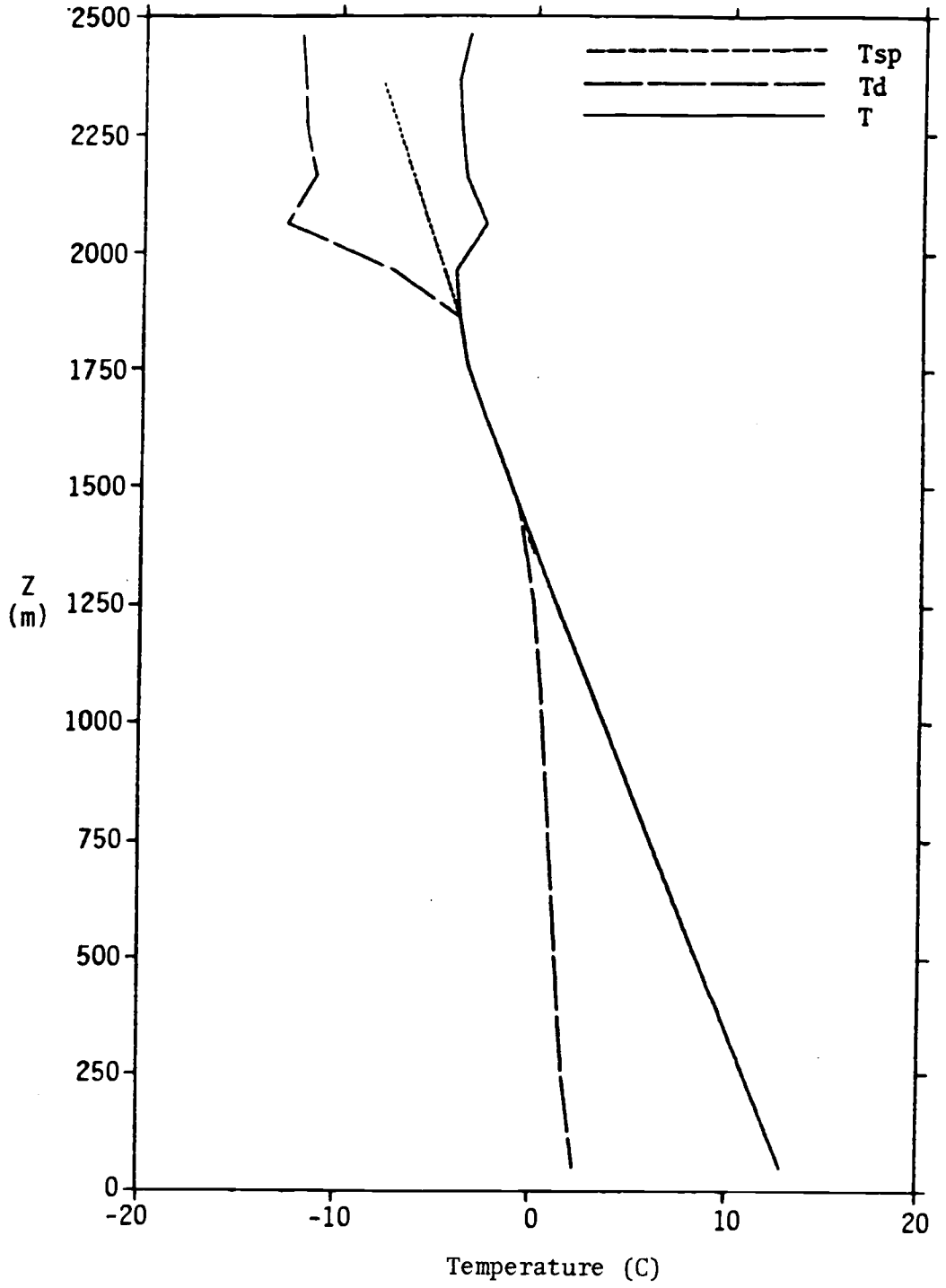

Figure 4.8. (Continued)

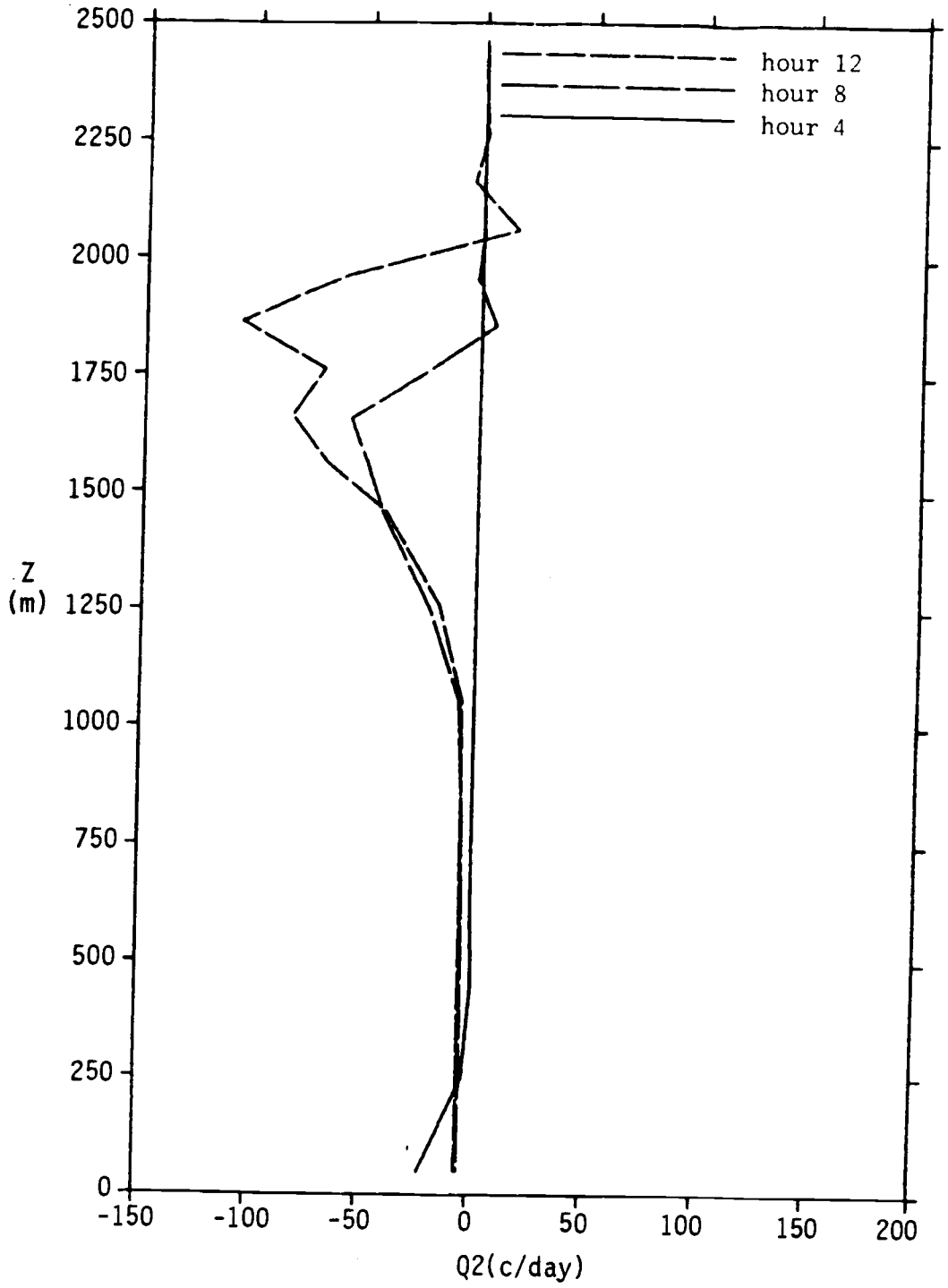

Figure 4.9. Model diagnostic Q2 profiles for the AMTEX case at hour 4, 8, 12 (a) with the OSU shallow convection scheme, and (b) without the OSU shallow convection scheme.

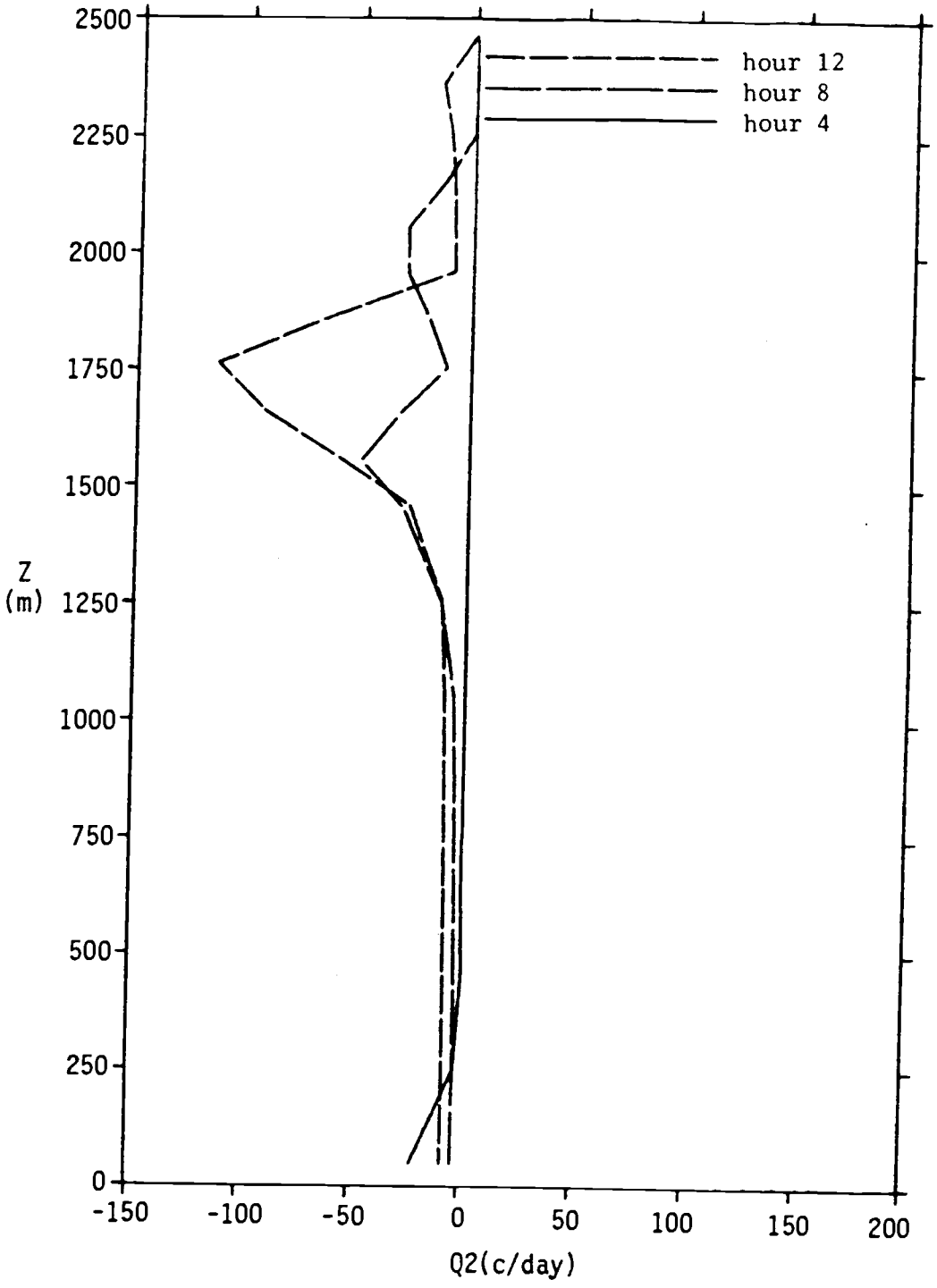

Figure 4.9. (Continued)

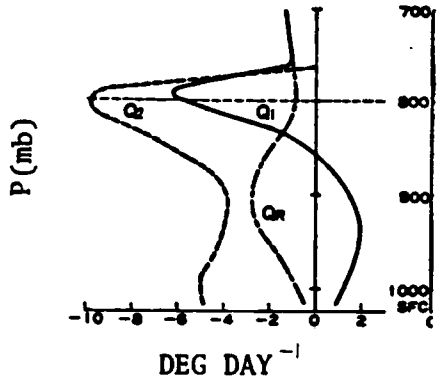

Figure 4.10a. Vertical profiles of large-scale apparent heat source Q1, apparent moisture sink Q2, radiation heating QR for AMTEX durning 14-16, Feb., 1974. Thin dashed line denote the inversion base.

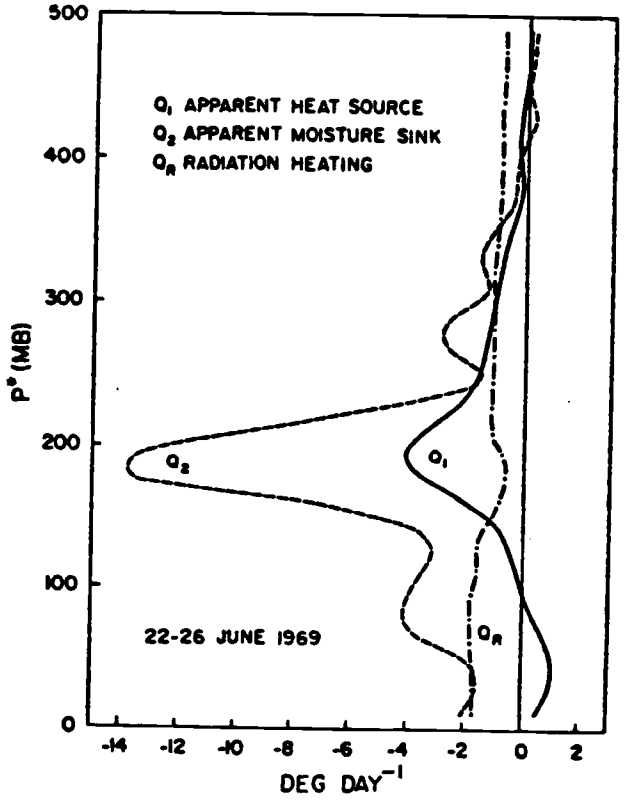

Figure 4.10b. Vertical profiles of apparent heat source Q1, apparent moisture sink Q2, and radiarion heating for the BOMEX undisturbed period.

observed Q2 profile. When shallow cumulus is included in the 1-D model, the predicted minimum in Q2 is nearly twice the observed minimum in magnitude (Fig 4.9a). This result can be explained by the fact that the model predicted moisture profiles become saturated after a few hours. As the moisture gradient across the inversion increases, the parameterized turbulent moisture flux also increases. In a recent effort to include the OSU boundary layer model in a global spectral primitive-equation model (to be reported elsewhere), the boundary layer structure over the ocean is closely monitored and is rarely found to be saturated. It is obvious that mechanisms such as horizontal advection, convective heating and large-scale precipitation are also important in determining the boundary layer moisture profiles.

In Table 4.1 we list the surface latent heat flux and virtual heat flux at hour 12 from the model calculation for the three data sets (unit is in W m^{-2}).

Table 4.1. Summary of the surface latent heat and virtual heat flux simulated with the OSU scheme. (note: * represents without the shallow convection.)

	Virtual heat flux (W m^{-2})	Latent heat flux (W m^{-2})
BOMEX	13 (9)*	194 (188)*
AMTEX	155 (153)*	675 (648)*
GATE	3*	55*

Comparing the model results and the observation (Table 2.1), we found that in general the model generates higher latent heat flux and lower sensible heat flux. This is because saturated sounding results in an over estimation of the cloud cover and enhancement of the cloud diffusivity as well as the surface moisture flux. The virtual heat flux is slightly under estimated. Because the potential temperature increases with height, enhancing the heat transport due to shallow cumulus would lead to a warmer temperature in the lower boundary layer. This would further reduce the sensible heat transport lending further support for not parameterizing the heat transport. The increase in the virtual heat flux with shallow cumulus (Table 4.1) is due to an increase in the turbulent moisture transport which results in a slightly drier lower boundary layer and a higher evaporation rate from the ocean.

In the AMTEX simulation both fluxes are overestimated at hour 12 and in the GATE case both fluxes are underestimated. However, as discussed in the previous section, for the AMTEX data set, the model takes 12 hours to adjust itself toward a steady state. After that the surface moisture flux became 302 W m^{-2} and sensible heat flux became 37 W m^{-2}. For the GATE data set, the model does not include the cumulus effect because the LCL is above the boundary layer.

For both the BOMEX and the GATE cases, the temperature field below the inversion initially decreases with time in both the model results and in the observations. This decrease has been attributed to the re-evaporation of liquid water detrained from the top of the

shallow cumulus. Diagonsis of the model output reveals that the cooling in the model forecast is due to strong turbulent mixing. We will examine this phenomenon using the excess temperature time series. The excess temperature is defined as

$$d\theta = TS + CGH(Z - Z2) - \theta(Z), \quad Z2 \leq Z \leq h \qquad (4.1)$$

where $d\theta$ is the excess temperature, $\theta(Z)$ is the potential temperature at Z, Z2 is the first model level, CGH is the counter-gradient [Eq. (3.6)], and TS is the surface temperature. For an unstable boundary layer, $d\theta$ is positive near the surface due to sensible heat transport. Turbulent mixing will attempt to reduce the excess. Near the top of the boundary layer, $d\theta$ usually becomes negative because of an increase in stability away from the surface. The large eddy turbulent mixing that is simulated in this model will actually mix colder air up and warmer air down (in the sense of the potential temperature). This can be seen in Fig. 4.11 where the excess temperature profiles for several forecast times are displayed. Over the first four hours, the boundary layer is unstable and strong mixing is seen to cool the upper boundary layer. When the surface air temperature eventually approaches the sea surface temperature, turbulence becomes weak and the upper boundary layer actually warms up slightly because of the imposed large-scale sinking motion (Fig. 4.1).

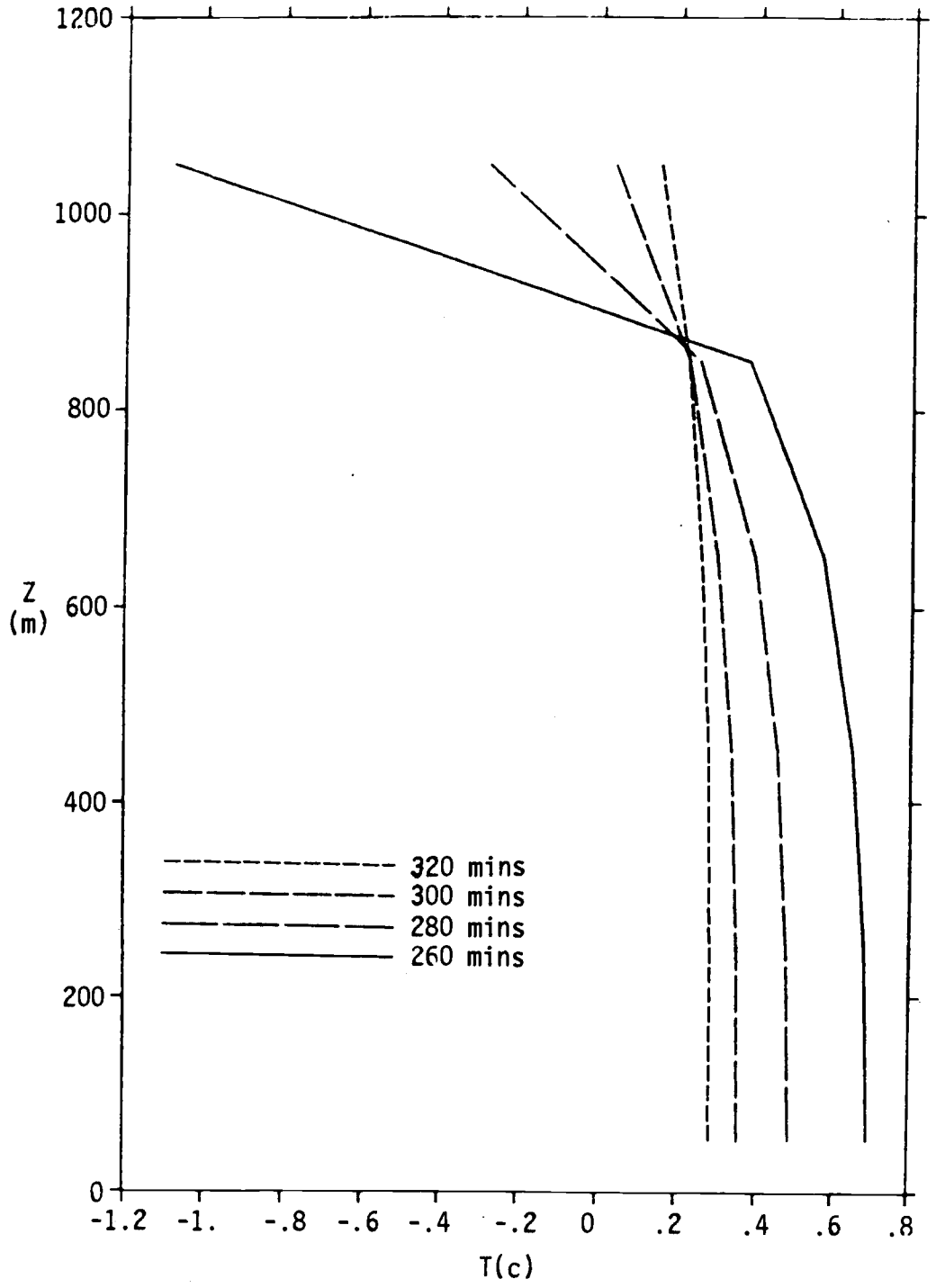

Figure 4.11. Predicted excess temperature profiles from the BOMEX case at several time steps.

4.3. Comparison With The ECMWF Scheme

Here we would like to compare the boundary layer parameterization scheme and the shallow convection scheme with the ECMWF schemes. Unlike our boundary layer parameterization scheme, the Louis formula used in the ECMWF model depends only on the Richardson number [Eq. (3.15)]. It is not necessary for the diffusivity coefficients K_m or K_h [Eq. (3.16)] to go to zero near h (top of the boundary layer), although the normal stability of the atmosphere is such that the K_m and K_h become very small above the boundary layer.

A recent ECMWF report (Louis, et al. 1981) shows two modifications of the Louis formula in order to increase the boundary layer turbulent mixing because, in day to day diagnostic of the global operational model, it became apparent that the model suffers from a lack of boundary layer mixing. The first modification includes a larger asymptotic mixing length of 300m to increase the K_m and K_h. The second modification not only slightly changes the formulation but also increases the asymptotic mixing length to 400m for heat and moisture. The modification is in response to artificial cooling of the stratospheric generated by the model and strong weakening of the jet stream in the model integrations. Essentially, the increased asymptotic mixing length for the heat and moisture will enhance the turbulent mixing processes and redistribute the heat and moisture into higher region. Furthermore, Tiedtke (1983) developed a simple shallow convection scheme

for ECMWF in response to deficiencies found in global integrations which is attributed to a lack of shallow convection.

In order to illustrate the difference between the OSU and the ECMWF boundary layer parameterization scheme, the coefficients of diffusivity using both models are presented in Fig. 4.12 (first modification of the Louis scheme is used for ECMWF). The initial state is the BOMEX case and the ECMWF scheme is used to predict for 24 hours. At hour 24 the coefficient of diffusivity based on our scheme is also calculated. It can be seen that the OSU parameterization scheme produces a profile of K_h that is about an order of magnitude greater than that from the ECMWF scheme. In addition, the K_h from the ECMWF scheme vanishes above .7h (the boundary layer height determination is based on Eq. (3.5)). This is a result of the chosen asymptotic mixing length that produces a maximum for K_h around 300m. Stronger mixing in the OSU scheme leads to warmer and drier surface air. This induces larger surface latent heat and sensible heat fluxes.

Here we implement both Louis's and Tiedtke's schemes in our boundary layer routine. Fig. 4.13-16 are the result from BOMEX and GATE initial states respectively (the AMTEX initial state leads to numerical instability and the inversion was wiped out within 3 hours so we will skip this case). Each of these runs uses asymptotic mixing length of 300m. Due to the weak turbulent mixing process as was shown above, it takes more than 24 hours for both ECMWF schemes to adjust the boundary layer structure from the initial

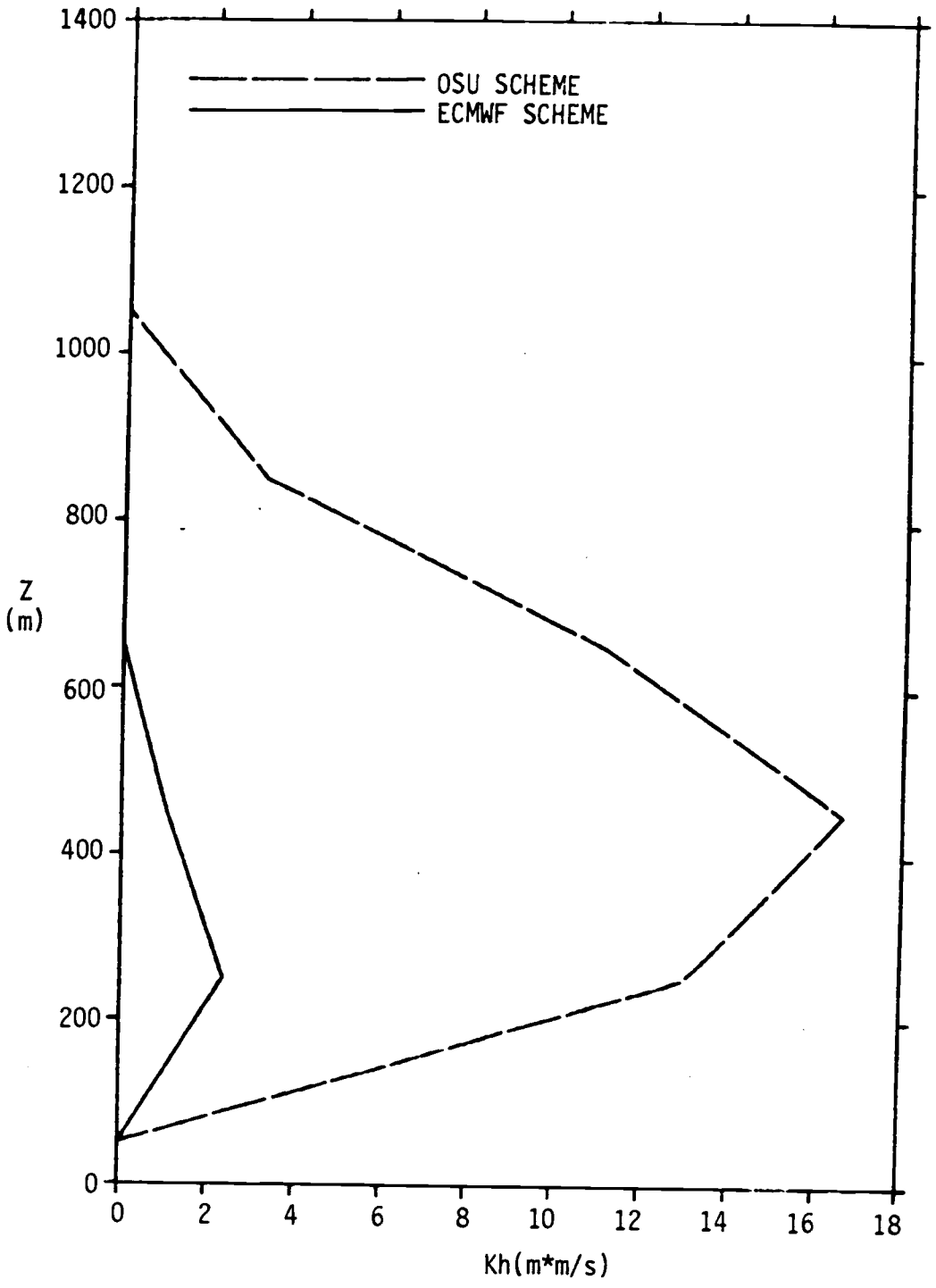

Figure 4.12. Vertical profile of the moisture diffusion coefficient for the OSU (dash line) and the ECMWF (solid line) schemes.

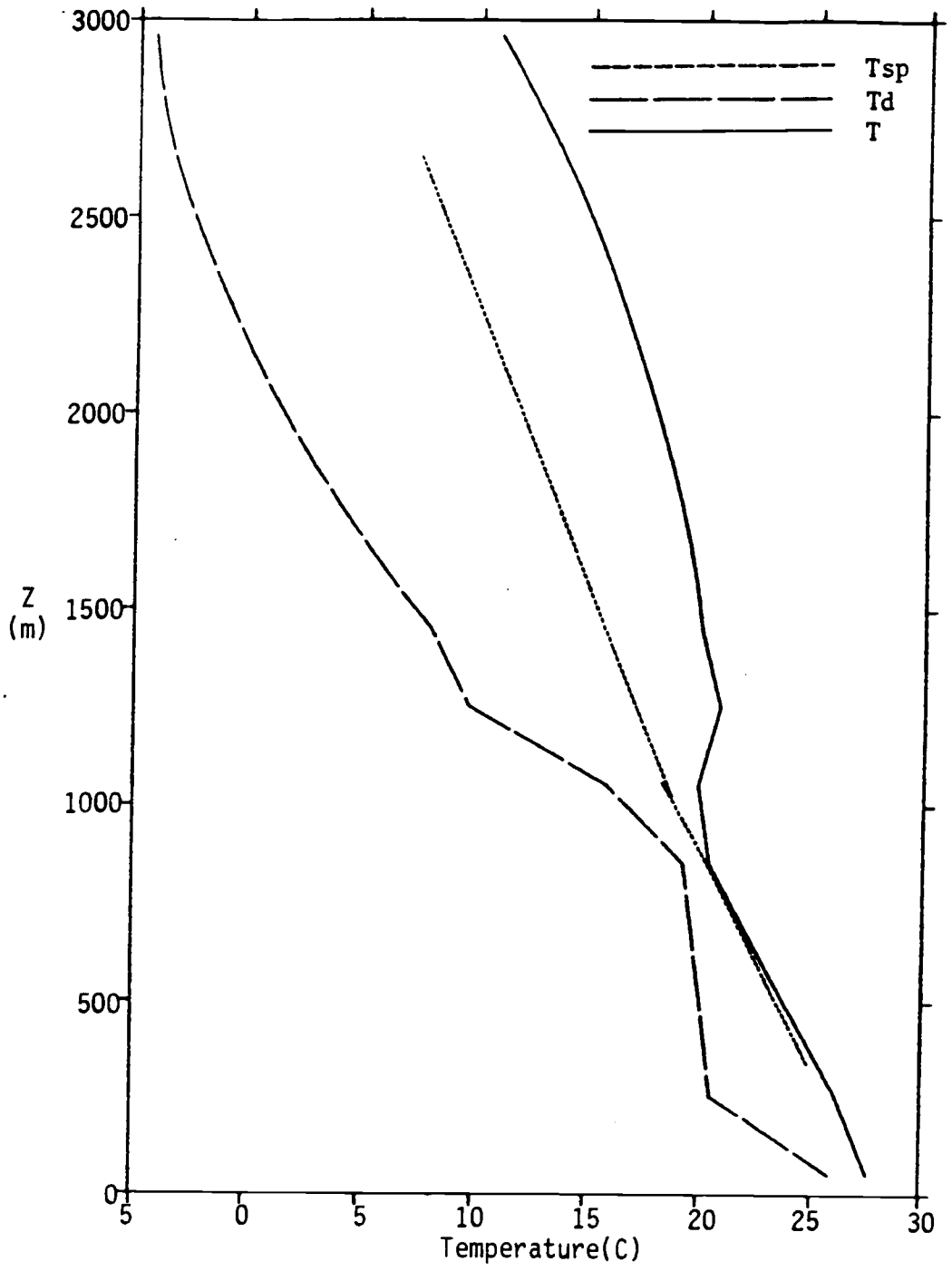

Figure 4.13. Temperature, dew point and saturation point profiles for the BOMEX case with the ECMWF shallow convection scheme (a) at hour 1, and (b) at hour 12.

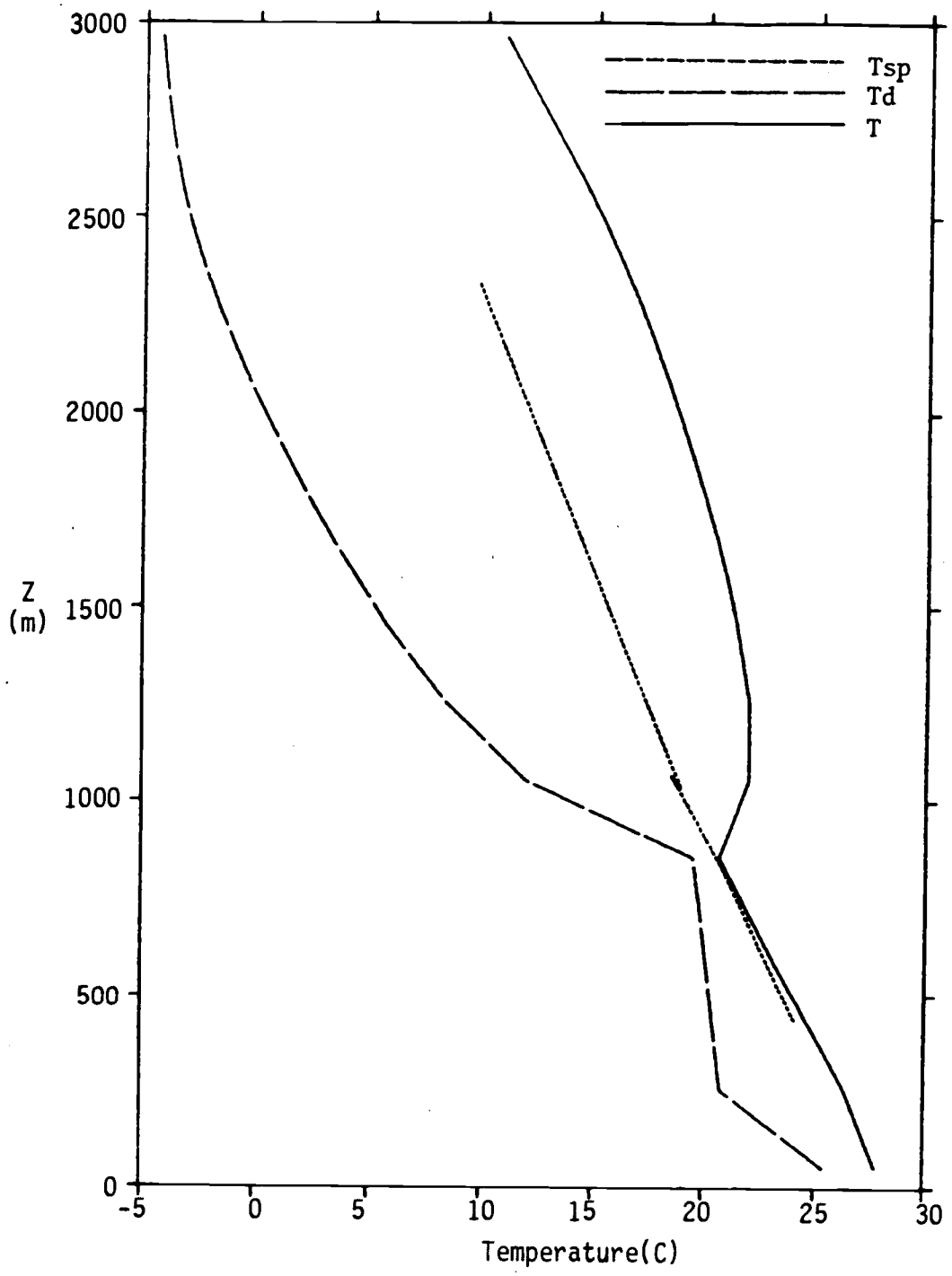

Figure 4.13. (Continued)

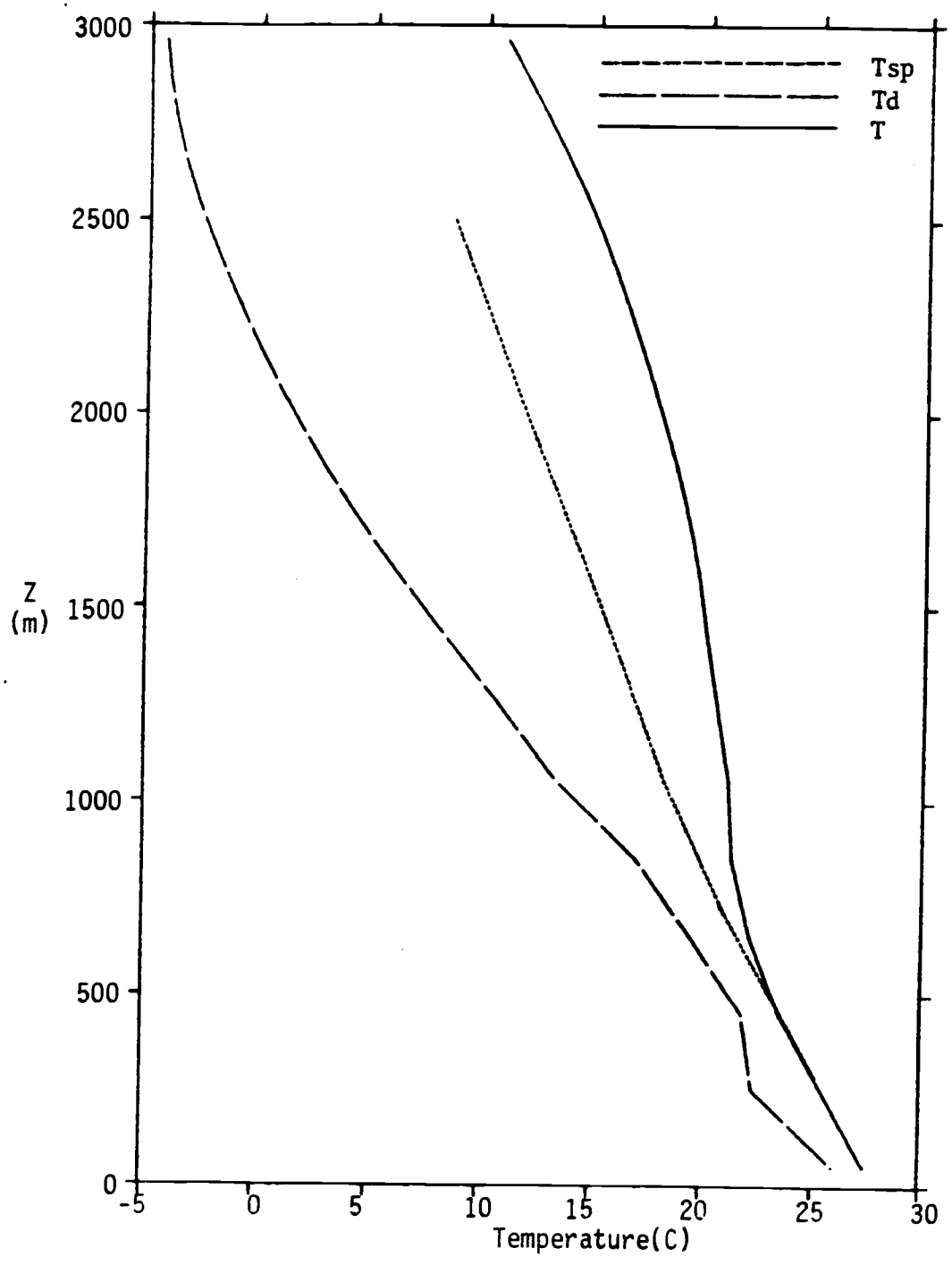

Figure 4.14. Temperature, dew point and saturation point profiles for the BOMEX case without the ECMWF shallow convection scheme. (a) at hour 1, and (b) at hour 12.

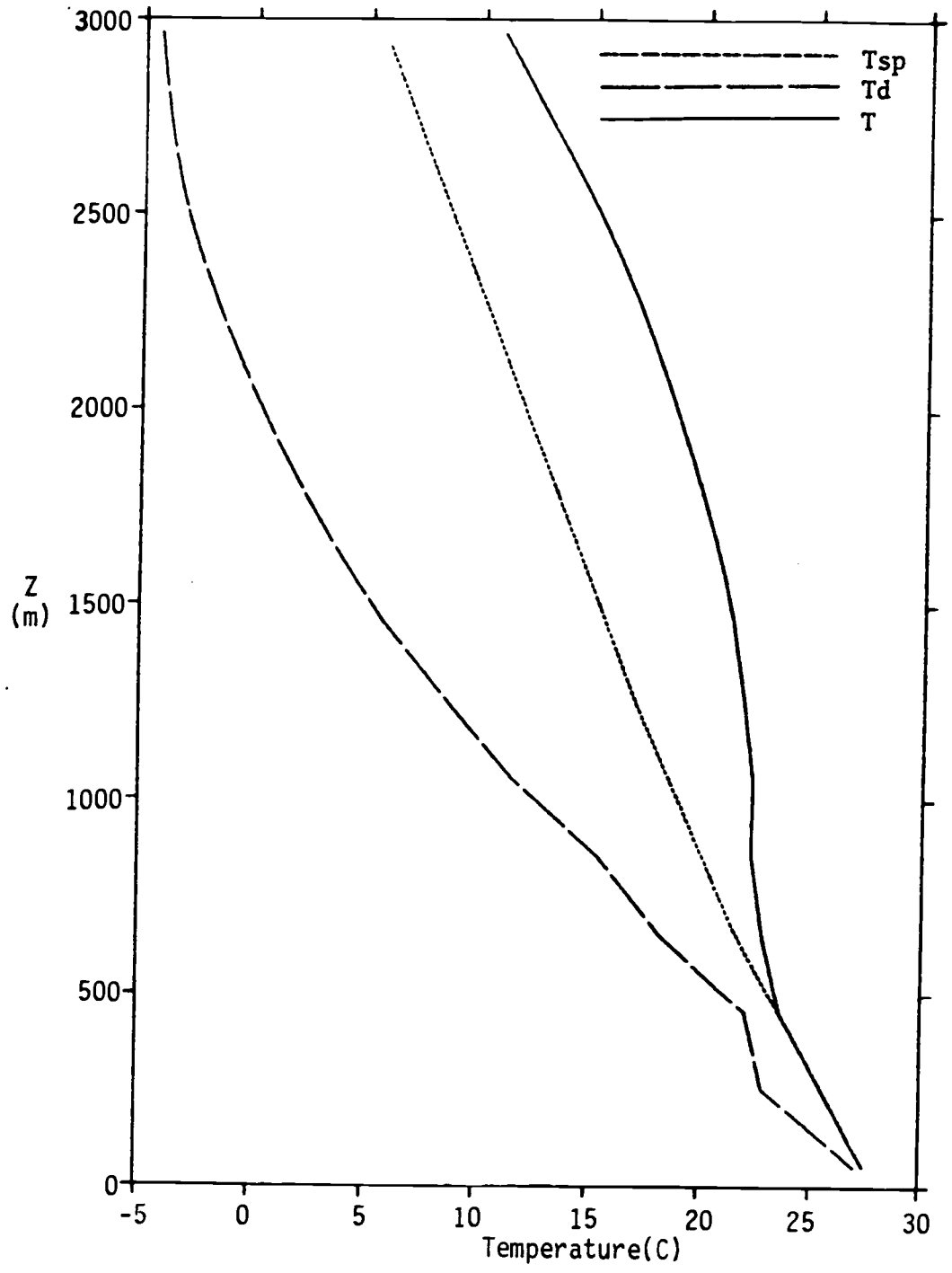

Figure 4.14. (Continued)

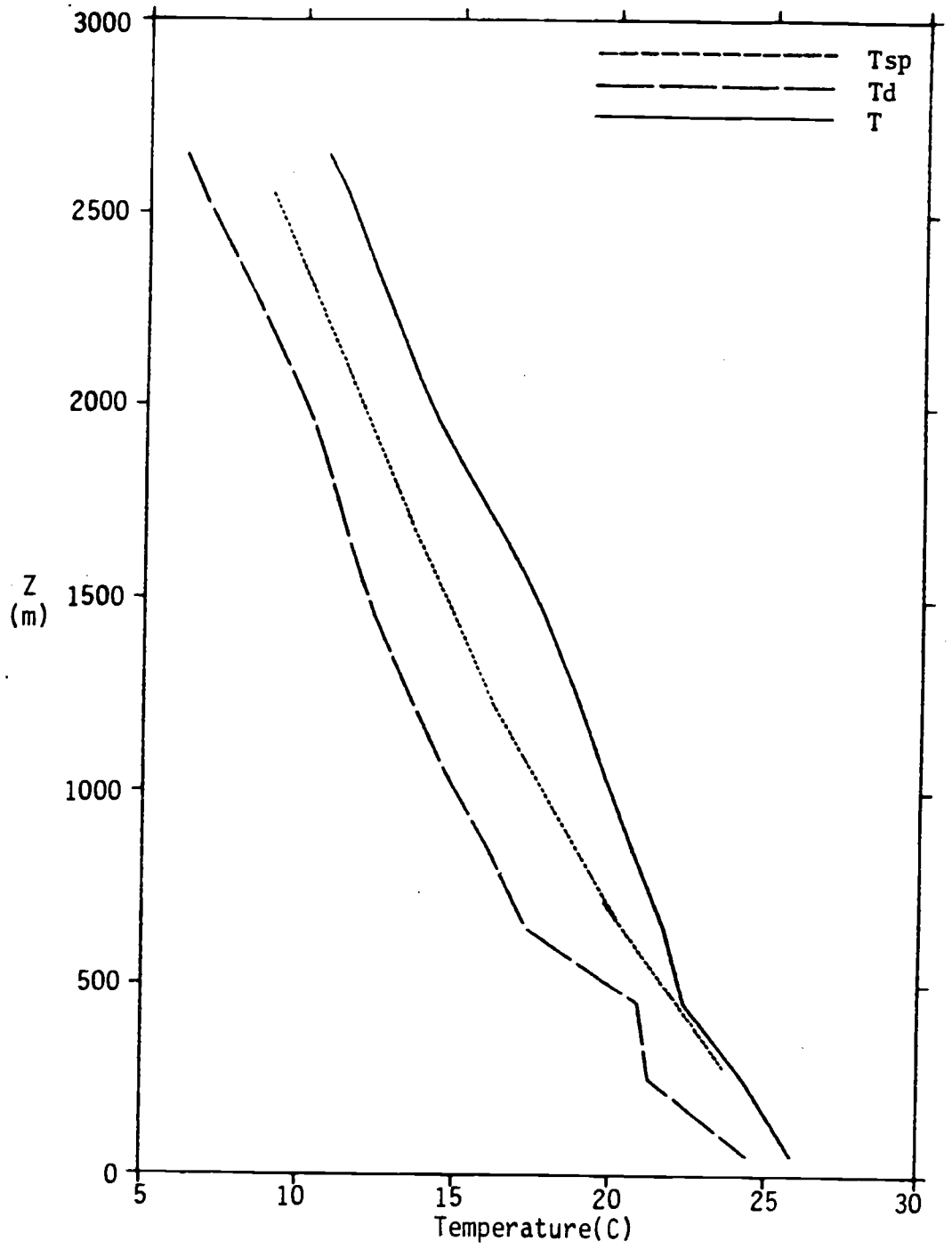

Figure 4.15. Temperature, dew point and saturation point profiles for the GATE case with the ECMWF shallow convection scheme (a) at hour 1, and (b) at hour 12.

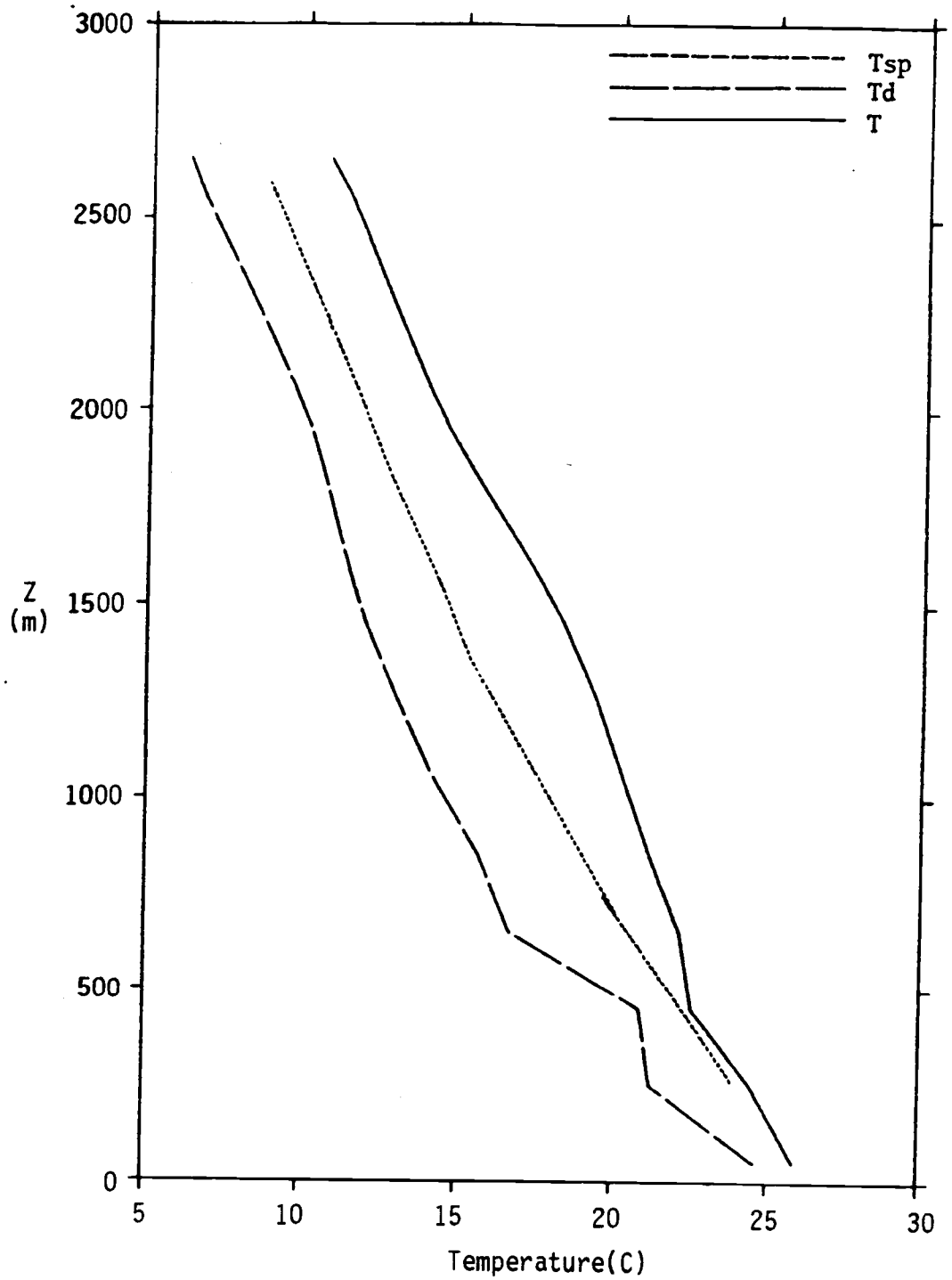

Figure 4.15. (Continued)

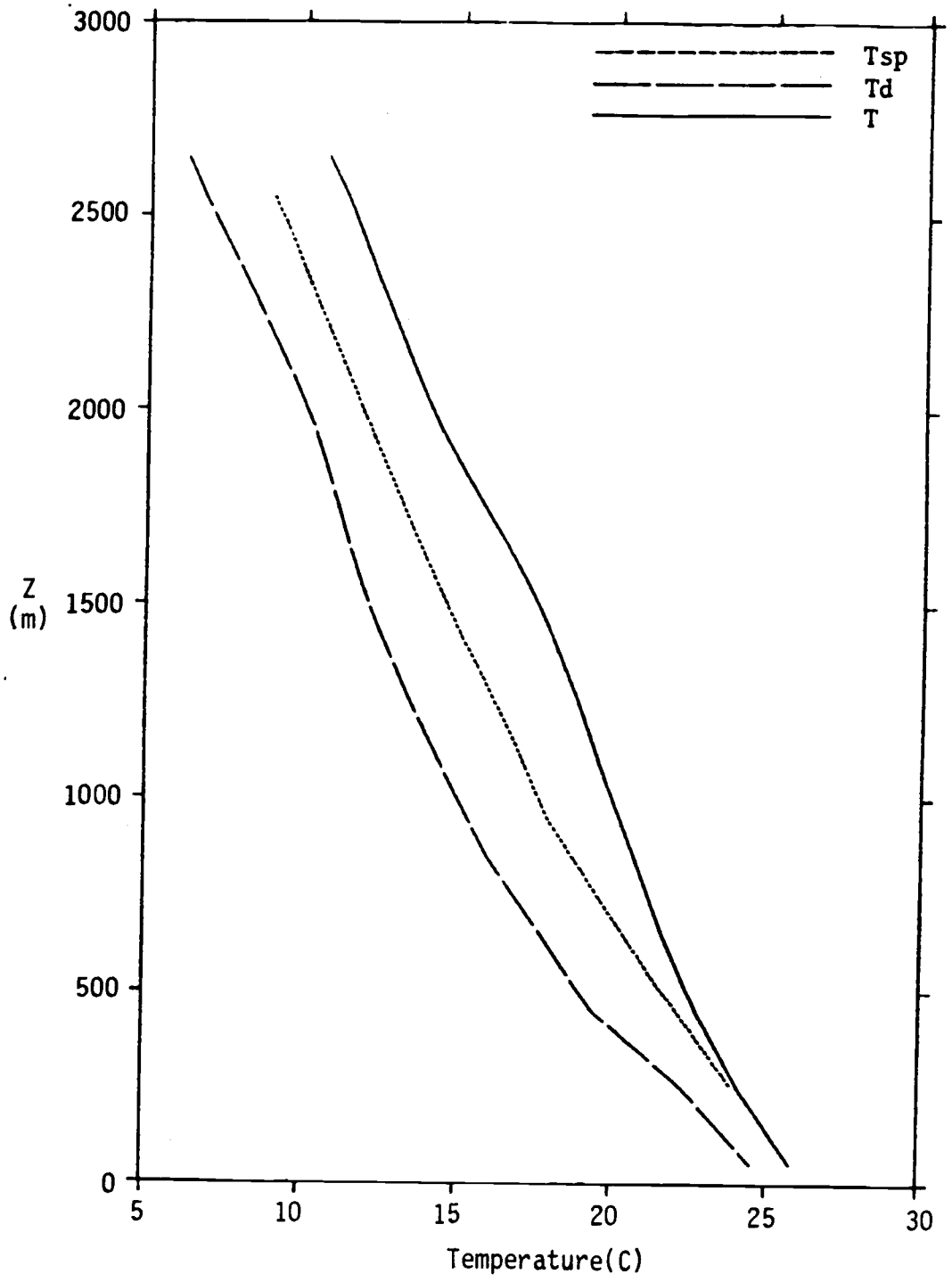

Figure 4.16. Temperature, dew point and saturation point profiles for the GATE case without the ECMWF shallow convection scheme (a) at hour 1, and (b) at hour 12.

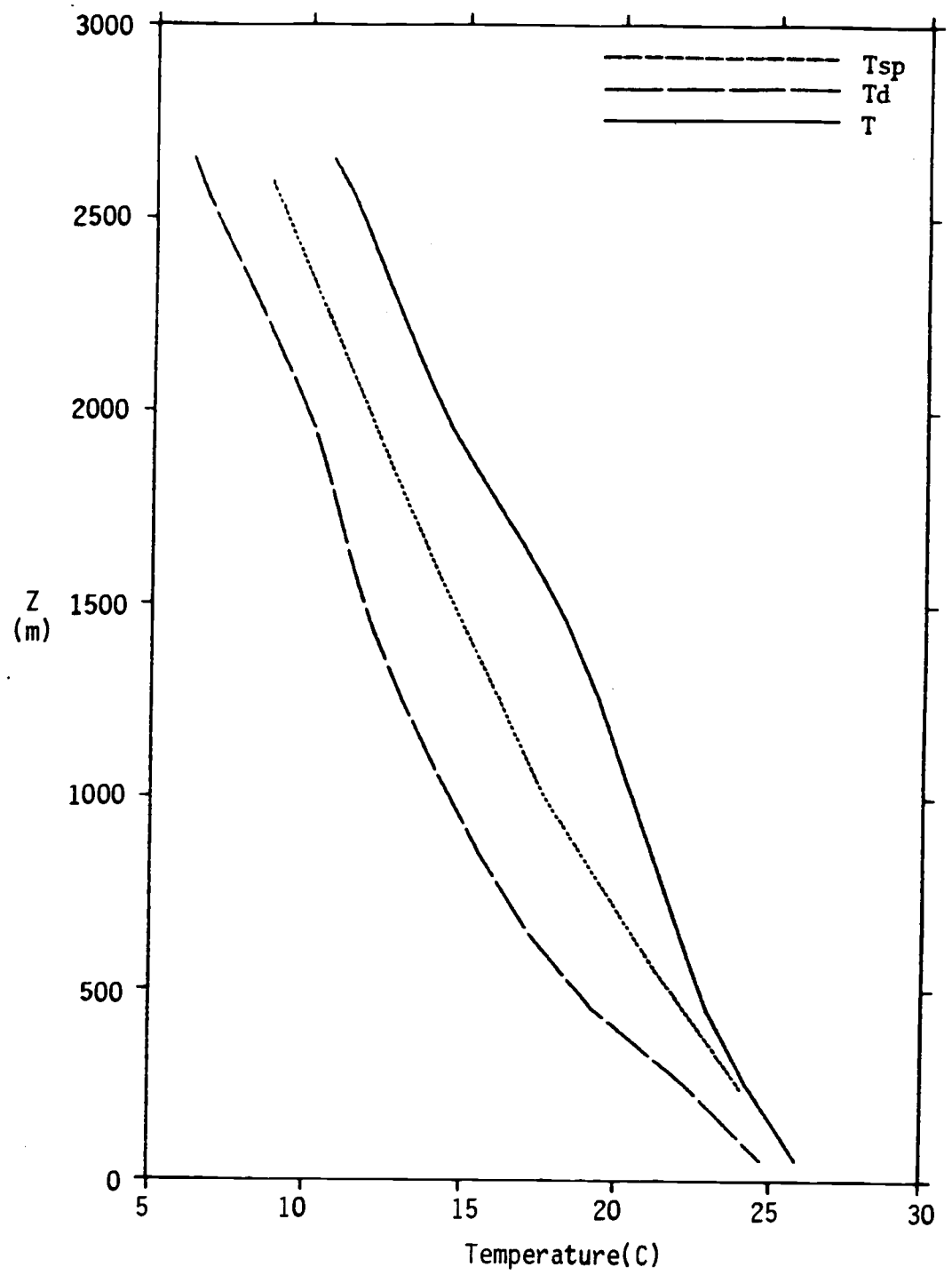

Figure 4.16. (Continued)

state to well-mixed. Compared to our result (less than one hour can result in a well-mixed lower boundary layer) the turbulent mixing for ECMWF scheme is relatively weak and slow. Hence we display model structures at hour 25 and 36. Table 4.2 lists the results at hour 36 from the ECMWF scheme.

Table 4.2. Summary of the surface latent heat and virtual heat flux simulated with the ECMWF scheme. (Note : * represents without the shallow convection)

Data	Virtual heat flux ($W\ m^{-2}$)	Latent heat flux ($W\ m^{-2}$)
BOMEX	1.5 (0.9)*	32 (18)*
GATE	0.45 (0.42)*	17 (13)*

The characteristics of the simulated GATE and BOMEX model structure are: 1) the predicted boundary layer height is lower, 2) a steady state structure can not be maintained for very long, and, 3) the upper boundary layer is not saturated with or without the shallow convection. With the shallow convection a well-defined inversion layer is obtained. Folding of the SP's profile above the inversion indicate the transition from the moist surface layer to the dryer mixed layer, but this is not very clear for the cases without the shallow convection due to the weaker turbulent mixing. Closer examination of the potential temperature (θ) and mixing ratio (q) profile can reveal more detail of the boundary layer model structure. For example, for the BOMEX case at hour 36 (see

Fig. 4.17-18) a deep mixed layer with it's top at 800 m is created with shallow convection, this is roughly twice the depth simulated without the shallow convection. Unlike our deeper and totally well-mixed boundary layer model structure at hour 12 (see Fig. 4.19- 20), the ECMWF result within the boundary layer shows a thick moist surface layer below 250 m which explains their smaller simulated surface virtual heat flux and latent heat flux (Table 4.2). Down-wind of the trade wind is the typical area where we can see the deep cumulus. It is very important to the development of the down-wind deep convection to transport moisture from the surface to the upper boundary layer. With the ECMWF scheme, however, moisture is trapped in the lower boundary layer and can not transported to the higher region without the shallow convection. Compared the Figs. 4.18b and 4.20b, at 1.3 Km the mixing ratio is rapidly drop off to 7 g Kg^{-1} from 17 g Kg^{-1} at 500 m for ECMWF scheme, while our scheme simulated a 1.1 Km depth well-mixed layer with a constant mixing ratio about 14.5 g Kg^{-1}. This may be the reason why the ECMWF global model needs the shallow convection to set up a deeper mixed-layer (Fig. 4.18a) and enhance the surface turbulent fluxes. In Fig. 4.20 our result indicates that the shallow convection only slightly increases the mixing ratio above the 1.3 Km and the profile below that level is not changed. But from the potential temperature point of the view (Fig. 4.19) the shallow convection creates a deeper transition layer above the boundary layer and the top of the boundary layer becomes lower.

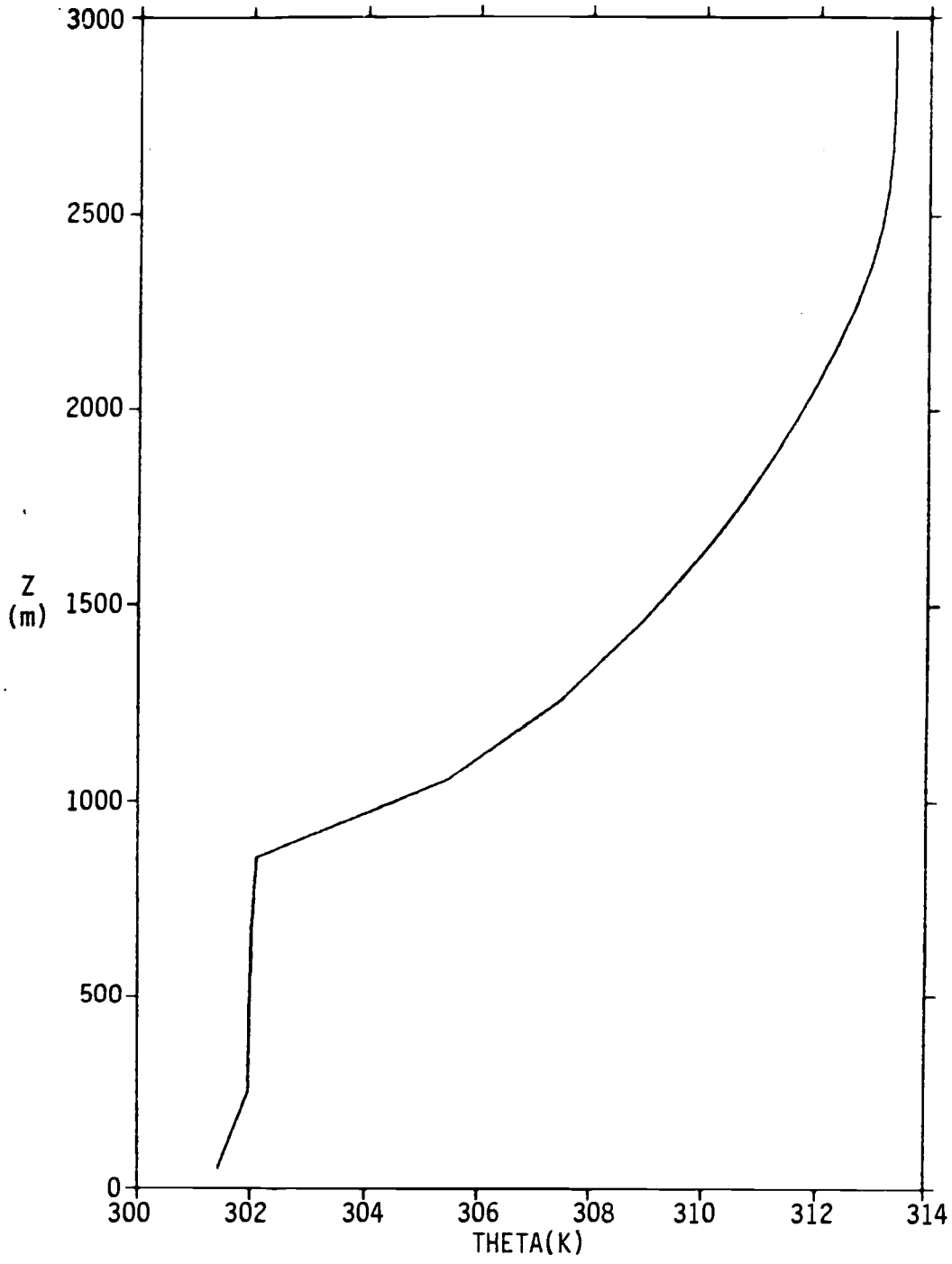

Figure 4.17. Predicted potential temperature profile for the BOMEX case at hour 36 (a) with the ECMWF shallow convection scheme, and (b) without the ECMWF shallow convection scheme.

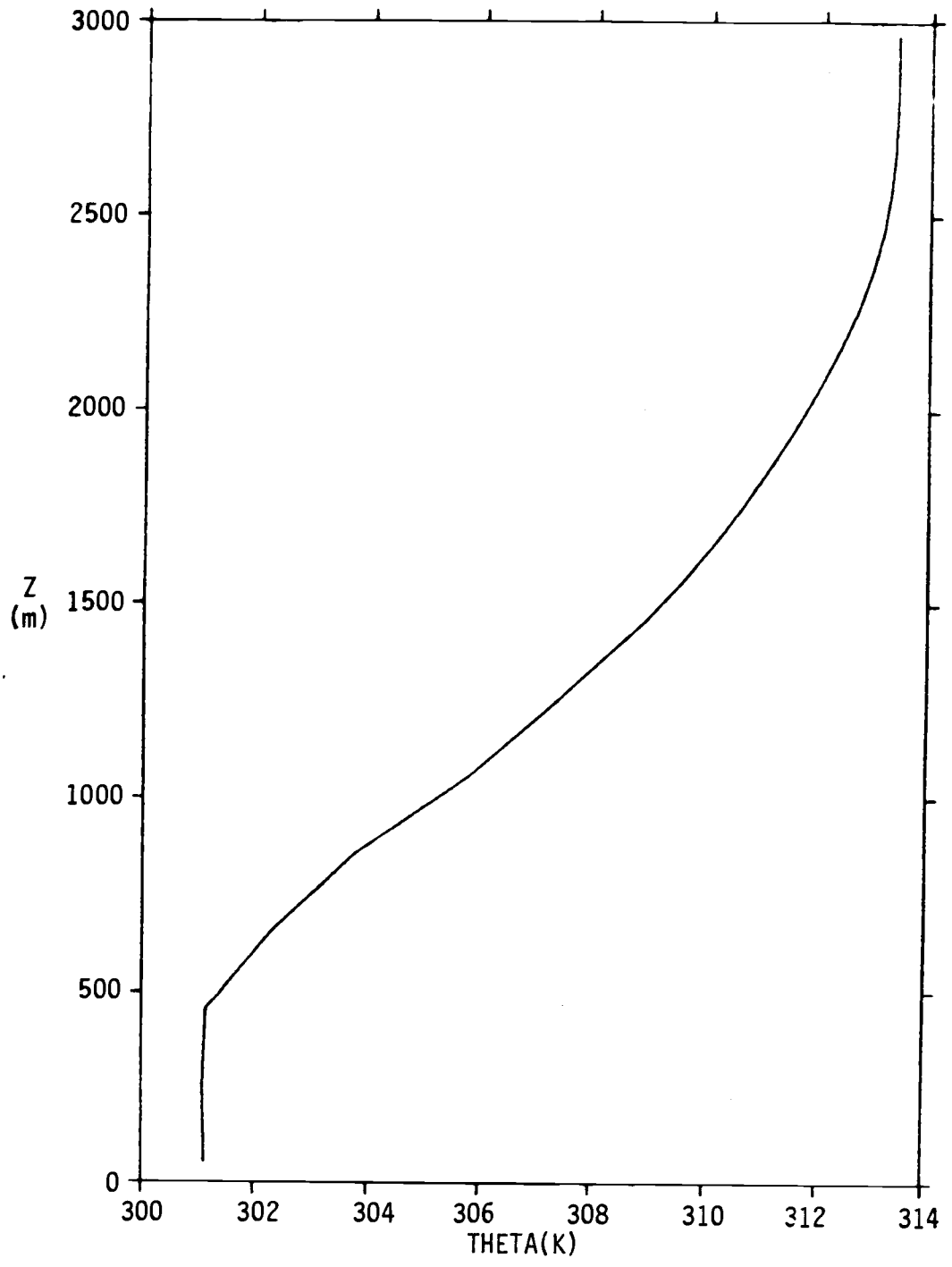

Figure 4.17. (Continued)

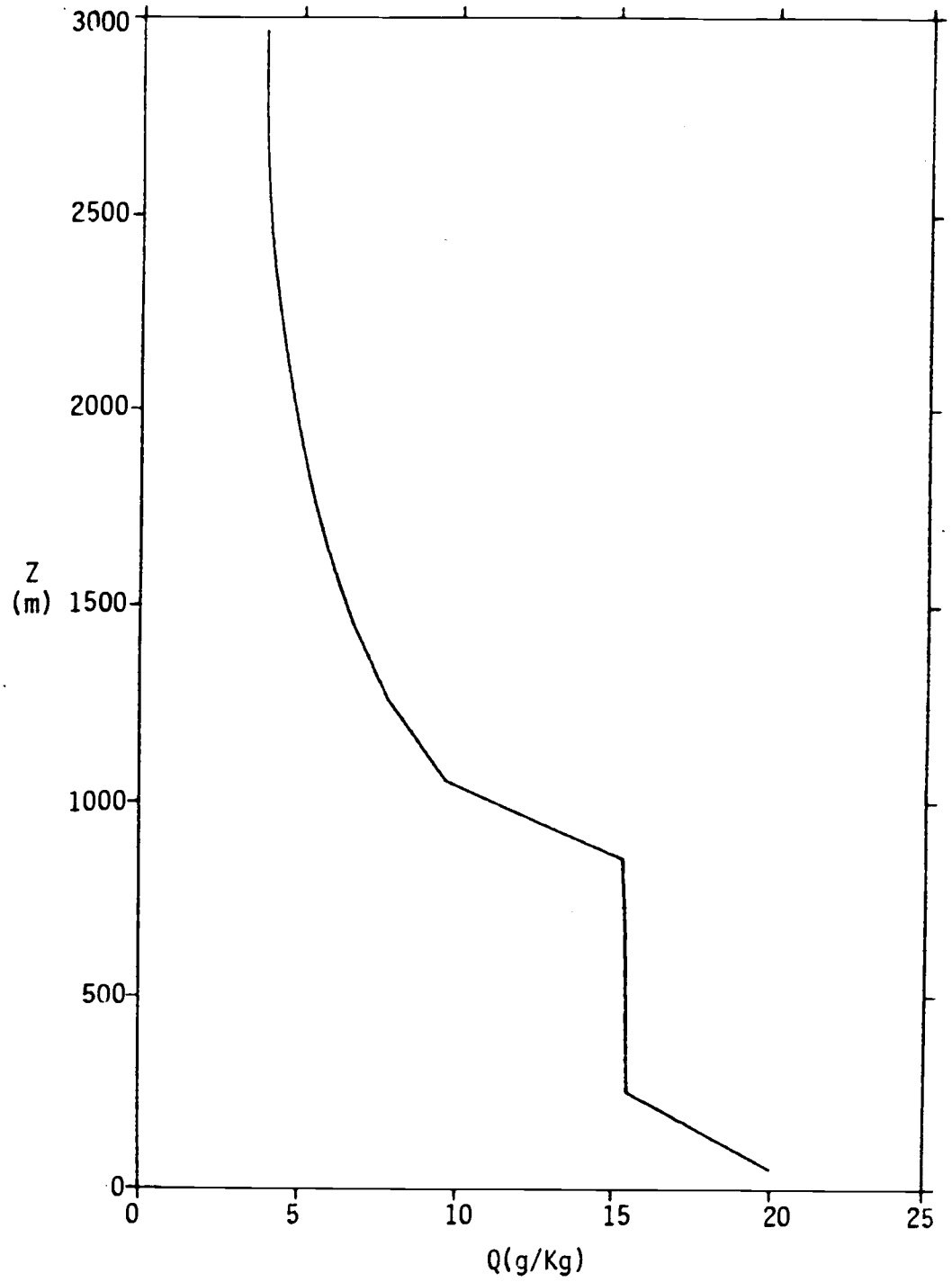

Figure 4.18. Predicted Mixing ratio profile for the BOMEX case at hour 36 (a) with the ECMWF shallow convection scheme, and (b) without the ECMWF shallow convection scheme.

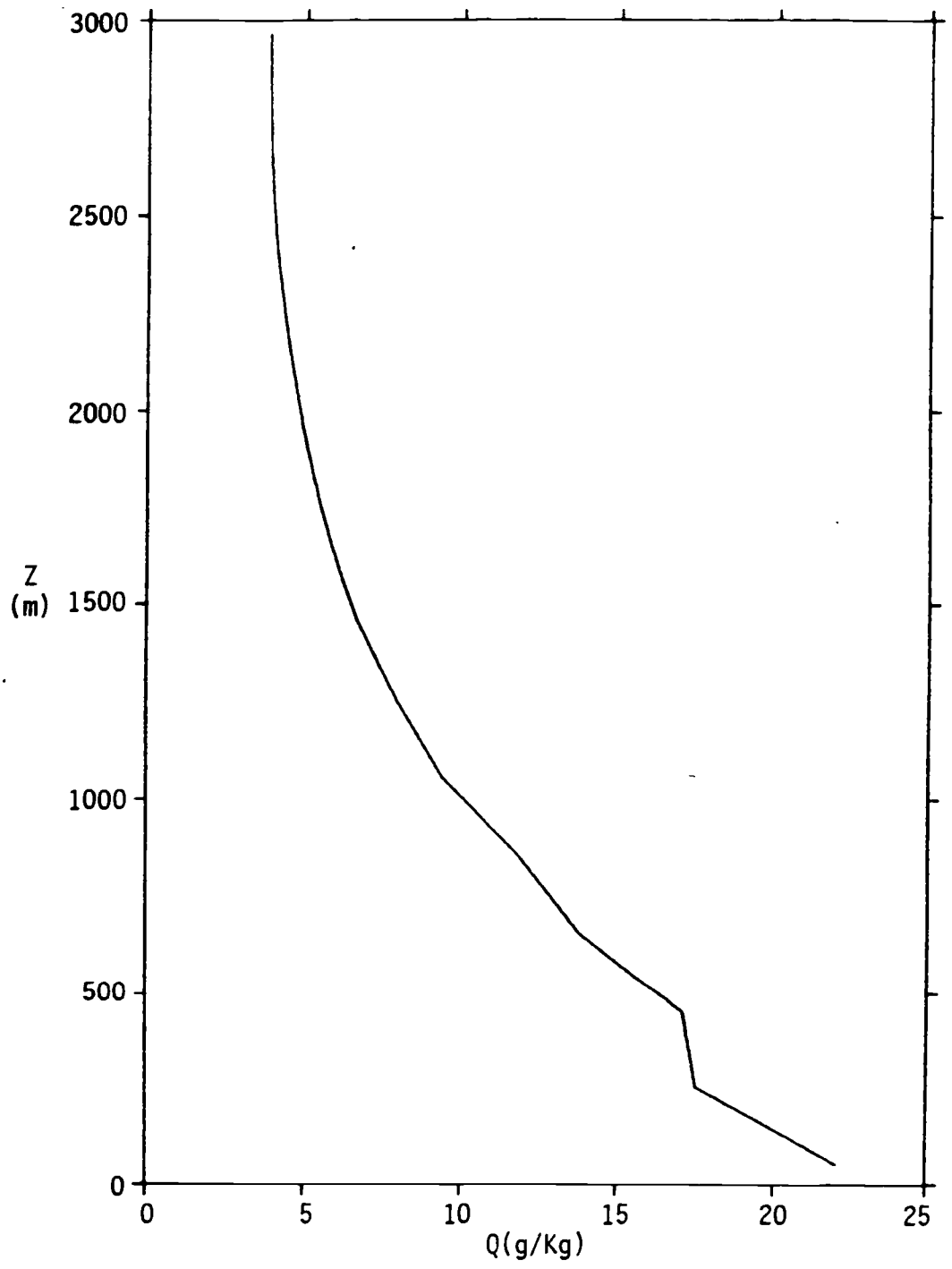

Figure 4.18. (Continued)

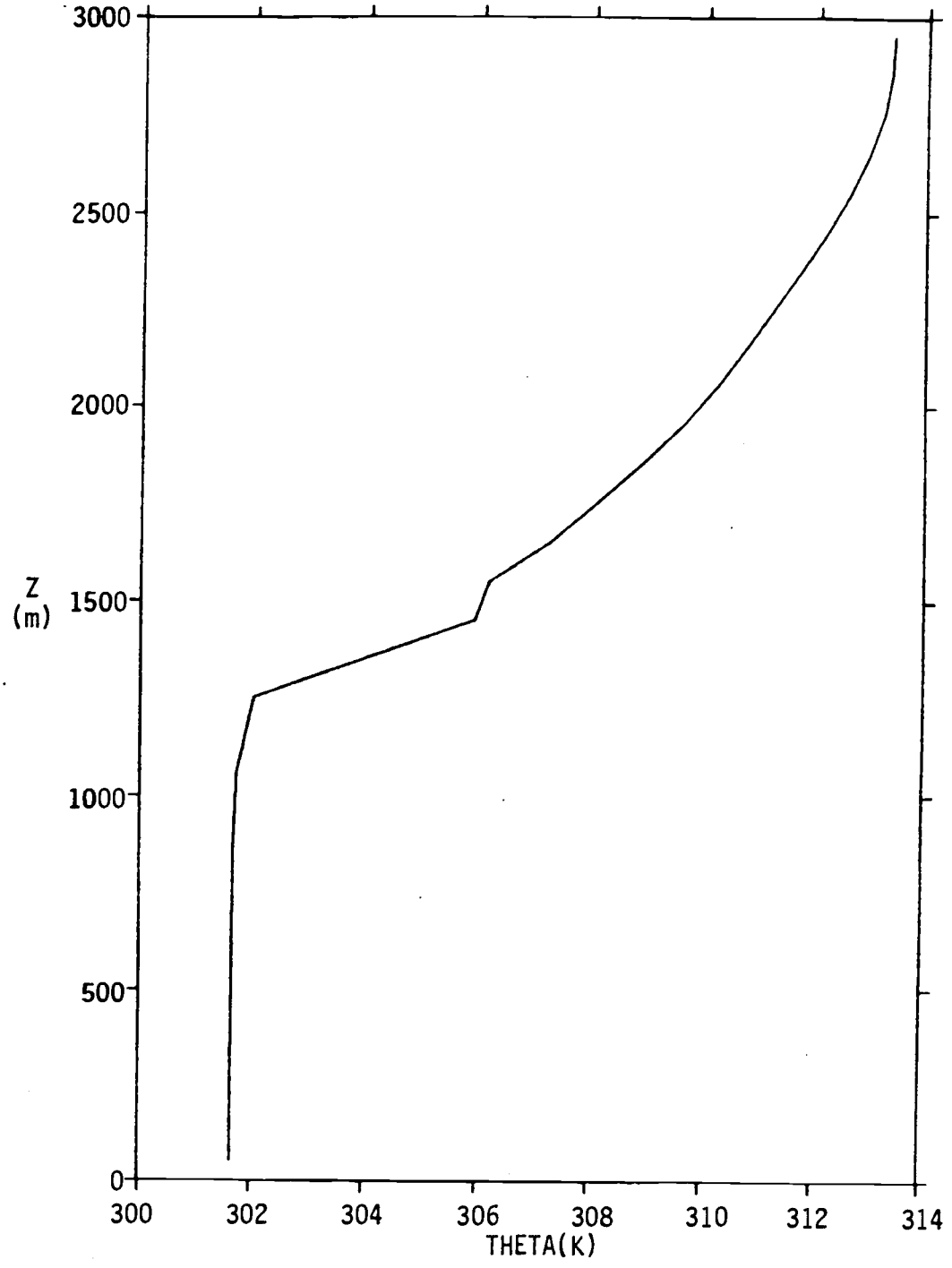

Figure 4.19. Predicted potential temperature profile for the BOMEX case at hour 12 (a) with the OSU shallow convection scheme, and (b) without the OSU shallow convection scheme.

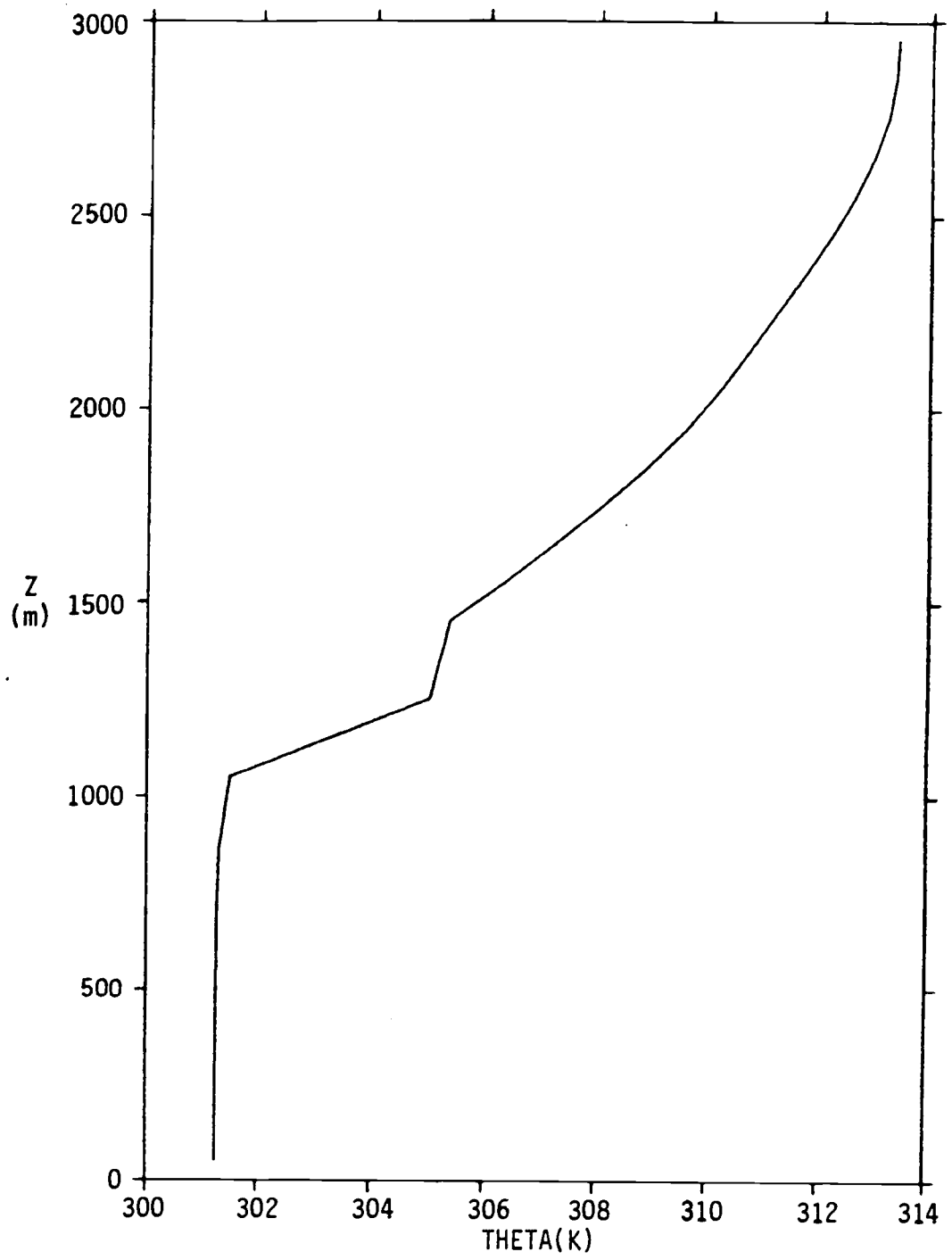

Figure 4.19. (Continued)

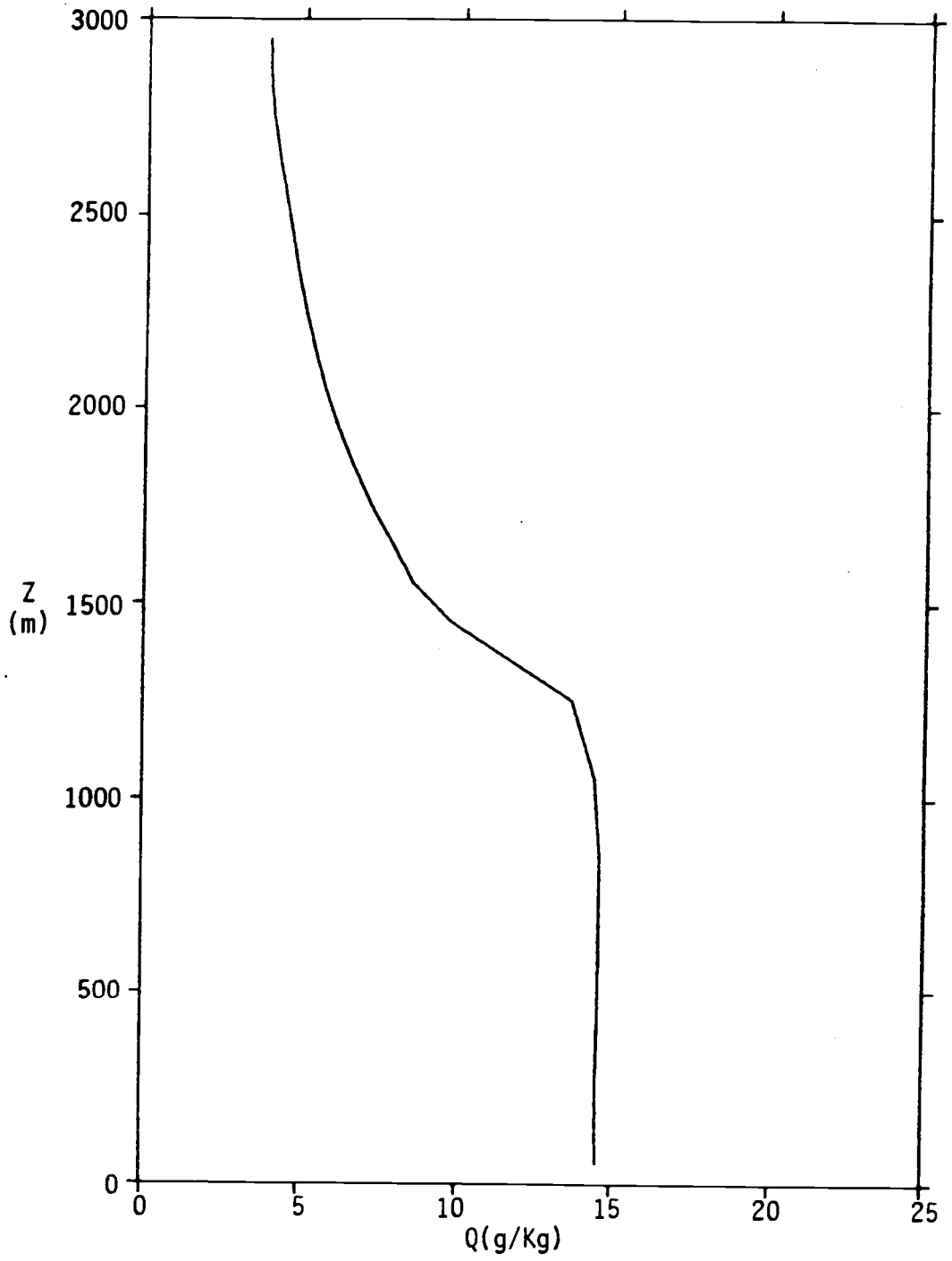

Figure 4.20. Predicted mixing ratio profile for the BOMEX case at hour 12 (a) with the OSU shallow convection scheme, (b) without the OSU shallow convection scheme.

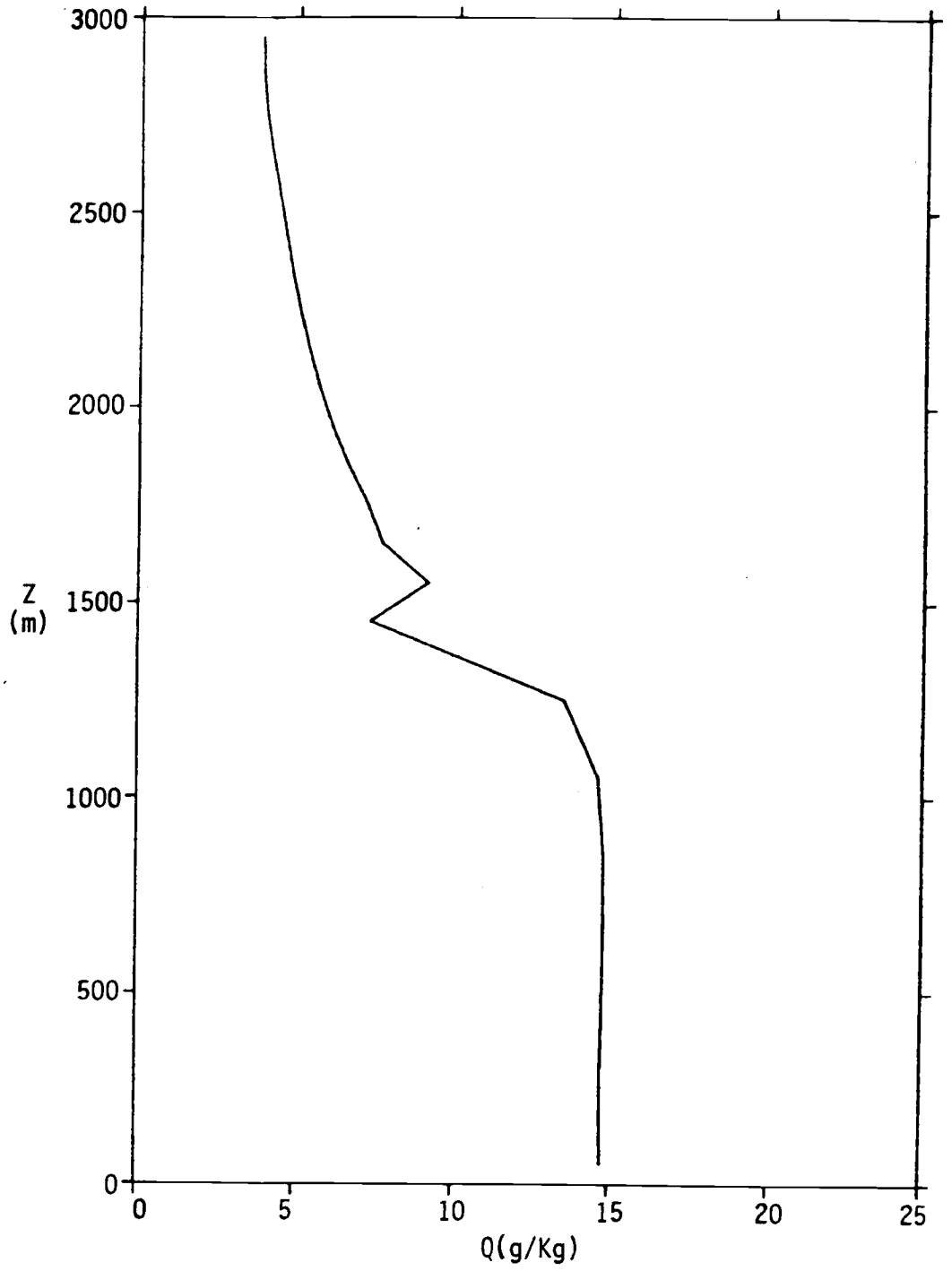

Figure 4.20. (Continued)

The primary difference between the schemes can be seen in the model diagnostic Q2 profiles at hour 36. For the BOMEX case (Fig. 4.21), the Q2 profile without shallow convection shows a large moisture flux convergence near the surface and a weaker one at the top of the mixed layer (400 m). When shallow convection is included the Q2 profiles shows only one minimum at the mixed layer top (800 m). This means the modeled shallow cumulus is working to prevent moisture from accumulating near the surface and to transport it from the lower boundary layer to the mixed layer top. This also enhances the surface sensible and latent heat transport. For the GATE case (Fig. 4.22), a similar result is obtained. Compare the case with the shallow convection to our result (which essentially is without the shallow cumulus), we found that both have a minimum point at 250m and the magnitude is slightly larger for the OSU model.

For the BOMEX case with shallow convection, the ECMWF scheme has a reasonable Q2 minimum compared to the observation. The boundary layer top (h) is much lower and the minimum point of the Q2 profile take places at the top of the mixed layer instead of the boundary layer top. However, the simulated thick moist surface layer is not observed in the real data. In contrast, our simulation has a deeper and well-mixed boundary layer (which is close to the observation) and a slightly overestimated moisture flux at the top of the boundary layer.

From the above discussion one can see that the role of the shallow convection is crucial to the ECMWF model because the

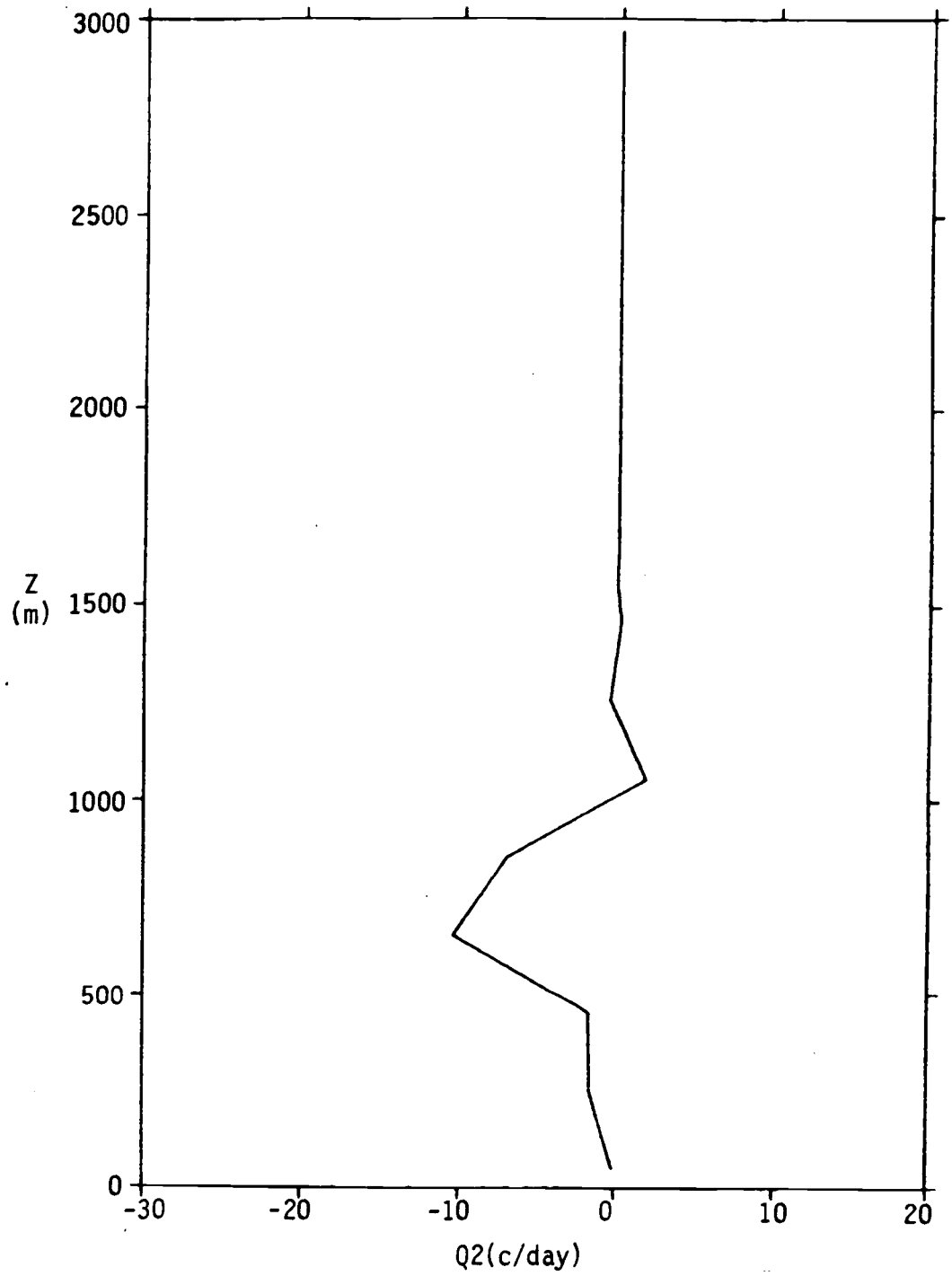

Figure 4.21. Predicted model diagnostic Q2 profiles for the BOMEX case at hours 4, 8, 12 (a) with the ECMWF shallow convection scheme, and (b) without the ECMWF shallow convection scheme.

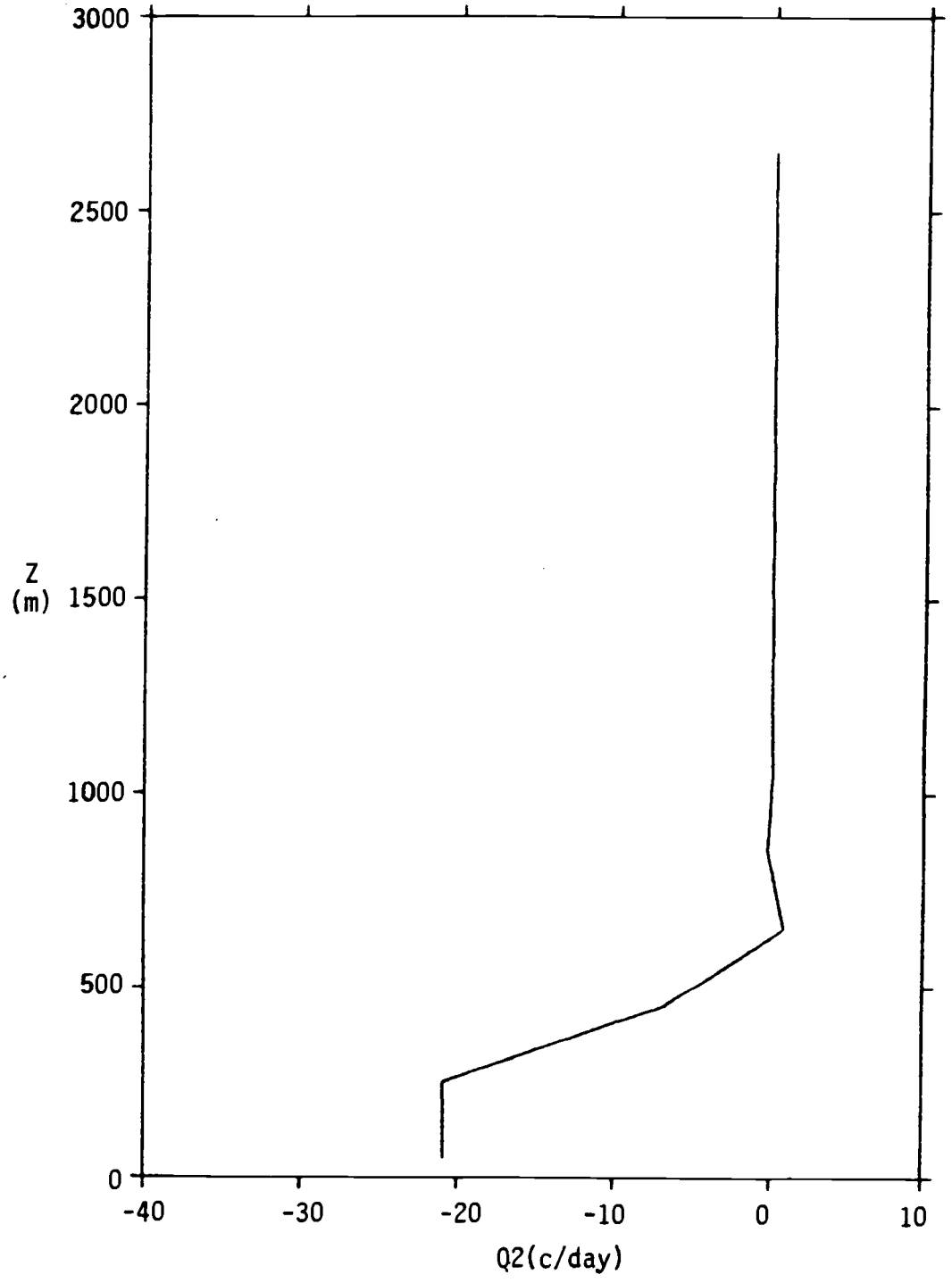

Figure 4.21. (Continued)

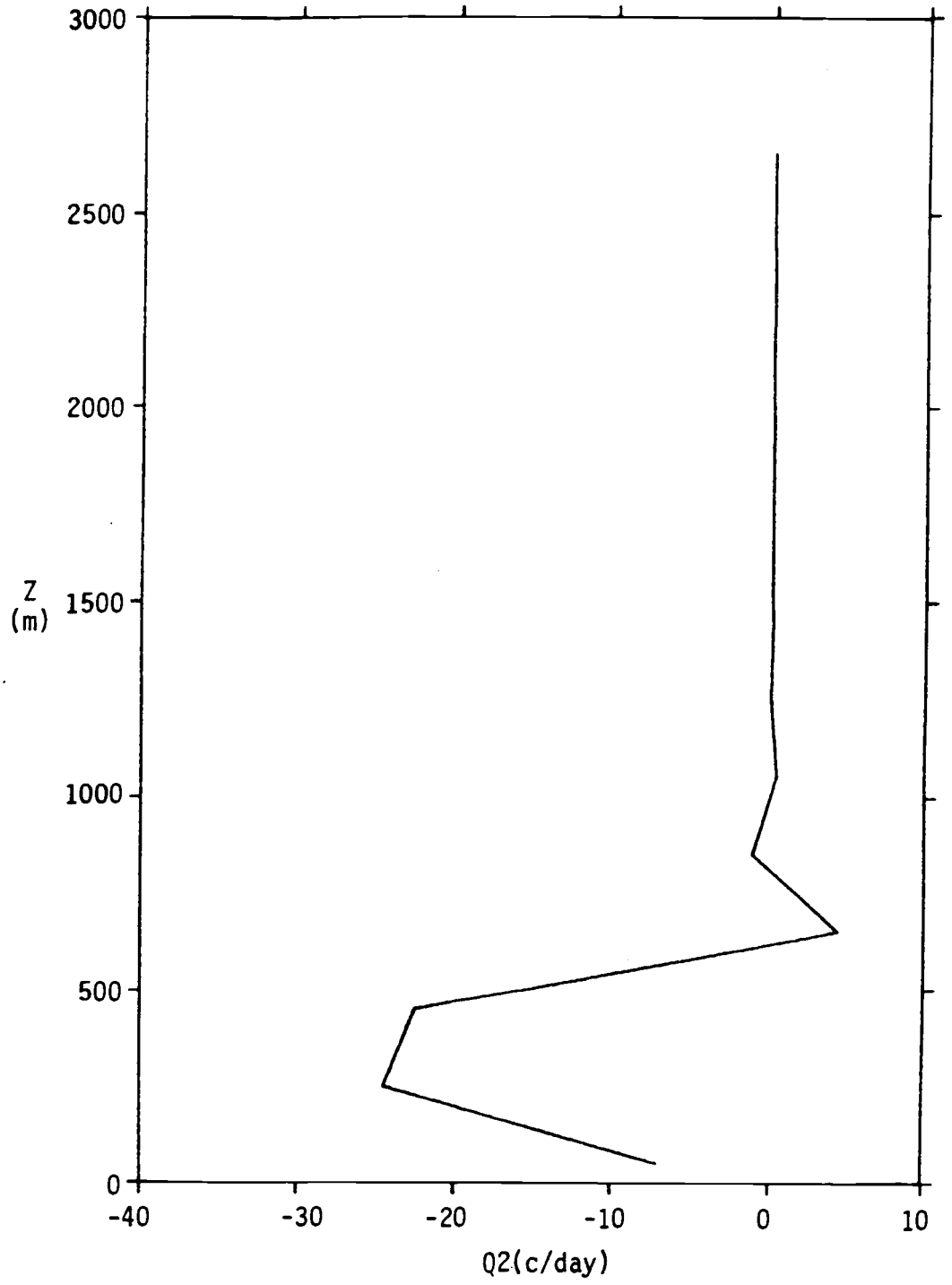

Figure 4.22. Predicted Q2 profiles for the GATE case at hours 4, 8, 12 (a) with the ECMWF shallow convection scheme, and (b) without the ECMWF shallow convection scheme.

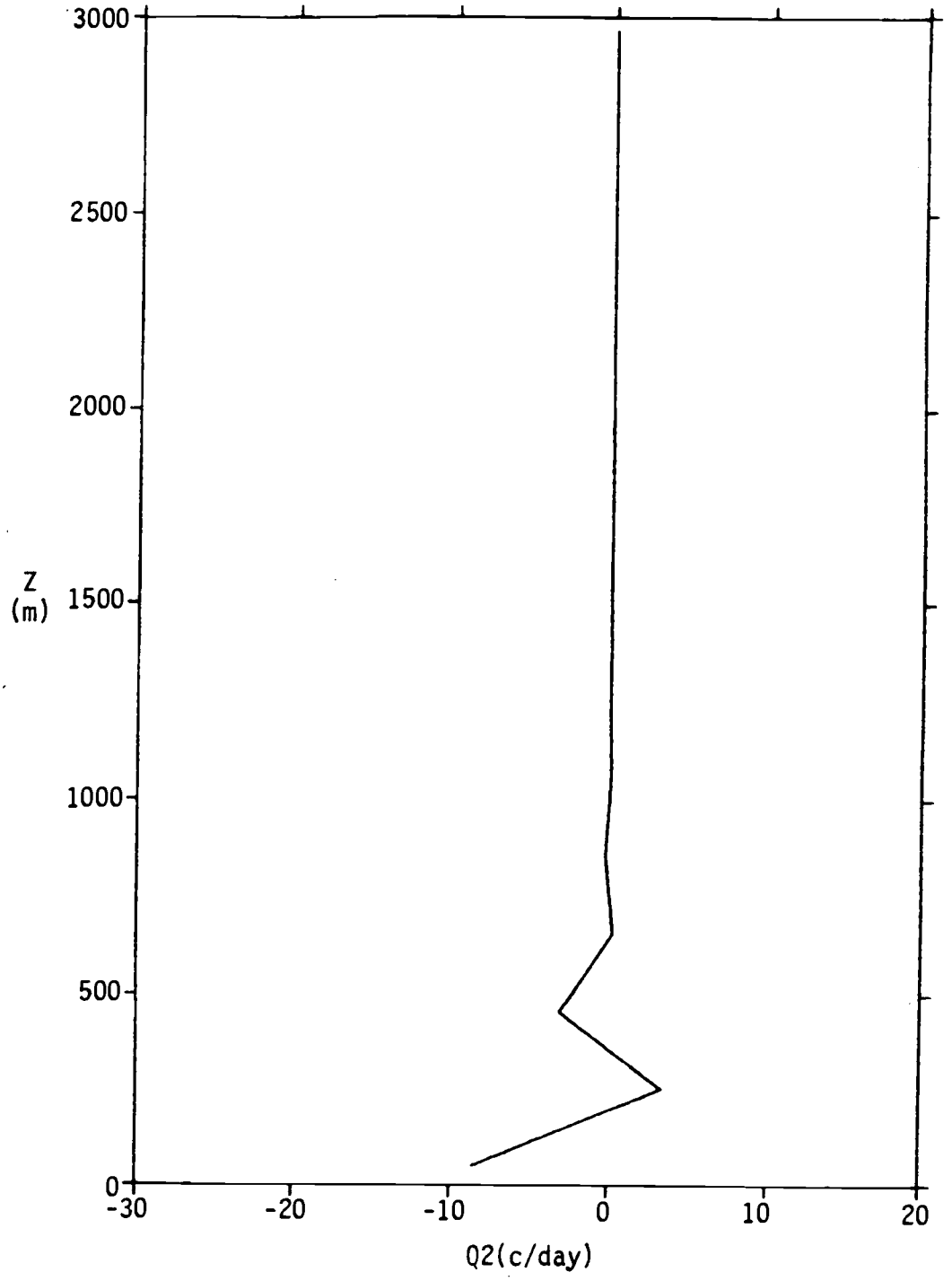

Figure 4.22. (Continued)

boundary layer mixing is too weak. By including the shallow convection in the model, the turbulent mixing is still not capable of reproducing the state that is close to the real data. These are due to the constraint of the asymptotic mixing length that prevents moisture and heat from mixed into higher atmosphere.

5. CONCLUSION AND DISCUSSION

The ECMWF global prediction model is considered by many the state-of-the-art weather prediction model at the present. It is the result of recent model diagnosis from the ECMWF that led to our interest in modeling the shallow cumulus. However, results based on our boundary layer parameterization scheme are quite different from the ECMWF experience. We found that our boundary layer parameterization can mix moisture into upper troposphere and created the observed Q2 profile while the ECMWF scheme cannot. The results indicate that the primary mechanism that transports moisture away from lower atmosphere is the boundary layer turbulent flux. The boundary turbulent mixing alone is capable of maintaining an apparent moisture source near the inversion. While the sensible heat flux over the ocean becomes quite small after a few hours, the virtual heat flux remains positive and the boundary layer remains in the unstable regime.

Due to the constraint of the asymptotic mixing length, we have found the ECMWF boundary layer mixing is restricted to the lowest 500 m of the boundary layer. Even with recent modification, the boundary mixing is still extremely small above 500 m. It is possible that the use of the diffusivity coefficient formula derived for a neutral boundary (Blackadar, 1962) in unstable situations may be inappropriate.

The effect of the shallow convection scheme in our 1-D model is to enhance the boundary layer turbulent mixing and the surface

turbulent fluxes and to reduce moisture flux convergence near the top of the boundary layer by mixing the air within the boundary layer with the free atmosphere. For the ECMWF model, the shallow convection scheme significantly improves the model results by enhancing the surface turbulent fluxes as well as the moisture flux convergence.

It is necessary to derive a proper boundary layer parameterization scheme before one tries to study the importance of the trade wind shallow cumulus. Without doing so, one can be very easily misled by the results and would have a wrong picture of the problem.

This study is primarily focused on the trade wind shallow cumulus. In the future, we would like to see the effect of the boundary layer and shallow convection scheme over other areas (e.g., over land situation) and would also like to focus on the impact on the 3-D models.

BIBLIOGRAPHY

Albercht B.A., R.S. Penc and W.H. Schubert, 1985: An observation study of cloud-topped mixed layers. J. Atmos. Sci., 42, 800-822.

Arakawa, A., and W.H. Schubert, 1974: Interaction of a cumulus cloud ensemble with the large-scale environment: Part I. J. Atmos. Sci., 31, 674-701.

Betts, A.K., 1978a: Saturation point analysis of moist convective overturning. J. Atmos. Sci., 39, 1484-1505.

_____, 1982b: Cloud thermodynamic models in saturation coordinates. J. Atmos. Sci., 39, 2182-2191.

_____, and M.J. Miller, 1984: A new convective adjustment scheme. ECMWF Technical Report No. 43.

Blackadar, A.K., and H. Tennekes, 1962: Asymptotic similarity in neutral barotropic planetary boundary layers. J. Atmos. Sci., 25(6), 1015-1020.

Brenner, S., C.-H. Yang and Y.K.S. Yee, 1982: The AFGL spectral model of the moist global atmosphere: documentation of the baseline version. A technical report to Atmospheric Prediction Branch, AFGL (AFGL-TR-82-0393).

Esbensen, S., 1975: An analysis of subcloud layer heat and moisture budgets in the western Atlantic trades. J. Atmos. Sci., 32, 1921-1933.

Kuo, H.-L., 1965: On formation and intensification of tropical cyclones through latent heat release by cumulus convection. J. Atmos. Sci., 22, 40-63.

LeMone, M.A., and W.T. Pennell, 1976: The relationship of trade wind cumulus distribution to subcloud layer fluxes and structure. Mon. Wea. Rev., 104, 524-539.

Louis, J.F., 1979: A parametric model of vertical eddy fluxes in the atmosphere. Bound.-layer Meteor., 17, 187-202.

Louis, J.F., M. Tiedtke and J.F. Gelyn, 1981: A short history of the operational PBL-parameterization at ECMWF. (Lecture given by J.F. Geleyn.) ECMWF Workshop on Planetary Boundary Layer Parameterization, 25-27 Nov. 1981, 59pp.

Murty, L.K., 1976: Heat and moisture budgets over AMTEX area during AMTEX'75. J. Meteor. Soc. Japan, 54, 370-381.

Nicholls, S., and M.A. LeMone, 1980: The fair weather boundary layer in GATE: The relationship of subcloud fluxes and structure to the distribution and enhancement of cumulus clouds. J. Atmos. Sci., 37, 2051-2067.

Nitta, T.S., 1976: Large-Scale heat and moisture budgets during the air mass transformation experiment. J. Meteor. Soc. Japan, 54, 1-14.

_____, and S.S. So, 1980: Structure and heat, moisture and momentum budgets of a convective mixed layer during AMTEX'75. J. Meteor. Soc. Japan, 58, 378-393.

Pan, H.-L., and L. Mahrt, 1986: Interaction between soil hydrology and boundary-layer development. Bound.-layer Meteor. (in press).

Tiedtke, M., 1983: The sensitivity studies of the time- mean large-scale flow to cumulus convection in the ECMWF model. ECMWF Workshop on Convection in Large-Scale Models, 28 Nov. - 1 Dec. 1983, 297pp.

Troen, I., and L. Mahrt, 1986: A boundary layer formulation for atmospheric models. Bound.-layer Meteor. (in press).

Wyngaard, J.C., and R.A. Brost, 1983: Top-down and bottom- up diffusion in the convection boundary layer. J. Atmos. Sci., 41, 102-112.

Yanai, M., S. Esbensen and J.-H. Chu, 1973: Determination of bulk properties of tropical cloud clusters from large-scale heat and moisture budgets. J. Atmos. Sci., 30, 611-627.